Emissions of methane and nitrous oxide from full-scale municipal wastewater treatment plants

Proefschrift

ter verkrijging van de graad van doctor

aan de Technische Universiteit Delft;

op gezag van de Rector Magnificus prof. ir. Karel Ch.A.M. Luyben;

voorzitter van het College voor Promoties

in het openbaar te verdedigen op dinsdag 14 oktober 2014 om 15:00 uur

door Matthijs Roger Juliette DAELMAN

bio-ingenieur, Universiteit Gent, België

geboren te Lokeren, België

Dit proefschrift is goedgekeurd door de promotoren:

Prof. dr. dr. h.c. ir. M.C.M. van Loosdrecht

Prof. dr. ir. E.I.P. Volcke

Samenstelling promotiecommissie:

Rector Magnificus	Technische Universiteit Delft, voorzitter
Prof. dr. dr. h.c. ir. M.C.M. van Loosdrecht	Technische Universiteit Delft, promotor
Prof. dr. ir. E.I.P. Volcke	Universiteit Gent, België, promotor
Prof. dr. ir. J.B. van Lier	Technische Universiteit Delft
Prof. dr. ir. I. Nopens	Universiteit Gent, België
Prof. dr. ir. N. Boon	Universiteit Gent, België
Prof. dr. J. Perez Canestro	Universitat Autònoma de Barcelona, Spain Technische Universiteit Delft
Dr. S. Gillot	Institut National de Recherche en Sciences et Technologies pour l'Environnement et l'Agriculture, France
*Prof. dr. ir. G.-J. Witkamp	Technische Universiteit Delft, reservelid

Table of contents

Summary

Since 1750, the year that commonly marks the start of the Industrial Revolution, the atmospheric concentrations of carbon dioxide, methane and nitrous oxide have risen about 40 %, 150 % and 20 %, respectively, above the pre-industrial levels due to human activity (IPCC, 2013b). These elevated greenhouse gas concentrations are held responsible for climate change, which has detrimental effects on the global ecosystem.

The treatment of municipal wastewater entails the emission of greenhouse gases. Carbon dioxide that is emitted directly during the microbial conversion of organic matter is short-cycle carbon, and therefore it does not contribute to the increased carbon dioxide concentrations in the atmosphere. Wastewater treatment also consumes fossil-fuel derived energy and synthetic chemicals, with indirect carbon dioxide emissions as a consequence. The processes leading to the indirect emission of carbon dioxide are well understood, and the magnitude of the emission can be estimated by life cycle assessment. Any decrease in the consumption of fossil fuel derived energy and synthetic chemicals will eventually mitigate the indirect emission of carbon dioxide. The origins of methane and nitrous oxide, both potent greenhouse gases with a global warming potential of respectively 34 and 298 CO_2-equivalents over a 100 year time horizon (IPCC, 2013b), are far less understood. This lack of insight hampers the mitigation of these emissions.

The present thesis discusses the emission of nitrous oxide and methane from municipal wastewater treatment plants. The final goal is to come up with guidelines to mitigate these emissions in order to decrease the climate footprint of wastewater treatment. This requires insight into the extent of the emissions and into the relationships between the emissions on the one hand and the plant's operational conditions on the other hand. This work fulfils the need for decent emission data by providing long-term, online emission data from a covered wastewater treatment plant that resulted in the most precise and accurate emission estimate from a full-scale plant to date. Given the importance of reliable data, particular attention is paid to sampling techniques (dissolved methane) and sampling strategies (nitrous oxide).

The **first chapter** briefly surveys what is known about the production pathways of methane and nitrous oxide in wastewater treatment plants. It continues with an overview of the presumed significance of methane and nitrous oxide emissions from municipal wastewater treatment in relation to the worldwide anthropogenic greenhouse gas emissions. The ways in which the emission is currently quantified is discussed as well, both for countrywide and for plantwide estimates.

The **second chapter** reports the results from a 16-month online monitoring campaign measuring nitrous oxide and methane emissions from a municipal wastewater treatment plant. Together with the carbon dioxide emission that was calculated from the plant's electricity and natural gas consumption, the emission data of methane and nitrous oxide were combined in a climate footprint of the plant. Both the methane and nitrous oxide

emissions at the Kralingseveer wastewater treatment plant under study exceeded the plant's indirect carbon dioxide emission related to electricity and natural gas consumption. Furthermore, the results of this study confirms the shortcoming the emission factors that are currently prescribed by the International Panel on Climate Change to estimate greenhouse gas emissions from municipal wastewater treatment. Exploratory measurements of methane removal efficiencies of compost, lava of activated carbon filters suggest that these techniques are of little or no use to remove methane from off- gases.

In the **third chapter**, the nitrous oxide emission dataset described in the previous chapter was used to evaluate a number of sampling strategies that had been used in previous studies to monitor such emissions. It was found that long-term sampling, be it grab-sampling or online monitoring, is indispensable to obtain an accurate and precise estimate of the yearly nitrous oxide emission from a plant. However, only online monitoring is able to provide insight in the diurnal dynamics of the emission. This chapter also demonstrates how to obtain the number of grab samples or online sampling periods that would have been required to obtain a sufficiently precise estimation of the emission. This makes it possible to balance effort and cost on the one hand, and precision of the estimate on the other hand.

The reasons behind the temporal variability of the nitrous oxide emission were investigated in the **fourth chapter**. The diurnal variability of the emission was compared with the diurnal variability of the concentration of the nitrogen species and oxygen in the reactors. The diurnal trend of the emission coincided with the diurnal trends of the nitrite and nitrate concentrations, but it could not be linked to fluctuations in the oxygen concentration. The effect of ammonium concentration and ammonium loading rate could not be unequivocally established. The diurnal variability of the emission was superimposed on a seasonal variability, but none of the investigated process variables could be linked to this long-term variability.

While chapter three and four focus on the emission of nitrous oxide, the **fifth chapter** elucidates the emission of methane during municipal wastewater treatment. To identify sinks and sources of methane on a municipal wastewater treatment plant and to establish the contribution of each unit process to the plant's total methane footprint, online monitoring data were combined with mass balances of methane over the different unit processes of the plant. This mass balance approach required measurements of dissolved methane, for which a sampling technique was developed. Sources of methane were the sewer and the unit processes related to the anaerobic digestion of primary and secondary sludge. The methane emission from the latter even superseded the carbon dioxide emission that is avoided by using the produced biogas in a combined heat and power system. The activated sludge tank appeared to be a sink for dissolved methane entering this tank, thus avoiding the emission of methane to the atmosphere.

Chapter six further investigated the biological conversion of methane in an activated sludge tank, using a simulation study. For this purpose, the well-established Activated Sludge Model nr. 1 was extended with growth and decay of methanotrophic organisms. The resulting model was implemented in Benchmark Simulation Model no. 1 to study the influence of process design and operating parameters on biological methane oxidation in a wastewater treatment plant. It was found that biological methane oxidation in an activated sludge tank can be optimized by accruate aeration control and at an aeration rate that is in agreement with optimal effluent quality. The deeper the aeration equipment is installed below the liquid surface, the more methane is converted for similar COD and nitrogen removal. In comparison with a plug flow reactor, a continuous stirred-tank reactor performas better with regard to methane conversion, but the perfomance of a plug flow reactor can be improved by avoiding excessive aeration at the entrance of the tank. High methane concentrations in the plant's influent benefit the conversion of methane. For the removal of methane from foul off gas, activated sludge has only limited potential as a bioscrubber.

To conclude, **chapter seven** offers some critical remarks on the implications of this thesis for monitoring and modelling greenhouse gas emissions. This chapter also contains some suggestions for future research and outlook to the effect of improving wastewater treatment technology on the extent of greenhouse gas emissions.

Samenvatting

Sinds 1750, het jaar dat doorgaans beschouwd wordt als het begin van de Industriële Revolutie, zijn de concentraties van koolstofdioxide, methaan en lachgas door toedoen van de mens respectievelijk gestegen met 40 %, 150 % en 20 % ten opzichte van de pre-industriële niveaus (IPCC, 2013a). Deze verhoogde concentraties veroorzaken klimaatverandering, met nadelige gevolgen voor het globale ecosysteem.

De behandeling van huishoudelijk afvalwater gaat gepaard met de emissies van broeikasgassen. Koolstofdioxide wordt rechtstreeks uitgestoten tijdens de microbiële omzetting van organische verbindingen. Dit is echter korte-cyclus koolstofdioxide en draagt dus niet bij tot de verhoogde concentraties aan koolstofdioxide in de atmosfeer. De behandeling van afvalwater verbruikt ook energie van fossiele herkomst en synthetische chemicaliën, met onrechtstreekse koolstofdioxide-emissies als gevolg. De processen die leiden tot de onrechtstreekse uitstoot van koolstofdioxide zijn bekend en de omvang van de emissie kan begroot worden met behulp van een levenscyclusanalyse. Een daling in het gebruik van fossiele energie en synthetische verbindingen zal uiteindelijk resulteren in een vermindering van de onrechtstreekse uitstoot van koolstofdioxide. De herkomst van de emissies van methaan en lachgas is nog niet geheel duidelijk. Beide gassen zijn krachtige broeikasgassen met een *global warming potential* van respectievelijk 34 en 298 CO_2-equivalenten. Dit gebrek aan inzicht staat een vermindering van deze emissies in de weg.

Deze thesis behandelt de emissie van lachgas en methaan uit rioolwaterzuiveringsinstallaties. Het uiteindelijke doel is om op de proppen te komen met richtlijnen om de uitstoot van deze gassen te verminderen, en om zo de klimaatvoetafdruk van waterzuivering in te perken. Dat vereist inzicht in de omvang van de emissies en in de relaties tussen de emissies enerzijds en de operationele omstandigheden in de zuivering anderzijds. Dit werk vervult de nood aan degelijke emissiedata door te voorzien in langetermijn, online emissiedata van een overdekte rioolwaterzuiveringsinstallatie. Het uiteindelijke resultaat is de meest precieze en accurate inschatting van broeikasgasemissies uit waterzuivering ooit. Gezien het belang van betrouwbare data werd hierbij bijzonder belang gehecht aan bemonsteringstechnieken (opgelost methaan) en bemonsteringsstrategieën (lachgas).

Het **eerste hoofdstuk** geeft een kort overzicht van de gekende manieren waarop methaan en lachgas gevormd worden in rioolwaterzuiveringsinstallaties. Het hoofdstuk gaat verder met een overzicht van het veronderstelde aandeel van methaan- en lachgasemissies uit waterzuivering in de totale anthropogene broeikasgasemissies. De manier waarop de emissie tegenwoordig wordt begroot, wordt ook besproken, zowel voor de emissie van een heel land als voor een individuële zuivering.

Het tweede hoofdstuk geeft de resultaten van een 16 maanden durende online meetcampagne waarbij lachgas- en meethaanemissies werden gemeten op een

rioolwaterzuiveringsinstallatie. Samen met de uitstoot van koolstofdioxide die werd berekend aan de hand van het elektriciteits- en aardgasverbruik van de zuivering, werden de gegevens over de uitstoot van methaan en lachgas gecombineerd tot een klimaatvoetafdruk van de zuivering. Zowel de emissie van lachgas als de emissie van methaan overstegen de indirecte uitstoot van koolstofdioxide die gepaard gaat met de consumptie van elektriciteit en aardgas van de zuivering. Verkennende metingen van de verwijderingsefficientie van methaan in compost-, lava- en actiefkoolfilters geven aan dat deze technieken weinig of geen zin hebben om methaan te verwijderen uit afgassen.

De lachgasdataset uit het vorige hoofdstuk wordt in het **derde hoofdstuk** gebruikt om een aantal bemonsteringsstrategieën uit vroegere studies te evalueren. Langetermijnbemonstering, of het nu gaat om steekmonsters of online bemonstering, blijkt de beste manier te zijn om tot een accurate en precieze inschatting te komen van de jaarlijkse lachgasemissie van een zuivering. Nochtans kan enkel online bemonstering inzicht verschaffen in de dagelijkse dynamiek van de van de emissie. Dit hoofdstuk toont verder hoe de precisie varieert in functie van het aantal steekmonsters of online bemonsteringsperiodes. Deze informatie toont hoeveel steekmonsters of online bemonsteringsperiodes nodig geweest zouden zijn om de gewenste precisie van de inschatting van de emissie te bereiken. Deze aanpak maakt het mogelijk om inspanningen en kosten enerzijds af te wegen tegen precisie van de inschatting anderzijds.

De oorzaken van de temporale variabiliteit van de lachgasemissie werden onderzocht in het **vierde hoofdstuk**. De dagelijkse variabiliteit van de lachgasemissie werd vergeleken met de dagelijkse variabiliteit van de stikstofconcentraties en de zuurstofconcentraties in de reactors. De dagelijkse trend van de emissie viel samen met de dagelijkse trends van de nitriet- en nitraatconcentraties, maar de trend van de emissie was niet gerelateerd aan de fluctuaties in de zuurstofconcentratie. Het effect van de ammoniumconcentratie en de ammoniumbelasting. De dagelijkse variabiliteit van de emissie was gesuperponeerd op een seizoenale variabiliteit, maar geen enkele van de onderzochte procesvariabelen bleek verband te houden met deze langetermijnvariabiliteit van de emissie.

Terwijl hoofdstuk drie en vier de uitstoot van lachgas behandelen, gaat het **vijfde hoofdstuk** over de uitstoot van methaan tijdens de behandeling van huishoudelijk afvalwater. Om de oorsprong en de bestemming van methaan in een rioolwaterzuiveringsinstallatie te identificeren en om de bijdrage van elk eenheidsproces aan de totale methaanvoetafdruk van de zuivering te bepalen werden online meetdata gecombineerd met massabalansen over de verschillende processen. Voor deze benadering met massabalansen was er nood aan metingen van opgelost methaan. Daarvoor werd in deze studie een meetmethode ontwikkeld. Bronnen van methaan waren de riolering en de eenheidsprocessen die dienen voor de anaerobe vergisting van primair en secundair slib. De methaanemissie van deze laatste onderdelen oversteg zelfs de koolstofdioxide-uitstoot die werd vermeden door het geproduceerde biogas te verbranden in een warmte-

krachtkoppeling. Opgelost methaan dat de actiefslibreactor binnenkwam bleek omgezet te worden waardoor de emissie van methaan werd gereduceerd.

De biologische omzetting van methaan in de actiefslibtank werd verder onderzocht in **hoofdstuk zes**. Hiervoor werd het wijdverspreide Activated Sludge Model nr. 1 uitgebreid met groei en sterfte van methanotrofe micro-organismen. Het resulterende model werd geïmplementeerd in Benchmark Simulation Model no. 1 om aan de hand van simulaties de invloed van ontwerp en bedrijfsvoering van een zuivering op de biologische methaanoxidatie na te gaan. Door een optimalisatie van de beluchting kan de conversie van methaan geoptimaliseerd worden. Bij deze optimale beluchting is ook de effluentkwaliteit optimaal. Hoe dieper de beluchtingsinstallatie zich onder het vloeistofoppervlak bevindt, hoe meer methaan verwijderd kan worden bij een gelijke CSV en stikstofverwijderingsefficientie. Een perfect gemengde tank is beter voor het omzetten van methaan dan een propstroomreactor, maar de methaanverwijdering in een propstroomreactor kan wel verbeterd worden door niet overtollig te beluchten aan de instroom. Hoge methaanconcentraties in het influent sijn gunstig voor de omzetting van methaan. De verwijdering van methaan uit afgas door het gas door actief slib te borrelen, is weinig efficiënt.

Tot slot bevat **hoofdstuk zeven** enkele kritische bemerkingen over de betekenis van deze thesis voor het bemonsteren en modelleren van broeikasgasemissies. Dit hoofdstuk reikt verder suggesties aan voor verder onderzoek en het biedt een blik op de toekomst met enkele speculaties over hoe verbetering van waterzuiveringstechnologie de omvang van de broeikasgasuitstoot zou kunnen verminderen.

1

General introduction

Climate change

On 27 September 2013, the Intergovernmental Panel on Climate Change (IPCC) accepted Working Group I's contribution to the Fifth Assessment Report. The IPCC's Fifth Assessment Report provides a clear view of the current state of scientific knowledge relevant to climate change (IPCC, 2013b). Working Group I's contribution to this report offers a comprehensive assessment of the physical science basis of climate change. It gives evidence for the increasing temperature of the atmosphere and the oceans, for a rise of sea levels, for shrinking ice sheets and glaciers, and increased atmospheric concentrations of the greenhouse gases carbon dioxide, methane and nitrous oxide. Since 1750, the year that commonly marks the start of the Industrial Revolution, the atmospheric concentrations of carbon dioxide, methane and nitrous oxide have risen about 40 %, 150 % and 20 %, respectively, above the pre-industrial levels due to human activity (IPCC, 2013b). These elevated greenhouse gas concentrations cause a growing radiative forcing, leading to an increase in atmospheric temperature with detrimental effects on Earth's ecosystems (IPCC, 2007c). According to the IPCC report "it is *extremely likely* [probability of 95 – 100 %] that human influence has been the dominant cause of the observed warming since the mid-20th century." Only by a substantial and sustained reduction of greenhouse gas emission can climate change be limited (IPCC, 2013b). This requires the identification of the sources of greenhouse gases and a thorough understanding of the mechanisms leading to their emission.

Overall objective

The present thesis discusses the emission of nitrous oxide and methane from municipal wastewater treatment plants. The final goal is to come up with guidelines to mitigate these emissions in order to decrease the climate footprint of wastewater treatment. This requires insight into the extent of the emissions and into the relationships between the emissions on the one hand and the plant's operational conditions on the other hand. This work fulfils the need for decent emission data by providing long-term, online data from a covered wastewater treatment plant that resulted in the most precise and accurate emission estimate from a full-scale plant to date. Given the importance of reliable data, particular attention is paid to sampling techniques (dissolved methane) and sampling strategies (nitrous oxide).

Greenhouse gases from wastewater treatment

Sewage treatment is one of the sources of anthropogenic greenhouse gas emissions. Carbon dioxide, methane and nitrous oxide are all emitted during the treatment of municipal wastewater. Nitrous oxide is the most potent of the three discussed GHGs. According to the IPCC's fourth assessment report, nitrous oxide has a global warming potential of 298 CO_2-equivalents over a 100 year time horizon, while methane has a global warming potential of 25 CO_2-equivalents over a 100 year time horizon (IPCC, 2007a). These numbers are used in chapter two and chapter five. At the time of writing this

introduction, however, the IPCC published its fifth assessment report with updated global warming potential numbers. Nitrous oxide still has a global warming potential of 298 CO_2-equivalents over a 100 year time horizon, but for methane, a new factor of 34 CO_2-equivalents over a 100 year time horizon is reported (IPCC, 2013b).

Carbon dioxide is emitted both directly and indirectly. Direct carbon dioxide emissions originate from the microbial respiration of organic matter in the aeration tanks. These emissions are generally considered as biogenic: the organic carbon in domestic wastewater can be traced back to the short-lived plants that serve as food for humans or as feed for livestock that is consumed by humans. During their lifetime, these plants assimilate carbon from the atmosphere. As such, the direct carbon dioxide emission from sewage treatment does not contribute to increased concentrations of carbon dioxide in the atmosphere. Yet, Law et al. (2013) reported that 4 – 14 % of the organic carbon in sewage influent is of fossil origin. If this carbon ends up in the atmosphere, e.g. after degradation by microorganisms in the activated sludge, it does indeed increase the carbon dioxide concentration in the atmosphere.
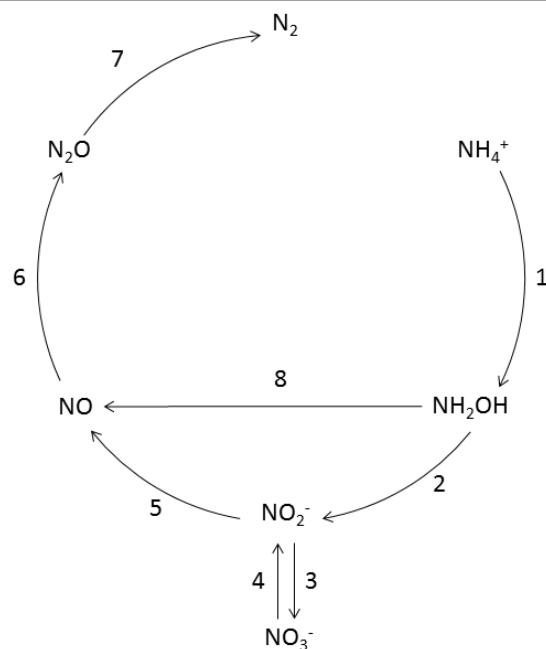
Sewage treatment also entails indirect carbon dioxide related to the plant's energy consumption and the dosing of fossil fuel derived chemicals such as flocculation and coagulation polymers, and methanol as electron donor for the denitrification process. This carbon dioxide originates from fossil carbon and as such its emission causes an increase of the carbon dioxide concentration in the atmosphere. The processes leading to the emission of indirect carbon dioxide are well understood, and the magnitude of the emission can be estimated by life cycle assessment. Any decrease in the consumption of fossil fuels and synthetic chemicals will eventually mitigate the indirect emission of carbon dioxide.

The second greenhouse gas, methane, is produced by methanogenic archaea when organic carbon is present in anaerobic conditions. Such conditions prevail in the sewer system, in particular in pressurized mains (Guisasola et al., 2008). Methane that is produced in sewers is either stripped from the sewage and emitted to the atmosphere through manholes and in pumping stations, or it remains dissolved and enters the WWTP with the influent. After entering the plant, the methane can again be stripped to the atmosphere or it can be biologically oxidised. Methane can also be produced on the plant itself, in particular during anaerobic digestion of sludge. In the latter case, methane is the intentional product of anaerobic digestion of sludge to biogas. This biogas is combusted in combined heat and power systems, and as such, anaerobic digestion of sludge contributes to a more sustainable and self-sufficient sewage treatment. However, methane can be emitted to the atmosphere from leakages, from sludge thickening and storage facilities, and as methane slip from the cogeneration unit. Methanogenesis is well understood but the quantification of the emission requires extensive monitoring.

Finally, the removal of nitrogen from wastewater can potentially lead to the production and emission of nitrous oxide, the most potent of the three greenhouse gases (Hanaki et al., 1992). In conventional activated sludge plants, nitrogen is removed via nitrification and subsequent denitrification (Figure 1.1). Nitrification consists of the oxidation of ammonium to nitrite via hydroxylamine by ammonia oxidizing bacteria (step 1 and 2 in Figure 1.1) and the oxidation of nitrite to nitrate by nitrite oxidizing bacteria (step 3 in Figure 1.1). Denitrification, the reduction of nitrate to nitrogen gas via nitrite, nitric oxide and nitrous oxide (step 4 to 7 in Figure 1.1), is usually performed by facultative aerobic heterotrophic bacteria, although some steps in this nitrogen reduction pathway are also performed by autotrophic nitrifying bacteria. Nitrite oxidizing bacteria have been observed to reduce nitrate to nitrite (step 4 in Figure 1.1) (Freitag et al., 1987), while ammonia oxidizing bacteria use the same enzymes as the heterotrophs to reduce nitrite to nitric oxide and nitrous oxide (step 4 to 6 in Figure 1.1) (Colliver and Stephenson, 2000).

Incomplete denitrification by heterotrophic denitrifiers can result in the accumulation and emission of nitrous oxide. It can also accumulate as a result of the denitrification pathway in ammonia oxidizing bacteria, since they lack the enzyme for the final denitrification step. Another pathway by which the ammonia oxidizing bacteria can produce nitrous oxide involves the biological oxidation of hydroxylamine to nitric oxide by hydroxylamine oxidoreductase (step 8 in Figure 1.1) or chemical decomposition of hydroxylamine to nitric oxide (Wunderlin et al., 2012). In its turn, nitric oxide is reduced to nitrous oxide (step 6 in Figure 1.1), but the exact mechanisms underlying this pathway are still debated, just as the relative importance of these two pathways in ammonia oxidizing bacteria (Schreiber et al., 2012).

Figure 1.1. Biological nitrogen conversions during nitrification and denitrification in a conventional wastewater treatment plant.

Step	Reaction	WWTP Process		Organism group		
1	Ammonium oxidation	Nitrifi-cation	Nitritation	Ammonia oxidizing bacteria		
2	Hydroxylamine oxidation to nitrite					
3	Nitrite oxidation		Nitratation	Nitrite oxidizing bacteria		
4	Nitrate reduction	Denitrification		Heterotr-ophic bacteria	Ammonia oxidizing bacteria	Nitrite oxidizing bacteria
5	Nitrite reduction					
6	Nitric oxide reduction					
7	Nitrous oxide reduction					
8	Hydroxylamine oxidation to nitric oxide			Ammonia oxidizing bacteria		

Nitrous oxide is not only produced biologically, but also chemically in a great number of chemical reactions involving nitroxyl (HNO), hydroxylamine (NH_2OH) and nitrite (NO_2^-) (Schreiber et al., 2012). Such reactions have been observed in soils (Van Cleemput, 1998) and in the atmosphere (Wiesen et al., 1995; Lammel and Cape, 1996). In wastewater treatment systems, such reactions could happen as well. In particular, chemical iron oxidation has been suggested as a possible cause for the formation of nitrous oxide in activated sludge (Kampschreur et al., 2011). The significance of chemical nitrous oxide formation in wastewater treatment has not yet been established.

Significance of wastewater treatment to total anthropogenic emissions

Methane and nitrous oxide contribute for 14.3 % and 7.9 % to the global anthropogenic greenhouse gas emissions, respectively, with the remainder consisting of carbon dioxide (76.7 %) and fluorinated gases (1.1 %) (IPCC, 2007b). The IPCC groups the global anthropogenic emissions in seven sectors, one of them being waste and wastewater. This sector as a whole is assumed to be responsible for 2.8 % of the global anthropogenic greenhouse gas emissions. In the USA, wastewater treatment and human sewage is reported to account for 0.1 % of the country's total anthropogenic greenhouse gas emission (EPA, 2013). In Australia, wastewater handling accounts for 13.3 % of the emissions from the IPCC's waste category, which equals about 0.4 % of the country's total greenhouse gas emission (Foley and Lant, 2008).

Considering methane and nitrous oxide separately, wastewater treatment accounts for 3.2 % of the global anthropogenic nitrous oxide emission (Kampschreur et al., 2009), while 4 – 5 % of the global anthropogenic methane emissions can be attributed to wastewater treatment (El-Fadel and Massoud, 2001; Conrad, 2009).

In comparison with other sectors such as agriculture, transportation and the electric power industry, the emissions of greenhouse gases from the wastewater treatment sector are modest. Nonetheless, as many industrial sectors, the wastewater treatment sector is committed to reducing its climate footprint. In that respect, it is worth noting that the emission of methane and nitrous oxide from wastewater treatment can exceed the emission of carbon dioxide related to electricity and chemicals consumption, transport etc. This warrants the focus on non-carbon dioxide emissions, despite their relatively small contribution to the total anthropogenic greenhouse gas emissions.

Estimation methods

Countrywide estimation
The abovementioned IPCC estimates of the wastewater treatment sector's contribution to the anthropogenic emissions are calculated using the 2006 IPCC Guidelines for National

Greenhouse Gas inventories (IPCC, 2006). As far as methane is concerned, the emission equals the amount of organic waste that is estimated to be treated multiplied by an emission factor minus the organics incorporated in the sludge and minus the methane that is recovered with combined heat and power. Depending on the availability of data, the emission factor can be tailored to reflect a country's wastewater treatment practices. In the Netherlands, the IPCC guidelines led to an emission factor of 0.007 kg CH_4 (kg $COD_{influent}$)$^{-1}$ for the water line and an additional 0.0015 kg CH_4 (kg $COD_{influent}$)$^{-1}$ for the sludge line (VROM, 2008). The VROM emission factor for the waterline includes the emission of methane that was formed in the sewer system and that is emitted upon entering the WWTP, although it is explicitly mentioned in the IPCC guidelines that **wastewater in closed underground sewers is not believed to be a significant source of CH_4** (IPCC, 2006). The exclusion of emissions from the sewers is rather surprising, since the abundance of organic material and the prevalence of anaerobic conditions in sewers are expected to give rise to methane production, as evidenced by Guisasola et al. (2008). Furthermore, the production of methane often accompanies the production of hydrogen sulphide, which is a widely recognized problem in sewers.

For nitrous oxide, direct emissions from nitrification and denitrification at wastewater treatment plants are considered minor in comparison with indirect emission from wastewater after discharge. Only for countries that have predominantly advanced centralized wastewater treatment plants with nitrification and denitrification steps, direct emissions need to be estimated (IPCC, 2006). For the indirect emission, a default emission factor of 0.005 (0.0005 – 0.25) kg N_2O-N kg^{-1} N discharged with the effluent is used, with the latter to be calculated from population protein intake, non-consumed protein and industrial waste protein. For the direct emission from advanced centralized wastewater treatment plants, the IPCC uses a default factor of 3.2 g N_2O person^{-1} year^{-1}, based on a single study by Czepiel et al. (1995) in which the nitrous oxide emission from a municipal plant not designed for nitrogen removal were measured using weekly grab samples over a period of 15 weeks. Assuming a protein intake of 100 g person^{-1} day^{-1} and 0.16 g N g^{-1} protein, Kampschreur et al. (2009) converted this IPCC emission factor into a ratio of 0.035 g N_2O N k^{-1} $TKN_{influent}$. As with methane, the IPCC does not consider sewers as a source of nitrous oxide. A recent study, however, reported a nitrous oxide emission of 1.7 g N_2O person^{-1} year^{-1}, which is about half of the emission factor used for WWTPs (Short et al., 2014).

As a number of studies already demonstrated, these fixed emission factors are problematic because they ignore the variability that many studies have exposed (Kampschreur et al., 2009; Foley et al., 2010; Law et al., 2012b; Aboobakar et al., 2014). In order to know to what extent wastewater treatment contributes to the global anthropogenic greenhouse gas emission, measurements of greenhouse gas emissions from full-scale wastewater treatment plants are indispensable.

Plantwide estimation

Obtaining accurate data of methane and nitrous oxide emissions from wastewater treatment is far from trivial due to the emission's spatial and temporal variability. Gaseous compounds are emitted dispersedly from the water surface of activated sludge tanks. Only if such tanks are completely covered and the off-gas is transported away from the tank through a duct, is it possible to obtain an accurate and precise estimate of the instantaneous mass flow rate, provided that the concentration and volumetric gas flow rate can be adequately measured. Nitrous oxide measurements from covered plants have been reported (e.g. Fred et al. (2009)) but most WWTPs are not covered. In that case, researchers have to resort to floating gas hoods (e.g. Ahn et al. (2010a); Foley et al. (2010); Desloover et al. (2011)), but these only cover a minor part of the reactor surface, raising concerns about the representativeness of the measurement. Indeed, the gaseous emissions from a bioreactor can be very heterogeneous across its water surface. In aerated zones, for instance, the fugitive compounds will be actively stripped from the liquid while the emission from non-aerated zones will be lower because in these zones mass transfer is governed by diffusion only. Especially in the case of surface aeration it is very hard to use floating hoods since the major part of the emission originates from the aerator zone while it is impossible to use such a device in the immediate vicinity of a surface aerator (Ye et al., 2014). In general, hydrodynamic effects in the reactor can cause concentration profiles of oxygen, COD and N-species (Gresch et al., 2010; Le Moullec et al., 2011). Particularly in plug flow reactors, such concentration profiles can be very pronounced.

Methane is also emitted at other locations than activated sludge tanks. Obviously, a sewer network is not an airtight system, causing methane to escape to the atmosphere via manholes, lids, pumping stations etc. Emissions from anaerobic sludge treatment are dispersed. Possible sources are leaks, dewatering and uncovered storage of digester effluent, maintenance, transport, incomplete combustion etc. From a practical point of view, such dispersed sources are hard to measure.

Other effects besides climate change

Emissions of methane and nitrous oxide should be avoided because they contribute to climate change, but there are a number of other environmental issues related to the emission of these gases as well.

Both methane and nitrous oxide affect stratospheric ozone levels (Portmann et al., 2012). Since the successful curbing of the use of halocarbons (CFCs) as a result of the Montreal protocol (1987), nitrous oxide has even become the single most important ozone depleting substance that is emitted to the atmosphere and it is expected to remain so well into the 21st century (Ravishankara et al., 2009).

The emission of nitrous oxide has also been suggested as an early warning signal of upset nitrification (Burgess et al., 2002a; Burgess et al., 2002b; Wunderlin et al., 2013b). Sivret et al. (2008) developed an aeration control concept using the nitrous oxide concentration in the off-gas of an activated sludge tank as a surrogate for the inhibition dynamics of the autotrophic nitrifiers. According to these studies, the emission of nitrous oxide goes hand in hand with increased ammonium concentrations in the effluent, which is an environmental problem by itself.

The anaerobic digestion of primary and secondary sludge produces biogas. By burning this biogas in a combined heat and power unit, WWTPs recover energy from the wastewater. Any biogas that is emitted to the atmosphere during the storage and handling of sludge represents a loss of energy and compromises the sustainability of anaerobic digestion.

Outline of the thesis

The **second chapter** of this thesis reports the results of the first long-term, on-line monitoring campaign measuring nitrous oxide and methane emissions from a municipal wastewater treatment plant. The emissions were recorded over a period of sixteen months. The indirect emission of carbon dioxide was calculated from the plant's consumption of electricity and natural gas from the grid. The acquired data enabled the construction of the plant's carbon footprint.

The **third chapter** focuses on the effect of monitoring strategies on the accuracy and precision of the estimate of the true nitrous oxide emission. The long-term dataset of continuous nitrous oxide emission measurements was used to evaluate different sampling strategies that had been used in previous studies to monitor these emissions. As a guideline to help balancing cost and precision, a method is presented to obtain the number of grab samples or online sampling periods that would have been required to obtain a sufficiently precise estimation of the emission.

Chapter four investigates the relationships between the diurnal and seasonal variability of the nitrous oxide emission on the one hand, and the plant's operational variables on the other hand. Numerous lab-scale and a number of full-scale studies came up with process conditions that are assumed to induce the production and emission of nitrous oxide. These findings were confronted with data from the first long-term, on-line monitoring campaign on a full-scale WWTP. The focus is on the correlation between the nitrogen species and the emission, and on the effect of the aeration regime.

The objective of **chapter five** is to further elucidate the emission of methane during municipal wastewater treatment. For each unit process on the plant, a methane mass balance was made. The combination of the methane mass balances with long-term monitoring data of the plant's total emission made it possible to identify sinks and sources of methane and to estimate their share in the plant's carbon footprint. The methane

emission associated with the anaerobic digestion of primary and secondary sludge (mainly related to sludge storage) superseded the carbon dioxide emission that is avoided by using the resulting biogas in a combined heat and power system. Also the sewer was found to be a significant source of methane, while activated sludge was found to be a sink for methane.

The latter observation motivated the study that the **sixth chapter** describes. The methane oxidizing potential of activated sludge was explored in a simulation study. For this aim, the widespread Activated Sludge Model no. 1 was extended with growth and decay of methanotrophic biomass. The resulting model was implemented in Benchmark Simulation Model no. 1 to study the influence of process design and operating parameters on biological methane oxidation in a wastewater treatment plant.

Finally, **chapter seven** offers some final considerations and conclusions, reaching out to the broader research field involved in investigating greenhouse gas emissions from wastewater treatment. The chapter discusses the need for adequate monitoring and the implications of the present work for modelling of greenhouse gas emissions from wastewater treatment. Some recommendations for future research are presented, as well as an outlook to the future evolution of wastewater treatment and the implications for future greenhouse gas emissions.

2

**Methane and nitrous oxide emissions from municipal
wastewater treatment – results from a long-term study**

Abstract

Methane and nitrous oxide emissions from a fully covered municipal wastewater treatment plant were measured on-line during sixteen months. At the plant under study, nitrous oxide contributed for three quarters to the plant's carbon footprint, while the methane emission was slightly larger than the indirect carbon dioxide emission related to the plant's electricity and natural gas consumption. This contrasted with two other wastewater treatment plants, where more than 80 % of the carbon footprint came from the indirect carbon dioxide emission. The nitrous oxide emission exhibited a seasonal dynamic, of which the cause remains unclear. Three types of air filters where investigated with regard to their effectiveness to remove methane from the off-gas.

Published as

Introduction

Municipal wastewater treatment plants are emission sources of the greenhouse gases methane (CH_4), nitrous oxide (N_2O) and carbon dioxide (CO_2) (Hofman et al., 2011). Carbon dioxide emissions contribute to climate change only insofar as they originate from the combustion of fossil fuels to generate the electricity that is required for the operation of the plant. Nitrous oxide is emitted during biological nitrogen removal from wastewater, through nitrification and subsequent denitrification. In both processes, nitrous oxide is formed, but a detailed understanding of the factors that induce nitrous oxide emissions is currently missing (Law et al., 2012b). Since nitrous oxide has a greenhouse gas potential of approximately 300 times that of carbon dioxide (IPCC, 2007a), it can potentially contribute heavily to a wastewater treatment plant's carbon footprint. Methane has a global warming potential of 25 CO_2-equivalents (IPCC, 2007a). It is emitted from those parts of the plant where anaerobic conditions prevail, such as the unit processes related to the anaerobic sludge treatment, but methane is also stripped from the sewage after it enters the plant (Guisasola et al., 2008).

The present study is the first long-term, on-line monitoring campaign measuring nitrous oxide and methane emissions from a municipal wastewater treatment plant. The objectives of this study were to quantify the emissions of methane and nitrous oxide and to calculate the contribution of methane, nitrous oxide and indirect carbon dioxide to the carbon footprint of a municipal wastewater treatment plant. Three types of air filters were tested as a possible mitigation option for methane emissions.

Materials and methods

Field site description

The monitoring campaign was performed at Kralingseveer WWTP, located in the municipality of Capelle aan den IJssel, near Rotterdam, the Netherlands (51° 54' 30" N 4° 32' 35" E). The plant treats the domestic wastewater of 360,000 population equivalents (PE). The excess sludge of the plant is treated in an anaerobic digester. The resulting biogas is used in a combined heat and power installation that fulfils about 60 % of the energy requirements of the plant. The remainder of the plant's energy requirements is met by electricity and natural gas from the grid.

The plant comprises two activated sludge systems: a plug flow reactor, and two parallel carousel reactors. After the wastewater has passed through a primary settling tank and a selector tank, where it is mixed with the return sludge, the mixed liquor enters the plug flow reactor. First, the mixed liquor passes through non-aerated, anoxic zone for denitrification, followed by an aerated zone for nitrification. From the aerated zone, the mixed liquor is recycled to the anoxic zone with a recycle ratio of three, while the remainder passes on to the two parallel carousel reactors. After passing through the

carousel reactors, the mixed liquor flows to the secondary settlers. A full description of the wastewater treatment plant under study is provided in Daelman et al. (2012, chapter 5 in this thesis).

Measurements of the methane removal efficiency of air filter systems
Three types of air filters on various wastewater facilities in the Netherlands were investigated with regard to their effectiveness to remove methane from the off-gas stream. At Kralingseveer WWTP, a compost filter treats the off-gas from the headworks, the primary settler, the storage tank for primary sludge, the buffer storage tank for digester effluent, the centrifuges and the storage tank for dewatered sludge. At Kortenoord WWTP, two lava filters treat the off-gas from the headworks and from the sludge dewatering centrifuges. At the Maassluis sewage pumping station, the off-gases are treated by a lava filter and a subsequent activated carbon filter, but only the activated carbon filter was accessible.

The methane concentration in the off-gas streams was determined by filling a gas bag and analysing its content with a gas chromatograph equipped with a flame ionization detector. The gas flow rates were determined with a hot-wire anemometer.

For the compost filter at Kralingseveer WWTP and the lava filters at Kortenoord WWTP, the ingoing and outgoing air flow rates were not equal due to the infiltration of false air. Therefore, the methane removal efficiency of the filters could not be calculated by merely measuring concentration. Instead, the methane flux was calculated by multiplying the respective air flow rates with the respective methane concentrations in the air flow. The difference between the ingoing and outgoing methane fluxes, divided by the ingoing methane flux, yielded the methane removal efficiency. For the activated carbon filter at the pumping station, the air flow rate could not be measured, but since no false air was entering the system, the methane removal efficiency was calculated by dividing the difference between the ingoing and outgoing concentration by the ingoing concentration.

Quantifying greenhouse gas emissions
All unit processes at Kralingseveer WWTP are covered, except for the secondary clarifiers. The air that comes from the compost filter is blown into the headspace of the carousel reactors. As a result, the off-gas from the carousel reactor also comprises the off-gas from the headworks, the primary settler, the storage tank for primary sludge, the buffer storage tank for digester effluent, the centrifuges and the storage tank for dewatered sludge. The off-gas from the plug flow reactor and from the two parallel carousel reactors is sent to an ozone washer for disinfection.

From 14 October 2010 until 26 January 2012, gas was withdrawn from the off-gas pipes going to the ozone washer. The gas was directed to a Servomex 4900 infrared gas analyser, measuring on-line the methane and nitrous oxide concentration in the off-gas flow. Every

minute, the methane and nitrous oxide concentrations were logged. The gas flow rates in the off-gas pipes were measured weekly using a hot wire anemometer. Since the blowers of the off-gas collection system are operated at constant power, the gas flow rates are constant. By multiplying the measured concentrations with the prevailing flow rate in the off-gas pipes, the methane and nitrous oxide fluxes from the plug flow reactor and the carousel were calculated.

The indirect carbon dioxide emission of the plant was calculated using the amount of electricity and natural gas that the plant consumed from the grid during the monitoring period to complement the energy that is recovered from the biogas in the cogeneration plant. The electricity consumption was multiplied with the amount of carbon dioxide that is emitted during the production of electricity using the typical Dutch mix of energy resources. According to the International Energy Agency, electricity production in the Netherlands emits $0.395 \text{ kg } CO_2 \cdot kWh^{-1}$ (IEA, 2010). The natural gas consumption was multiplied with an emission factor of $1.8 \text{ kg } CO_2 \cdot Nm^{-3}$ (Heslinga and van Harmelen, 2006).

Results

Magnitude of the emission

Table 2.1 summarizes the amount of greenhouse gas that is emitted from the plant. To allow comparison with the emission from other wastewater treatment plants and other studies, the emission values were normalized by magnitude of the population served and by the average amount of wastewater treated during the monitoring period. Typically, the methane and nitrous oxide emission is also expressed relative to the incoming COD and nitrogen, respectively. For each day when the incoming COD and incoming nitrogen data were available from the plant's lab analysis, the daily methane emission was divided by the daily COD and the daily nitrous oxide emission was divided by the nitrogen load. Lab analyses were available on a weekly basis, resulting in 78 emission factors for each gas. For this study, the average emission factors were $11 \text{g } CH_4 \cdot (\text{kg } COD_{influent})^{-1}$, or 1.1 % of the incoming COD, and $28 \text{ g } N_2O\text{-}N \cdot (\text{kg } TKN_{influent})^{-1}$, or 2.8 % of the incoming nitrogen.

Table 2.1. Absolute and normalized emission values of methane and nitrous oxide, and the indirect carbon dioxide emission related to electricity and natural gas consumption. Conversions to CO$_2$-equivalents are according to the IPCC (2007a) emission factors.

	Methane	Nitrous oxide	Carbon dioxide
ton.y^{-1}	107	52	1,622
ton CO$_2$-eq..y^{-1}	2,687	15,609	1,622
kg (CH$_4$, N$_2$O, CO$_2$ respectively).PE^{-1}.y^{-1}	0.39	0.19	5.8
kg CO$_2$-eq..PE^{-1}.y^{-1}	9.6	56	5.8
g.(m^3 wastewater)$^{-1}$	3.3	1.6	50
g.CO$_2$-eq..(m^3 wastewater)$^{-1}$	83	483	50

The monthly averaged methane emission from Kralingseveer WWTP is shown in Figure 2.1A, together with the atmospheric temperature. The methane emission varies between 211 and 429 kg CH$_4$.d^{-1}. At first sight, the emission appears the highest during the summer months (June and July), suggesting an effect of temperature, but there was no meaningful correlation between daily average methane emission and temperature (R^2 = 0.18).

Figure 2.1B summarizes the monthly averages of the nitrous oxide, as well as the wastewater temperature measured in the carousel reactors. Since nitrous oxide is produced in the mixed liquor, the water temperature is more relevant than the atmospheric temperature. The nitrous oxide emission exhibits a seasonal dynamic, but this dynamic lags two to three months behind the water temperature dynamic. In October and November 2010 there is almost no nitrous oxide emitted at all. When the water temperature drops below 15 °C in December 2010, the emissions starts to increase. When the temperature reaches its minimum in January 2011, the emission has increased to a monthly average of 39 kg N$_2$O-N.d^{-1}. When the temperature starts to go up again in February 2011, the emission keeps on increasing to reach a maximum monthly average of 271 kg N$_2$O-N.d^{-1} in March 2011. Only from April onwards, when the temperature climbs above 15 °C again, the emission starts to decrease again. In the autumn and early winter of 2011 – 2012, it is hard to distinguish any trend.
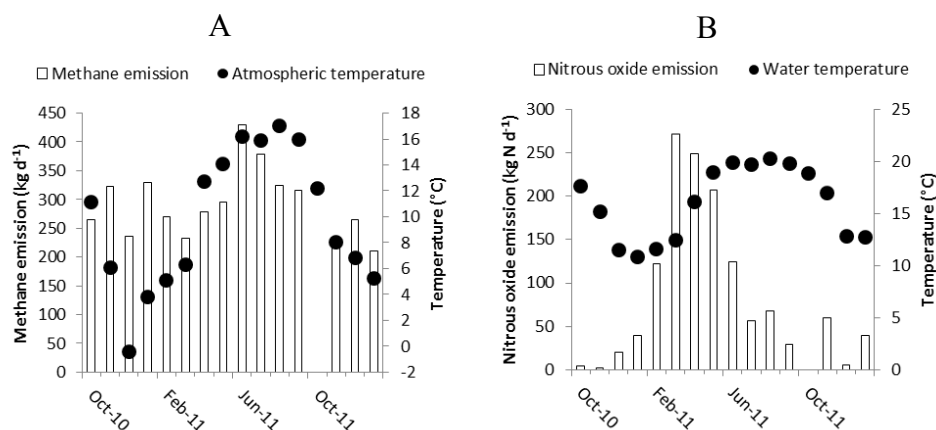
Figure 2.1. Monthly averaged methane emission with atmospheric temperature (A) and monthly average nitrous oxide emission with water temperature (B).

Carbon footprint

Figure 2.2 displays the share of each of the three gases in the plant's total greenhouse gas emission. At Kralingseveer WWTP, nitrous oxide dominated the greenhouse gas footprint. The methane emission amounted to 13.5% while the share of the nitrous oxide emission was 78.4 %. Both greenhouse gases contributed more to the overall plant footprint than the carbon dioxide emission (8.1%) related to the plant's electricity and natural gas consumption.
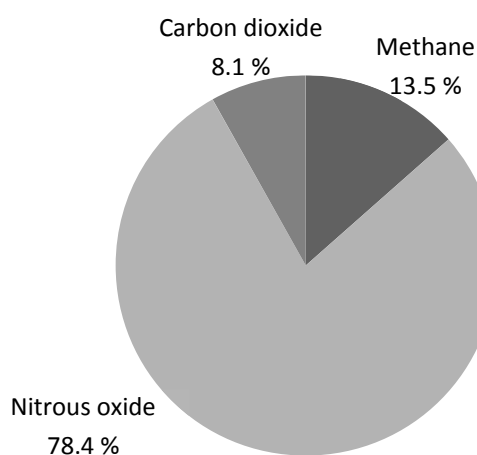

Figure 2.2. Contribution of the three greenhouse gases to the plant's total greenhouse gas footprint, expressed as CO_2-equivalents. The carbon dioxide emission comprises the emissions related to electricity and natural gas consumption.

The only other study that actually measured the complete climate footprint of a WWTP is STOWA (2010). Those results are shown in Table 2.2. In this study, the emissions from two plants, Kortenoord and Papendrecht, were measured during one week, and for a third plant, Kralingseveer (the same plant as the one in the present study), the emissions were measured during one week in October and during one week in February to take into account the effect of temperature.

For the plants of Papendrecht and Kortenoord, the indirect carbon dioxide contributes most to the carbon footprint, 81 % and 84 %, respectively. When expressed in terms of population equivalents, the plant of Kralingseveer (Table 2.1) emits about twice as much methane, 60 to 90 times more nitrous oxide and about four times less carbon dioxide than the plants of Kortenoord and Papendrecht (Table 2.2).

Table 2.2. Normalized emission (kg.PE^{-1}.y^{-1}) and relative contribution to the carbon footprint (%) for the three plants investigated in STOWA (2010).

	Methane		Nitrous oxide		Carbon dioxide	
Papendrecht	0.212	17 %	0.002	2 %	25.4	81 %
Kortenoord	0.153	13 %	0.003	3 %	24.0	84 %
Kralingseveer – October 2008	0.438	36 %	0.022	21 %	12.8	43 %
Kralingseveer – February 2009	0.230	5 %	0.222	88 %	10.4	7 %

Effectiveness of air filters for methane removal

Table 2.3 provides an overview of the methane removal efficiency of three types of air treatment filters. The lava filter at the sludge treatment facility of Kortenoord WWTP and the activated carbon filter at the sewage pumping station only remove 4 % of the methane in the off-gas, while the compost filter at Kralingseveer WWTP and the lava filter at the headworks of Kortenoord WWTP remove 14 % and 25 %, respectively.

Table 2.3. Methane removal efficiency of three types of air filters.

Filter type	Location	# measurements	Removal efficiency
Compost	Kralingseveer WWTP	4	14 % ± 48% *
Lava	Kortenoord headworks	1	25 %
Lava	Kortenoord sludge treatment	1	4 %
Activated carbon	Sewage pumping station	1	4 %

* mean ± standard deviation

Discussion

Emission of nitrous oxide

As far as nitrous oxide is concerned, the IPCC (2006) proposes an emission factor of 3.2 g N_2O-N.PE^{-1}, which amounts to 0.35 g N_2O-N.(kg $TKN_{influent}$)$^{-1}$ for developed countries, characterized by a high protein intake (Kampschreur et al., 2009). This emission factor, which is based on a single study by Czepiel et al. (1995), is eighty times lower than the 28 g N_2O-N.(kg $TKN_{influent}$)$^{-1}$, i.e. 2.8 % of the incoming nitrogen, of the present study. However, the value from this study falls within the wide range of emission factors from previous studies. A review study of Kampschreur et al. (2009) listed emission factors ranging from 0.001% to 14.6 % of the in-coming nitrogen. A wide variety in emission factors was also found in a national nitrous oxide measurement survey in the USA by Ahn et al. (2010b), who found values ranging from 0.01% to 1.8 % of incoming nitrogen. In a survey of seven WWTPs in Australia by Foley et al. (2010), emission factors of 0.06% to 25.3 % of nitrogen denitrified were found. The wide variability between the normalized nitrous oxide emissions from the different plants that were monitored in STOWA (2010) (Table 2.2) and the normalized emission that was determined during the present study (Table 2.1) demonstrates again the meaninglessness of the use of a single emission factor, as also pleaded by Kampschreur et al. (2009) and Ahn et al. (2010b). Furthermore, the temporal variability of the nitrous oxide emission (Figure 2.1B) also sheds a light on how short term monitoring studies such as the one-week campaigns by STOWA (2010) or the one-day campaigns of Ahn et al. (2010b) introduce a high variability as well. If the present study had been performed during only one week October or November 2010, the estimated emission would have been less than ten times lower than the present estimate, while it would have been almost thirty times higher if the monitoring would have been performed in March 2011.

The seasonal pattern of the nitrous oxide emission in the present study is in agreement with the results from STOWA (2010), i.e. high emissions during the monitoring week in February 2009, and low emissions during the monitoring week in October 2008. However, according to Figure 2.1A, there is a time lag of two to three months between the emissions and the water temperature. The observation that the emission increases with decreasing temperature may be related to the change of the sludge residence time (SRT). When temperature drops, the nitrification rate of the microorganisms in the activated sludge decreases. The ammonia conversion efficiency of the plant remained constant over the entire monitoring period (data not shown). With a lower nitrification rate during winter, a constant ammonia conversion over all seasons can only be achieved by prolonging the SRT. In which way exactly a longer SRT relates to higher nitrous oxide emissions remains unclear, and should be investigated in further research.

At Kralingseveer, the nitrous oxide emission per population equivalent and the share of nitrous oxide in the total climate footprint are higher than for Papendrecht and Kortenoord plants of the study by STOWA (2010). Since those two plants were only monitored during one week each, an interpretation of the emission data is delicate, especially taking into account the seasonal variability that was found at the Kralingseveer plant. However, the higher emission of the Kralingseveer plant may be attributed to the higher average sludge nitrogen loading rate of Kralingseveer (0.019 kg N.kg $MLSS^{-1}.d^{-1}$) in comparison with the other two plants (0.010 and 0.012 kg N.kg $MLSS^{-1}.d^{-1}$, STOWA (2010)), since high nitrogen conversion rates are assumed to induce nitrous oxide emissions (Law et al., 2012b).

Emission of methane

The IPCC calculates the methane emission using the maximum amount of methane that can be produced from a given quantity of organics and a correction factor indicating the extent to which this methane producing capacity is realized in each type of treatment and discharge pathway and system (IPCC, 2006). For the Netherlands, the implementation of this calculation method results in a methane emission factor of 8.5 g CH_4.(kg $COD_{influent}$)$^{-1}$ for plants with anaerobic sludge treatment, which is 23 % lower than the 11 g CH_4.(kg $COD_{influent}$)$^{-1}$ of Kralingseveer WWTP. Other data about methane emissions are scarce. Only two peer-reviewed studies about the topic were found: Czepiel et al. (1993) and Wang et al. (2011a), with emission factors of 1.6 g CH_4.(kg $BOD_{influent}$)$^{-1}$ and 0.8 g CH_4.(kg $COD_{influent}$)$^{-1}$, respectively, which is lower than the methane emission of Kralingseveer. Also the plants of Papendrecht and Kortenoord had lower emissions than Kralingseveer (0.212 and 0.153 kg.PE^{-1}.y^{-1}, respectively, versus 0.39 kg.PE^{-1}.y^{-1}. Cf. Table 2.1 and Table 2.2). Of all these plants, Kralingseveer WWTP is the only one that has anaerobic sludge treatment.

On the one hand the presence of anaerobic sludge treatment implies that more methane will be emitted at WWTPs with sludge digestion, since the anaerobic sludge digestion facility causes methane emissions (Daelman et al., 2012, Chapter 5 in this thesis). On the other hand, the indirect carbon dioxide emission per population equivalent is lower at a plant with anaerobic sludge digestion since it produces biogas that enables the plant to be (partially) self-sufficient concerning its electricity demand. On the contrary, plants that do not produce biogas by anaerobic sludge digestion consume relatively more electricity, explaining the higher carbon dioxide emissions of these plants. This observation suggests that in order to judge the sustainability of biogas production from wastewater sludge, one should consider the trade-off between the emissions of methane on the one hand and the avoidance of carbon dioxide emission by utilizing biogas on the other hand. For completeness' sake, also the way in which the dewatered digestate or the undigested dewatered sludge is processed after it leaves the plant should be taken into account.

Effectiveness of air filters for methane removal from off-gas streams
In the Netherlands, many wastewater treatment plants and sewage pumping stations dispose of air filter systems to get rid of odorous compounds in the off-gas streams from the headworks and sludge treatment. Although these systems are not designed to remove methane from the off-gases, this study investigated the possible use of such filters to mitigate methane emissions.

At first, the data suggest that common types of air filters are not or only to a small extent able to remove methane from the gas stream. Nevertheless, the variability of the efficiency data from several measurements of the same filter and the variability between different filter types is high, and the number of measurements are limited, making the results in Table 2.3 delicate to interpret. Therefore these measurements should be considered as exploratory. For instance, the difference between ingoing and outgoing methane flux may be due to temporal variation of the flux between the respective measurements, rather than to a different methane removal efficiency. Still, the methane removal efficiency may depend on operational variables, such as concentration differences in the gas stream to be treated, or the temperature in the filter. Further research may bring conclusive proof of the methane removal efficiency of common air treatment filters, and the effect of operational conditions.

Conclusions

- This long-term study of greenhouse gas emissions from a wastewater treatment plant confirms the shortcoming of fixed emission factors to estimate the emissions.
- Both the methane and nitrous oxide emissions at the Kralingseveer wastewater treatment plant under study exceeded the plant's indirect carbon dioxide emission related to electricity consumption.

- The plant under study showed a relatively high methane emission in comparison with other plants, which was related to the presence of anaerobic sludge treatment.
- The nitrous oxide emission showed a seasonal dynamic, which is yet not fully understood.
- Exploratory results suggest that compost, lava of activated carbon filters remove methane from off-gas only to a small extent or not at all.

Acknowledgements

3

Influence of sampling strategies on the estimated nitrous oxide emission from wastewater treatment plants

Chapter 3

Abstract

In the last few years, the emission of nitrous oxide from wastewater treatment plants hasbecome a topic of increased interest, given its considerable impact on the overall climatefootprint of wastewater treatment plants. Various sampling strategies to estimate nitrousoxide emission from wastewater treatment plants have been applied in different studies.The present study addresses the influence of sampling strategies on the estimated emissionby analysing the variability of an extensive dataset of nitrous oxide emissionsresulting from a long-term online monitoring campaign at a full-scale municipal wastewatertreatment plant. It is shown that short-term sampling is inadequate to accuratelyestimate the average nitrous oxide emissions from a particular wastewater treatmentplant, while online monitoring is indispensable to capture the short-term variability(diurnal dynamics).

Published as

Introduction

Wastewater treatment plants (WWTPs) are known as emission sources of the greenhouse gas nitrous oxide (N_2O) (Hanaki et al., 1992; Kampschreur et al., 2009; Desloover et al., 2012; Law et al., 2012b). Nitrous oxide is expected to be emitted during biological nitrogen removal from wastewater, through nitrification and subsequent denitrification (Kampschreur et al., 2009). In one study, nitrous oxide was found to make up 88 % of the emitted carbon dioxide equivalents of a particular WWTP (STOWA, 2010), while Daelman et al. (2013, chapter 2 in this thesis) established the share of nitrous oxide at the same WWTP as 78 % based on the long-term, online monitoring campaign that yielded the dataset that is used in the present study. Since nitrous oxide has a global warming potential of 298 CO_2-equivalents over a 100 year time horizon, even a low emission contributes significantly to a WWTP's greenhouse gas footprint (IPCC, 2007a).

Table 3.1 provides an overview of the reported monitoring studies of full-scale municipal wastewater treatment plants and the applied sampling strategies. The various strategies differ in aspects such as the duration of the sampling campaign (ranging from a single day to 1.5 years) and the sampling frequency (ranging from a single grab sample to online sampling). The nitrous oxide emissions obtained from these studies display a huge variability, both over time and between different WWTPs. In their review, Kampschreur et al. (2009) reported nitrous oxide emissions ranging from 0 to 14.6 % of the nitrogen load. During a study in the Netherlands (STOWA, 2010), the emission of nitrous oxide was monitored at three WWTPs. Two plants were monitored during one week each, while the third plant was monitored during one week in October 2008 and one week in September 2009. The emission showed a variability of 0.040 to 6.1 % of the incoming nitrogen between the WWTPs, and of 0.42 to 6.1 % between October and February respectively, for the same WWTP. Ahn et al. (2010b) also demonstrated the short-term variability of nitrous oxide emission over a single day.

The influence of different sampling strategies on the reported nitrous oxide emission of different studies has not been assessed up till now. It can, however, be reasonably expected that the sampling strategy will influence the estimated total nitrous oxide emission from such a dynamic process. In the field of wastewater treatment, the challenge of monitoring dynamic phenomena has also been addressed by Ort and Gujer (2006), Ort et al. (2010a) and Ort et al. (2010b) in the case of pharmaceuticals and personal care products in sewer systems, while Gevaert et al. (2009) discussed the monitoring of the substances on the priority list of the European Water Framework Directive. In these studies, monitoring scenarios are tested by applying different sampling modes to a simulated dataset that results from dynamic models describing the presence of pollutants in sewers and water bodies. In the present study, a similar approach is taken, but instead of using simulated data, this contribution compares and evaluates the reported monitoring strategies for nitrous oxide

emissions by applying strategies from previous studies to the dataset of a long-term, online measuring campaign.

The objective of this study is to expose the caveats to be expected during monitoring of nitrous oxide emission from wastewater treatment by illustrating the effect of sampling strategies on the estimation of the emission. These days, numerous research groups are engaging in sampling campaigns in order to quantify the nitrous oxide emission and to identify the mechanisms behind it. Often, the complexity and the cost of sampling limit these campaigns to a small number of samples or to a short measurement period. The present study demonstrates that results obtained from such limited measurements lead to unreliable estimates of the amount of nitrous oxide emitted.

Table 3.1. Overview of sampling strategies for the determination of nitrous oxide emissions from full-scale WWTPs, applied in previous studies.

Study	Sampling strategy (frequency and duration)
Czepiel et al. (1995)	Weekly grab samples from one WWTP during 15 weeks
Wicht and Beier (1995)	Single grab samples from 25 WWTPs
Sümer et al. (1995)	Biweekly grab samples from one WWTP over one year
Kimochi et al. (1998)	Online over four 2 hour aeration cycles of a single WWTP
Sommer et al. (1998)	(Bi)weekly grab samples from one WWTP over 1.5 years
Peu et al. (2006)	Online over one / three weeks from two WWTPs
STOWA (2010)	2 WWTPs: online over one week 1 WWTP: online over one week in autumn and one week in winter
Ahn et al. (2010a); Ahn et al. (2010b)	Online over 24 h at 12 different WWTPs
Foley et al. (2010)	Grab samples taken in the morning and afternoon of two consecutive days for 7 WWTP

Materials and methods

The long-term, online dataset

To assess the influence of monitoring strategies on the estimated nitrous oxide emissions from WWTPs, several monitoring scenarios have been applied to an extensive dataset of a long-term online monitoring campaign at a completely covered WWTP. The nitrous oxide mass flow rate was calculated from measurement data of the concentration and volumetric gas flow rate of the off-gas coming from the covered activated sludge tanks. The sampling protocol is added as supplementary material. The dataset contained 23.280 data points of the total nitrous oxide emission from the plant and covered the entire measurement period from October 14, 2010 to January 26, 2012, with a month-long interruption in October 2011 due to a technical failure. In total, the dataset covered 416 days, one data point being available for every 25 minutes during this period. By integrating all the data points of the entire dataset, an estimate of the plant's total emission was obtained: 91 kg N_2O-N d^{-1}. This value is further referred to as the true average emission.

The emission pattern shows a distinct variability, both on the long term (seasonal) and on the short term (diurnal). Figure 3.1 shows the seasonal variability of the daily nitrous oxide emission. In October and November 2010 the emission is lower than 10 kg N_2O-N.d^{-1}. November 2010 has even two weeks during which no nitrous oxide is emitted at all. In December 2010, the emission starts to increase to reach a maximum daily emission of 455 kg N_2O-N.d^{-1} in March 2011. From April onwards, the emission starts to decrease again. In the autumn and early winter of 2011-2012, it is hard to distinguish any trend.
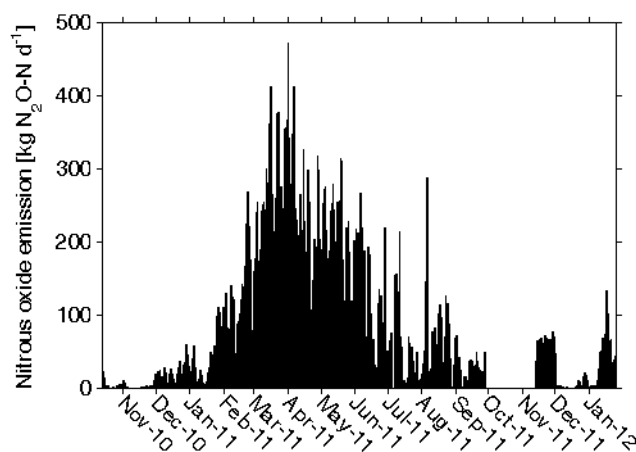

Figure 3.1. Daily nitrous oxide emission from 14 October 2010 to 26 January 2012 (the gap in October 2010 is due to equipment downtime).

Figure 3.2 shows the diurnal variability during one week in December 2010. During this week, the emission peaked at midnight and was lowest in the morning. The results of this week were chosen as a mere illustration of the diurnal variability that could possibly be encountered. It should be noted that the diurnal emission pattern during this week in December 2010 is not at all representative for the entire period.
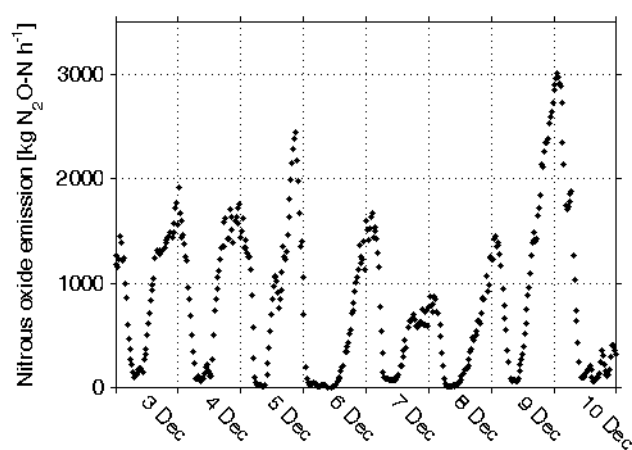
Figure 3.2. Online nitrous oxide emission from 3 to 11 December 2010. The vertical gridlines indicate midnight.

Implementation of different sampling strategies

The long-term online dataset that came forth from this monitoring campaign was subjected to different sampling strategies based on the ones that have been used in the previous studies mentioned in Table 3.1. The evaluated sampling strategies are presented in Table 3.2.

Table 3.2. Overview of the characteristics of the evaluated sampling strategies.

Sampling strategy
24 hour online sampling
7 day online sampling
Long-term weekly grab sampling
Single grab sample

24 hour online sampling

A 24 h online sampling strategy was applied by Ahn et al. (2010b). The exact sampling frequency is not mentioned. Presumably, such a monitoring campaign would last e.g. from 11 a.m. on a working day until 11 a.m. the next working day. The average over this 24 h period would yield an estimated daily emission flow rate (kg N_2O-N d^{-1}). This strategy was applied to every 24 h period of the present online long-term dataset, starting at 11 a.m. on a Monday, a Tuesday, a Wednesday or a Thursday (it was presumed that a WWTP cannot be accessed during the weekend, so a measurement campaign has to start and end on a weekday). Of each such period, the average emission was calculated, resulting in 237 calculated values of the daily nitrous oxide emission of the plant. Each of these 237 emission estimates is a possible outcome of a 24 h online sampling campaign. All the possible outcomes were collected in a histogram with a bin width of 10 kg N_2O-N d^{-1} (Figure 3.6).

7 day online sampling

Online sampling campaigns lasting for one week were carried out by Peu et al. (2006) and by STOWA (2010). By averaging the emission over seven days of online sampling, an estimate of the daily emission (kg N_2O-N d^{-1}) is obtained. For the present study, this strategy was applied to every period of 7 consecutive days of the complete dataset, excluding the 7 day periods that started on Saturday or Sunday (again it was presumed that a WWTP cannot be accessed during the weekend, so also a 7 d online measurement campaign has to start and end on a weekday). 7-day moving averages over the long-term online dataset were calculated, starting and ending at 11 a.m., excluding the 7 day periods that started on Saturday or Sunday, resulting in 289 calculated values of the daily nitrous oxide emission of the plant. Similarly to the previous case, each of these 289 emission estimates is a possible outcome of a 7 d online sampling campaign. All the possible outcomes were collected in a histogram with a bin width of 10 kg N_2O-N d^{-1} (Figure 3.6).

Long-term weekly grab sample

Czepiel et al. (1995), Sümer et al. (1995) and Sommer et al. (1998) took (bi)-weekly grab samples over a longer period (fifteen weeks, 1 year and 1.5 year, respectively). According to this sampling scheme, one takes a single grab sample on a specific day of the week, e.g. each Monday, at some time between 9 a.m. and 5 p.m., during several weeks or longer. The average of all the grab samples is the final estimate of the average emission. This long-term weekly grab sampling strategy was implemented by randomly selecting a daytime emission value from the long-term online dataset for each working day of the week, mimicking five long-term weekly grab sampling campaigns of 58, 59 or 60 weeks (not all days of the week were equally represented in the long-term online dataset due to interruptions in the online sampling campaign), each of which was performed on a specific day of the week. For all days of the week of the dataset, these 58, 59 or 60 randomly selected values were averaged per day, resulting in seven calculated values of the daily emission, one for each day of the

week. With about 20 data points available between 8 a.m. and 5 p.m. each day, and 58 to 60 days per sampling campaign, the possible ways in which to conduct a long-term weekly sampling campaign are all but infinite (20^{60}). In contrast to the three previous strategies, it is therefore nearly impossible to obtain the full number of possible outcomes for each of the seven weekly sampling campaigns. Instead, the procedure was repeated 1000 times for each day, so each repetition yielded 1000 calculated values per day of the week. This procedure was also performed for a random working day per sampling week, mimicking a monitoring campaign during which a weekly sample is taken on a random working day instead of a fixed day of the week. This procedure was repeated 1000 times as well. For each of the seven sampling campaigns using a fixed day and for the sampling campaign using a random weekday, the 1000 values are possible outcomes of the respective sampling strategies. All the possible outcomes were collected in a histogram with a bin width of 10 kg N_2O-N d^{-1} (Figure 3.7).

Single grab sample

Wicht and Beier (1995) determined the nitrous oxide emission of 25 WWTPs by taking a single grab sample at each plant. To evaluate grab sampling, every value of the online dataset that was logged on working days between 9 a.m. and 5 p.m. is considered a potential value of a grab sample, since grab samples are usually taken during working hours. This resulted in 5504 possible estimates. Again, each of these 5504 emission estimates is a possible outcome of a sampling campaign consisting of a single grab sample. All the possible outcomes were collected in a histogram with a bin width of 10 kg N_2O-N d^{-1} (Figure 3.6).

Precision as function of sampling campaign duration

For each of the investigated sampling strategies, the relative error between the true average emission and the simulated estimate is determined in function of the number of sampling instances, similarly as Ort and Gujer (2006). For the 24 h and the 7 d online sampling strategy it concerns the number of random, not necessarily consecutive 24 h periods; or random, not necessarily consecutive weeks of online monitoring, respectively. For the long-term weekly grab sampling strategy it is determined how many weeks such a campaign should last to yield a satisfying estimate. Finally, the number of completely random grab samples that is required, is determined as well.

24 hour online sampling

From the collected dataset of 24 h averages that start and end on 11 a.m. on a working day, containing 237 values (cf. section Implementation of different sampling strategies), a number of 24 h averages could be selected randomly. This number is called n, and it does not necessarily concern consecutive periods. These n 24 h averages represent a subset of the long-term online dataset. Figure 3 illustrates the way in which a sampling scheme of n = 20 randomly picked 24 h periods is mimicked. The average of the entire dataset

represents the true average nitrous oxide emission from the WWTP, while the average of the subset of 20 randomly picked sampling days represents a possible estimate of the true average nitrous oxide emission.
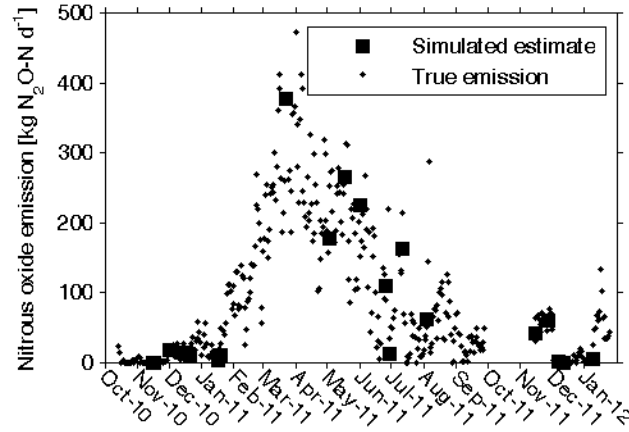
Figure 3.3. Comparison of a possible sampling scheme comprising 20 periods of 24 h starting at 11 a.m. (squares) with the true daily nitrous oxide emission (midnight to midnight) over the entire long-term online measurement campaign (dots).

This procedure was repeated for every number n of sampling periods (from 1 to 237, cf. section Implementation of different sampling strategies), resulting in a different simulated estimate for any value of n. For each value of n, the relative error ε was calculated as

$$\varepsilon = \frac{\text{Simulated average emission} - \text{True average emission}}{\text{True average emission}} \tag{3.1}$$

When ε is plotted against n, a graph like in Figure 4 is obtained.
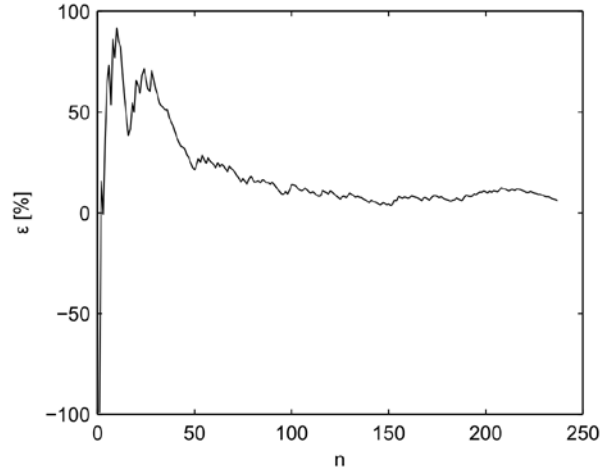
Figure 3.4. Relative error between estimated and true total nitrous oxide emission vs. the number of not necessarily consecutive 24 h sampling periods.

Per value of n, this was repeated 1000 times. This yielded a distribution of the relative errors as a function of the number of sampling periods, $\varepsilon(n)$. Figure 3.5 shows this distribution of ε for n = 20.
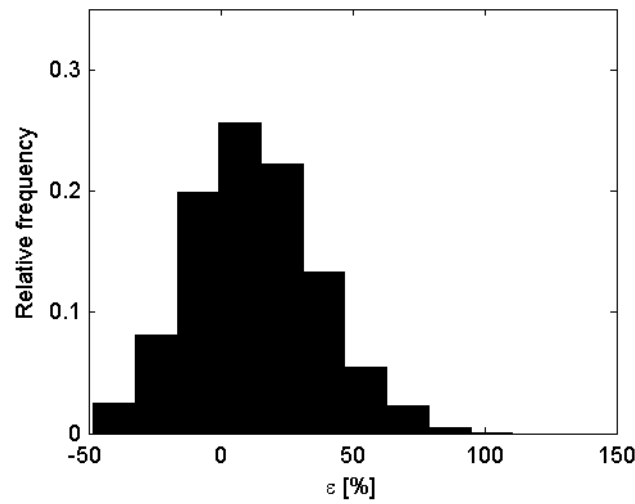
Figure 3.5. Histogram of the relative error for 1000 simulations of a sampling scheme consisting of 20 days of 24h online measurements.

The average μ and the standard deviation σ of this distribution were determined for each value of n. $\mu - 2\sigma$ and $\mu + 2\sigma$ are uncertainty bounds for ε. If the 1000 instances of ε for a certain n are normally distributed (such as in Figure 3.5), this interval is a 95 % confidence

interval around the mean. For each n, the normality of ε was verified using the Kolmogorov-Smirnov test.

7 day online sampling

The precision of the estimate as a function of the number of online sampling weeks was evaluated similarly as for the number of 24 h online sampling periods. In total, 289 moving averages were calculated, one for each period of seven consecutive days starting and ending at 11 a.m. on a weekday (cf. section Implementation of different sampling strategies). A monitoring campaign could consist of any number n of random non-overlapping weeks during which the nitrous oxide emission was measured online, up to a maximum of 58, the maximum number of non-overlapping periods starting and ending at 11 a.m. on a weekday in the long-term, online dataset. As in the case of 24 h online sampling, all the data points over the n 7d periods are averaged for each n. This average is an estimate of the plant's total average emission. For each value of n, the relative error ε was calculated according to eq.(3.1). For each value of n, this was repeated 1000 times, resulting in 1000 simulated estimates and relative errors per value of n. Again, this yielded a distribution of the relative errors as a function of the number of sampling periods, ε(n). The average μ and the standard deviation σ of this distribution were determined for each value of n. The uncertainty bounds for ε are μ - 2σ and μ + 2σ. If the 1000 instances of ε for a certain n are normally distributed, this interval is a 95 % confidence interval. For each n, the normality of ε was verified using the Kolmogorov-Smirnov test.

Long-term weekly grab sampling

Long-term weekly grab sampling was mimicked without the restriction that the sample was taken on a specific day of the week. Such a strategy would take a grab sample in every consecutive week, no matter what day of the week, during n weeks. To simulate this, the daytime values of the weekdays were pooled per week. Next, n weekly grab sampling campaigns of 1 to n weeks were simulated by randomly selecting a value from the weekly pooled data for n consecutive weeks, starting with a random week. However, when n consecutive weeks are randomly chosen from 62 weeks, the first and the last n – 1 weeks have a lower probability to be selected than the weeks in between. To avoid this misrepresentation, any series of n consecutive weeks that started less than n weeks before the end of the dataset was completed with the required number of consecutive weeks at the beginning of the dataset. This ensures that the weeks in the beginning and the end of the long-term dataset have an equal chance to be randomly chosen.

For each value of n, the n weekly emission values were averaged, resulting in 62 estimates. For each estimate, the relative error ε was calculated according to eq. (3.1). Again, this procedure was repeated 1000 times, resulting in 1000 simulated estimates and 1000 values of ε for each of the 62 values of n. For each n, the average μ and the standard deviation σ of the 1000 relative errors were determined, with μ - 2σ and μ + 2σ as uncertainty bounds.

Again, the Kolmogorov-Smirnov test was used to determine for which values of n the 1000 relative errors were normally distributed. In the latter case, μ - 2σ and μ + 2σ are the bounds of a 95 % confidence interval.

Completely random grab sampling

The long-term online dataset contained 5504 values that were logged on working days between 9 a.m. and 5 p.m. All these values are possible results of grab samples. A grab sampling campaign could consist of one to any number n of completely random grab samples, but from a practical point of view, the maximum number of grab samples is limited to n = 200. To mimic n completely random sampling campaigns, n random values were picked from the 5504 daytime values of the long-term online dataset. For each n, the n grab samples were averaged, resulting in 200 simulated estimates of the nitrous oxide emission, one for each value of n. 1000 repetitions of this procedure result in 1000 simulated estimates and 1000 relative errors (calculated according to eq. (3.1)) for each value of n. For each n, the average μ and the standard deviation σ of the 1000 relative errors were determined, with μ - 2σ and μ + 2σ as uncertainty bounds. Again, the Kolmogorov-Smirnov test was used to determine for which values of n the 1000 relative errors were normally distributed. In the latter case, μ - 2σ and μ + 2σ are the bounds of a 95 % confidence interval.

Results

Evaluation of the different sampling strategies when applied to the long-term online dataset

A histogram of the possible estimates of the daily nitrous oxide emission was made for each simulated sampling strategy that was applied to the long-term online dataset. Figure 3.6 shows the histograms of the three short-term sampling strategies, while Figure 3.7 shows the histograms of the possible emission estimates that result from implementing the long-term weekly grab sampling strategy to the long-term, online dataset.
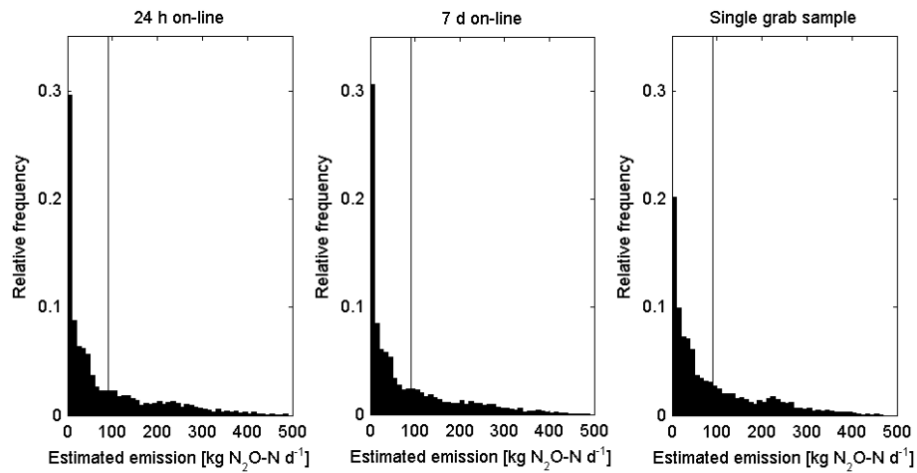
Figure 3.6. Histograms of the possible emission estimates that result from implementing different short-term sampling strategies: a single 24h period of online measurements, a single 7 d period of online measurements and a single grab-sample, respectively. The vertical line indicates the true average nitrous oxide emission as determined by the long-term, online sampling campaign.
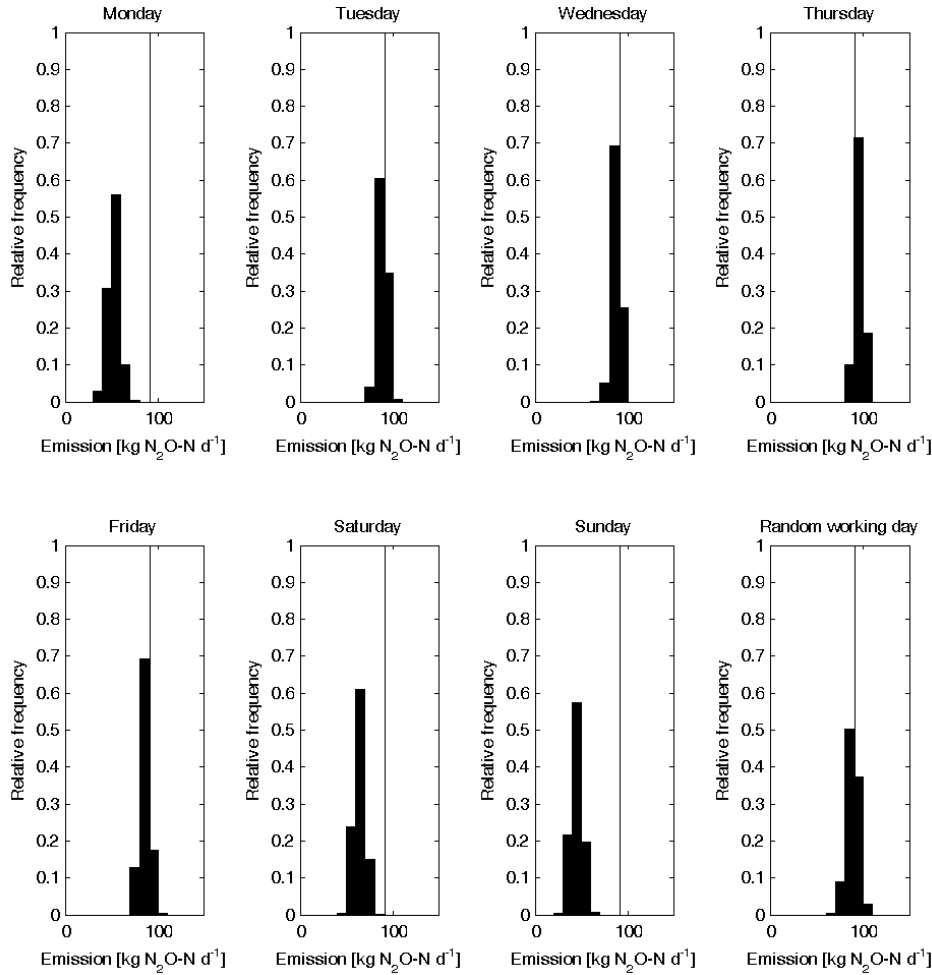
Figure 3.7. Histograms of the possible emission estimates that result from implementing the long-term (58, 59 or 60 weeks, depending on the day of the week) weekly grab sampling strategy to the long-term, online dataset. The first seven plots show the outcome per day of the week separately, while the last plot shows the result when the weekly sample is taken on a random workday. The vertical line indicates the true average nitrous oxide emission as determined by the long-term, online sampling campaign.

For the three short-term sampling strategies shown in Figure 3.6, about 20 % to 30 % of the simulated estimates are in the lowest quantile of the histogram. This implies that these sampling schemes have a relatively high chance to severely underestimate the true average nitrous oxide emission of 91 kg N_2O-N d^{-1}. However, these three distributions also have long tails: the chance to end up with an estimate equal to the double of the true emission is

about the same as the chance to obtain an estimate that is equal to the true emission (i.e. 2 %). In contrast, the long-term weekly grab sampling campaigns (Figure 3.7) appear to have a relatively high chance to obtain an accurate estimate of the true emission, except for the ones during which the samples are taken on a Saturday, a Sunday or a Monday. The latter three distributions have their mean left of the true average emission of 91 kg N_2O-N d^{-1}, resulting in an underestimation of the emission. This agrees with the true average emission per day, calculated from all the online data points per day, shown in Table 3.3. Besides a higher accuracy, the long-term weekly grab sampling strategy also results in a higher precision than the short-term sampling campaigns, as indicated by the lower dispersion of the simulation results (note different scales of X-axes).

Table 3.3. Average true emission of N_2O from the Kralingseveer WWTP per day of the week. The left column contains the values from midnight to midnight, while the right column contains the average of all daytime values (9 a.m. to 5 p.m.).

Day of the week	True average daily emission over 24 hours (kg N2O-N d-1)	True average daily emission from 9 am to 5 pm only (kg N_2O-N d^{-1})
Monday	75.8	52.9
Tuesday	106.4	90.5
Wednesday	103.2	87.9
Thursday	108.8	96.2
Friday	97.0	85.4
Saturday	81.7	65.5
Sunday	66.6	45.2

Precision as function of number of samples or duration of sampling campaign

24 hour online sampling

Using the long-term online dataset, it was possible to simulate 237 sampling periods of 24h, starting and ending at 11 a.m. on a working day. A sampling campaign could consist of any number n of random, not necessarily consecutive 24h periods, with n ranging from 1 to 237. Each n results in an estimate that deviates to some extent from the true average emission, resulting in a relative error ε for each value of n. The relative error ε will generally approach to zero with increasing n, as is confirmed in Figure 3.4. Nonetheless, the relative error does not coincide with zero when n becomes 237, because these 237 sampling periods only comprise 24 h periods starting and ending at 11 a.m. on weekdays, while the true average emission is estimated using the entire long-term online dataset of 417 days, including weekends. The precision of the estimate in function of the number of random 24h online sampling days is inferred from Figure 3.8A. By running 1000 simulations for each n, 1000 values of the relative error are obtained for each n. For each n, one can plot μ

- 2σ and μ + 2σ as uncertainty bounds. For n > 7 and n < 230, the 1000 relative errors are normally distributed. In those cases, the uncertainty bounds are the bounds of a 95 % confidence interval around the average.

From Figure 3.8 it is clear that ten random 24 h periods of online sampling would yield an estimate whose relative error has 95 % chance to lie between -62 and 78 %. A subset of 50 sampling periods of 24 h yields a relative error between -22 and 35 % in 95 % of the cases. An increase in the number of sampling days results in an ever decreasing marginal improvement in precision. It should be noted that the graph shows a slight bias towards a positive error. That is because the true emission is based on the entire long-term, online dataset (417 days) while the simulation of the sampling strategy is limited to 24 h periods starting and ending on working days only (237 days). Therefore, the maximum number of 24 h sampling days results in a simulated dataset that still contains less data than the long-term, online dataset that includes the weekends as well. When n equals 237, the estimate and the concomitant relative error is the same for each of the 1000 iterations, since there is only one way in which to sample 237 days. At that point, the lower and upper uncertainty bounds coincide.

7 day online sampling
A similar approach was adopted for determining the relative error in function of the number of not necessarily consecutive 7 d periods during which the emission is measured online. In total, there were 289 periods that qualified for simulation. Taking into account that those periods were not allowed to overlap, a sampling campaign could consist of any number n of random, not necessarily consecutive 7 d periods, with n ranging from 1 to 57. The precision of the estimate in function of the number of random 7 d online sampling periods can be inferred from Figure 3.8B, in a similar way as for the number of 24 h online sampling periods. Only for n > 7 and n < 57 are the uncertainty bounds also the bounds of the 95 % confidence interval around the average, since the relative error ε follows a normal distribution for those values of n. Sampling online for 10 not necessarily consecutive weeks would result in an estimate whose relative error has a 95 % confidence interval between -55 % and 59 %. To obtain an estimate with a relative error that has a 95 % confidence interval of about 10 %, one would need to sample during more than 53 (not necessarily consecutive) weeks. In the case 7 d online sampling periods, the upper and lower uncertainty bounds do not coincide when the maximum number of sampling weeks is obtained, since a campaign of 57 online sampling periods of 7 days can start on each working day of the week. So, even with 57 sampling periods of 7 d, the estimate will differ depending on the day of the week on which the mimicked campaign starts.

Long-term weekly grab samples
In section Evaluation of the different sampling strategies when applied to the long-term online dataset it was established that long-term weekly grab sampling on a random working

day during the entire length of the dataset yields the most accurate estimate of the average nitrous oxide emission. When such a sampling strategy is simulated for different campaign durations, i.e. a weekly grab sample over a different number of consecutive weeks, Figure 3.8C is obtained. Only from 59 weekly grab samples onward, the relative errors are normally distributed. So, only for those values of n are the uncertainty bounds also the bounds of the 95 % confidence interval around the mean. Figure 3.8C demonstrates that the relative error decreases with an increasing length of the sampling campaign. Just as in the case of 7 d online sampling, the upper and lower uncertainty bounds do not coincide, because even at the maximum of 62 sampling weeks, the possible ways to obtain weekly samples are sheer infinite.

Completely random grab sampling
Finally, the accuracy of a campaign consisting of completely random grab samples is verified. In this case, the simulated relative errors are normally distributed for each n starting from 3.

Figure 3.8D shows that a sampling scheme of 20 completely random samples results in a 95 % confidence interval of [-64%, 42%], narrowing down to [-29%,13%] for 100 samples, but the marginal improvement becomes smaller with an increasing number of samples.

Discussion

What is the best sampling strategy?

Duration and timing of the sampling campaign
The long-term, online dataset of the present measurement campaign exhibits an enormous variability, both on the long term (Figure 3.1) and on the short term (Figure 3.2). The exact causes of this variability are beyond the scope of the present study, but this variability has severe implications for the sampling strategy that is used to estimate the average amount of nitrous oxide that is emitted from a WWTP.

From Figure 3.6 it is evident that the simulated short-term sampling campaigns, be it a single grab sample, 24 h or 7 d online monitoring, are unable to result in a good estimation of the yearly nitrous oxide emission from the municipal WWTP under study. If such a short-term monitoring campaign was simulated for October 2010, the resulting estimate of the nitrous oxide emission would result in a severe underestimation of the yearly nitrous oxide emission from the WWTP, while a simulated short-term campaign during Spring 2011 would lead to a serious overestimation (Figure 3.1). This emission pattern is consistent with the results from a previous study at the same WWTP, where the emission was measured during one week in October 2008 and one week in February 2009 (STOWA, 2010). In that study, the emission was low in October and high in February.

The histograms of the simulated estimates resulting from short term sampling campaigns are heavily skewed to the right, indicating that such campaigns have a higher chance to result in an underestimation of the emission. Therefore short-term sampling strategies are ill suited to obtain an accurate estimate of the average nitrous oxide emission of the Kralingseveer plant under study. The long-term weekly sampling strategy performs better, as shown in Figure 3.7. Nonetheless, the resulting simulated estimates from a long-term weekly grab sampling strategy depend on the day on which the sample is taken. If the weekly sample is taken on a Saturday, a Sunday or a Monday, the resulting estimate is an underestimation of the true average emission. Indeed, for reasons that are beyond the scope of this paper, the true emission on those days of the week is lower than on the other days (Table 3.3). In fact, a long-term weekly grab sampling strategy during which samples are taken on a fixed day of the week, results in an estimate of the true daytime emission on that particular day of the week. Since it is not possible to know beforehand which days of the week have a deviant emission, sampling on a random day is the better option to get an estimate of the yearly average nitrous oxide emission.

Sampling frequency
Although long-term weekly grab samples give the most accurate and precise estimate of the yearly nitrous oxide emission from the WWTP, such a sampling strategy cannot discern the diurnal emission pattern that is illustrated in Figure 3.2. If during this period samples are taken during daytime only, as is usually the case with grab sampling, the total emission during this period is underestimated since the emissions at this particular WWTP and during this particular period are at their lowest during the daytime. As already mentioned above, this diurnal pattern is not representative for the entire measurement period. During other periods the daytime emissions were actually higher than the night-time emissions. That is why the long-term grab sampling strategy, although using only daytime samples, still results in acceptable simulated estimates of the yearly emission, but this cannot be known before actually measuring online during 24 hours.

For research purposes, diurnal patterns may be very helpful to identify the mechanisms behind the nitrous oxide emission, since many operational parameters of a WWTP also show diurnal variability (e.g. dissolved oxygen, nitrogen load, influent flow etc.). In order to correlate these parameters with emissions, high frequency data of both the emission and the parameters are needed, and that can only be achieved with high frequency, online sampling. Kampschreur et al. (2008b) already mentioned that the registration of their dynamics is a prerequisite to determine the relationship between the emissions and the operational conditions. Their online measurements on a full-scale nitritation reactor showed that nitrous oxide emissions depend mainly on dissolved oxygen level, nitrite concentration and aeration rate. In their turn, Ahn et al. (2010a) were able to establish a correlation between diurnal variability in the emission of nitrous oxide and the diurnal total Kjeldahl nitrogen loadings on a full-scale municipal WWTP. In a pilot-scale study, Lotito et

al. (2012) exposed a diurnal pattern of nitrous oxide emissions during the day. This pattern was correlated to the ammonia and nitrite peaks in the tank. Finally, Aboobakar et al. (2013) used online data of emissions and several process conditions of a full-scale WWTP in a statistical analysis and found out that the emissions were negatively correlated with the dissolved oxygen level.

From the studies mentioned above, it is clear that a consensus about the causes of the emission is still lacking. Yet, it is obvious that insight in the short-term dynamics of both the nitrous oxide emission and the process conditions is essential in the discussion about which process conditions induce nitrous oxide emissions. As the present study demonstrates, the short-term dynamics of the nitrous oxide emission can only be revealed by high-frequency (online) sampling.

Precision as function of sampling campaign duration

The precision of the estimate resulting from a sampling campaign increases with the length of the campaign. This is also evident from Figure 3.8. However, sampling requires a considerable effort and cost, resulting in a trade-off between precision and resources. To decide how long a sampling campaign should last or how many samples should be taken, the precision of the final estimate as a function of the campaign length or the number of samples was assessed in this study.
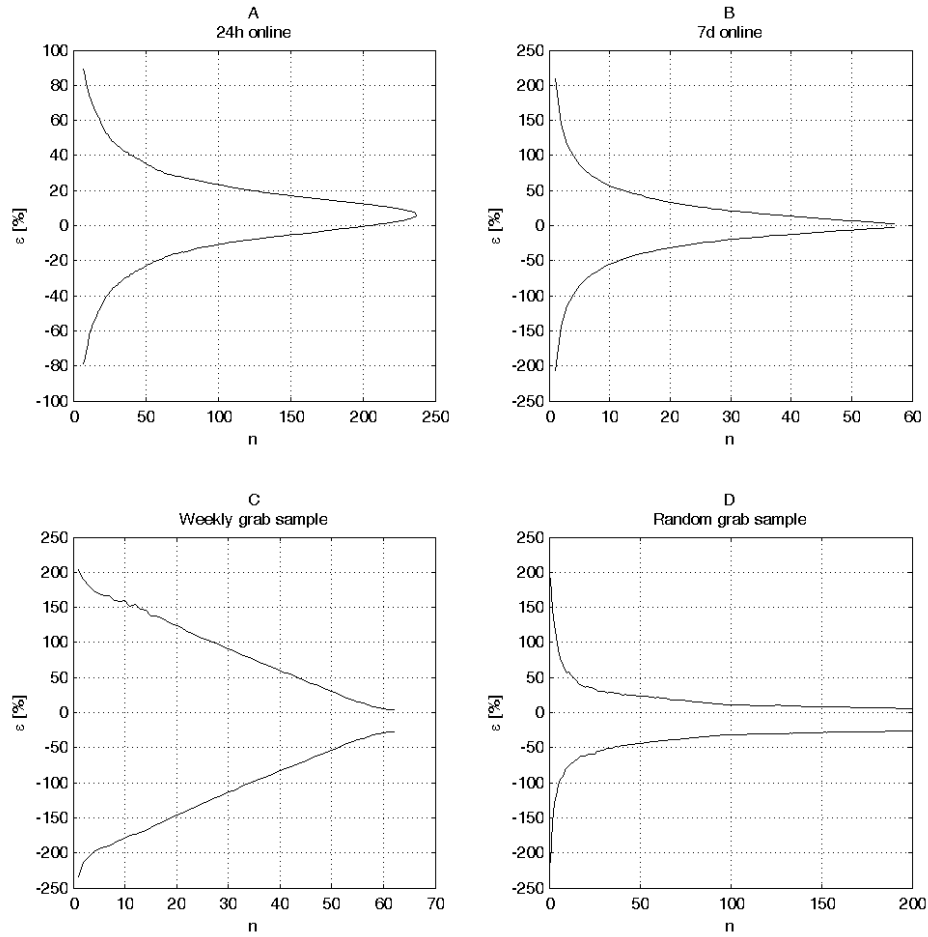
Figure 3.8. Uncertainty bounds of the relative error ε versus the number n of 24 online sampling periods (A), 7 d online sampling periods (B), weekly grab samples (C) and completely random grab samples (D). These results are based on 1000 iterations.

Grab sampling

From the evaluation of different sampling strategies in section What is the best sampling strategy? it was concluded that, of all the discussed sampling strategies (cf. Table 3.1), a weekly sampling campaign over the entire measurement period, during which the samples are taken on a random working day results in the most precise estimate of the true nitrous oxide emission from this WWTP. This was concluded after simulating such a campaign for the entire length of the long-term online monitoring period, i.e. 62 weeks. Nevertheless, depending on the desired precision, a shorter monitoring period might have been

sufficient. In Figure 3.8C it was shown that the relative error decreases linearly with the number of consecutive sampling weeks, until about 60 weeks, when there is a 95 % chance that the absolute value of the relative error is smaller than 25 %. When grab samples are taken completely randomly instead of weekly, the same precision can never be obtained (Figure 3.8D). If the 60 grab samples are taken randomly instead of weekly, the absolute value of the relative error has a 95 % chance to be smaller than 41 % (Figure 3.8D). However, when only 30 samples are taken completely at random, the relative error still has a 95 % chance to be smaller than 50 % (Figure 3.8D), while 30 grab samples taken in consecutive weeks result in uncertainty bounds between -112 % and 91 % (Figure 3.8C). Considering the cost of sampling, this may be a clue to determine the length of a weekly grab sampling strategy that should have been applied to estimate the yearly nitrous oxide emission from Kralingseveer WWTP.

Weekly grab sampling campaigns that are shorter than the complete dataset, perform relatively poorly, because such campaigns do not capture the seasonal variability in the complete dataset. When planning a weekly sampling campaign, one should try to cover the variability that can be reasonably expected. On a WWTP, the seasonal variability is caused by the seasonal variations in ambient temperature. To cover the entire temperature range, one has to sample at least one year, which amounts to about fifty weekly grab samples. However, in the case of grab sampling, the cost is primarily associated with taking and analysing the sample, rather than with the duration of a campaign. Considering this, it is better to take only a limited number of samples spread randomly over the year, than to take the same number of samples every week.

Online sampling
Grab sampling strategies cannot bring insight into the diurnal variability of the emission, in contrast to online monitoring strategies such as the 24 h of 7 d online monitoring campaigns. Of course, one could consider to repeat several 24 h or 7 d online monitoring campaigns over a longer period in order to take the long-term variability into account as well. The precision of the simulated estimate in function of the number of such sampling events is shown in Figure 3.8A and Figure 3.8B. To obtain a relative error that has 95 % chance to be smaller than 50 %, one would need 25 random periods of 24 h online sampling or 12 random periods of 7 d online measurements. Considering the effort it takes to install, calibrate and dismantle the measuring equipment it is worthwhile to measure online over a longer period, preferably one year to cover the entire temperature range, instead of several short periods. But when budgetary or other constraints limit the use of online analysing equipment to a limited number of days or weeks, it is better in terms of precision to spread the measurements over the entire year than to measure during consecutive periods.

What about the emission from other WWTPs?

The present study is entirely based on a dataset of nitrous oxide emission of the WWTP of Kralingseveer from 14 October 2010 to 26 January 2012. These data were used to identify the way of sampling that would have resulted in the best estimate of the average emission at this particular WWTP in this particular period. One could argue that the conclusions from this study are not necessarily valid for other plants. Indeed, the values of the confidence interval bounds, for instance, cannot be directly applied to other studies. The variability that was encountered in the nitrous oxide emission from Kralingseveer WWTP is not necessarily representative for other plants. Yet, the lack of other long-term online datasets of full-scale nitrous oxide emission makes it impossible to assess to what extent the tremendous variability at Kralingseveer is generally applicable. In two other water-related fields, this lack of data was countered by testing different monitoring scenarios against simulated data from dynamic models of the presence of pollutants in sewers Ort and Gujer (2006) and water bodies Gevaert et al. (2009). For nitrous oxide emission, a reliable mechanistic model that is able to describe the dynamics of nitrous oxide emission from full-scale WWTPs is not available (yet). Overall, rather than prescribing the exact way in which to sample, this study reveals the caveats involved in sampling nitrous oxide emissions from full-scale WWTPs.

Conclusions

A long-term dataset of continuous nitrous oxide emission measurements from a municipal WWTP was used to evaluate different sampling strategies that have been used in previous studies to monitor these emissions. A reliable determination of the actual average nitrous oxide emission of a WWTP requires long-term sampling, be it online or grab sampling, covering the entire temperature range that can possibly be encountered. For long-term grab sampling, night-time and weekend samples contribute significantly to a more accurate estimate.

If the interest of the monitoring campaign is in the short-term variability, rather than in the mere average nitrous oxide emission, (long-term) grab sampling is not sufficient. In that case, e.g. when researchers want to compare the diurnal dynamics of the emission with the diurnal dynamics of the plant's process conditions, high-frequency (online) sampling is indispensable. Especially in the case of online sampling, long-term sampling is very resource-demanding. As a guideline to help balancing cost and precision, a method was presented to obtain the number of grab samples or online sampling periods that would have been required to obtain a sufficiently precise estimation of the emission.

Acknowledgements

Appendix 3A

Sampling protocol for monitoring nitrous oxide emissions at Kralingseveer WWTP.
From October 14, 2010 to January 26, 2012 the emission of nitrous oxide was measured at the wastewater treatment plant of Kralingseveer, located in the municipality of Capelle aan den IJssel, near Rotterdam, the Netherlands (51° 54' 30" N 4° 32' 35" E). The plant has a capacity of 360,000 population equivalents. The activated sludge reactors of this WWTP are covered. The collected off-gas is directed through four pipes to an ozone washer for disinfection before it is released through the flue gas stack. Figure 1 shows the configuration of the pipes.
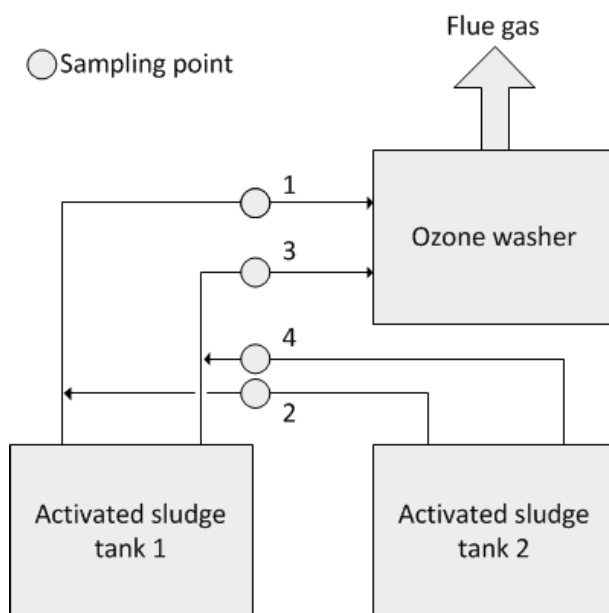
Figure 1. Configuration of the ventilation pipes directing the off-gas of the reactors to the ozone washer. The sampling locations are labelled 1 to 4.

The off-gas that goes to the ozone washer was sampled, allowing for an accurate estimation of nitrous oxide in the overall off-gas flow leaving the reactors. After passing through a condenser unit, the gas was directed to an online Servomex 4900 infrared gas phase analyser. The concentrations measured in the off-gas were corrected with measured atmospheric background concentrations. The gas flow rates in the four off-gas pipes were measured weekly using a Tesco 435 hot wire anemometer. Since the blowers of the off-gas collection system were operated at constant power, the gas flow rates could be assumed to be constant. It was indeed verified that the standard deviation of the weekly gas flow rate measurements over the entire measurement campaign was smaller than the measurement

error as calculated according to the manual of the anemometer. By multiplying the measured concentrations with the prevailing gas flow rates in the four pipes, the nitrous oxide fluxes in the four pipes were calculated. The four pipes were sampled sequentially according to the scheme in Figure 2. Per cycle and per sampling point, the four logged values were averaged (every first minute was used for purging after switching). The average of sampling point 1 and 3 were added to obtain the total emission. Every cycle lasted for 25 minutes, so the resolution of the online dataset is 25 minutes. In total, the dataset comprised 23.280 data points (Figure 3).

Time (minutes)	Sample point 1	Sample point 2	Sample point 3	Sample point 4	Ambient air
1	Purging				
2	Logging				
3	Logging				
4	Logging				
5	Logging				
6		Purging			
7		Logging			
8		Logging			
9		Logging			
10		Logging			
11			Purging		
12			Logging		
13			Logging		
14			Logging		
15			Logging		
16				Purging	
17				Logging	
18				Logging	
19				Logging	
20				Logging	
21					Purging
22					Logging
23					Logging
24					Logging
25					Logging

Purging
Logging

Figure 2. One cycle of the sequential sampling scheme, illustrating the order of sampling.
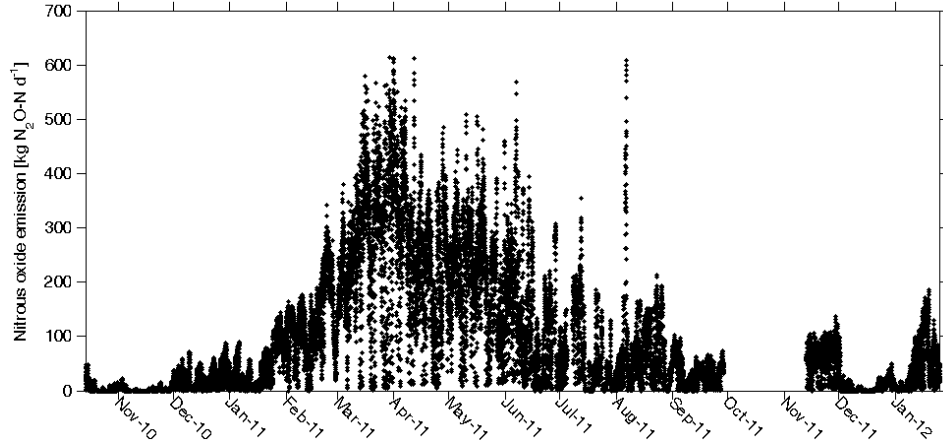
Figure 3. Plot of the 23.280 data points in the complete, online dataset, i.e. one point every 25 minutes from 14 October 2010 to 26 January 2012 (the gap in October 2010 is due to equipment downtime).

Error analysis

For each of the four sampling points, the measurement error of the gas flow rate measurement was estimated according to the manual of the anemometer (Testo 435 hot wire anemometer). The relative errors for each measuring point are shown in

Figure 4. Relative error of the gas flow rate measuremts for each of the four sampling points.

Sampling point	Relative error
1	5.4 %
2	6.5 %
3	5.4 %
4	6.7 %

According to the specification of the Servomex gas analyser, the measurement error on both the methane and nitrous oxide measurements was either 0.5 ppm or 1 % of the reading, whichever is the larger.

To estimate the maximal value of the error on the total emission, the error of the highest value (2011-03-29 21:30) was determined. Since a mass flow rate is the product of a concentration and a gas flow rate, the relative error is the square root of the sum of squares of the relative errors of the concentration and gas flow rate errors, respectively. So, for sampling point 1 and 3, the relative error of the mass flow rate is

$$\sqrt{(5.3\text{ \%})^2 + (1.0\text{ \%})^2} = 5.4\text{ \%}$$

The total emission equals the sum of the emission from sampling point 1 and 3. To obtain the absolute measurement error of the sum of two measurements, their respective absolute errors have to be added. The total emission is the sum of the emission from sampling point 1 and sampling point 2.

$$11.5 \ kg \ N_2O - N \ h^{-1} + 14.0 \ kg \ N_2O - N \ h^{-1} = 25.6 \ kg \ N_2O - N \ h^{-1}$$

The absolute error of this sum is

$$(5.4 \ \% * 11.5) kg \ N_2O - N \ h^{-1} + 5.4\% * 14.0) \ kg \ N_2O - N \ h^{-1}$$
$$= 1.38 \ kg \ N_2O - N \ h^{-1}$$

As a result, the relative error on the maximal value of the total emission is 5.4 %.

Calibration procedure

The drift of the zero measurement is 1 ppm per week and the drift of the span measurement is 1ppm or 2 % of the reading per week (whichever is the larger). About once a week, the necessity of calibrating was verified by sending a span gas with a certified concentration of the measured compounds through the analyzer.

4

Seasonality of nitrous oxide emissions from full-scale municipal wastewater treatment

Chapter 4

Abstract

During nitrogen removal in conventional activated sludge processes, nitrous oxide can be emitted. With a global warming potential of 298 CO_2-equivalents it is an important greenhouse gas that affects the sustainability of wastewater treatment. The present study reports nitrous oxide emission data from a 16 month monitoring campaign on a full-scale municipal wastewater treatment. The daily emission demonstrated a pronounced seasonal variability. This seasonal variability was compared with the long-term variability of a number of process variables that are commonly monitored during municipal wastewater treatment. On a seasonal timescale, none of the investigated variables correlated with the emission. This makes it difficult to predict the emission of wastewater treatment and it suggest that the variability of the emission may be related to time-lagged phenomena, such as microbial community dynamics and microbial adaptation dynamics.

Introduction

Since about two decades it has been recognised that nitrous oxide (N_2O) is emitted during the biological treatment of wastewater (Hanaki et al., 1992). Considering its global warming potential of 298 CO_2-equivalents over a hundred year time horizon, the emission of nitrous oxide can contribute significantly to the climate footprint of a wastewater treatment plant (IPCC, 2013b). At the WWTP that is also the location for the present study, nitrous oxide was found to make up 78.4 % of the plants climate footprint, expressed as CO_2-equivalents, the remainder of the emissions being methane (13.5 %) and the indirect carbon dioxide related to the plant's energy consumption (8.1 %) (Daelman et al., 2013, chapter 2 in this thesis). Besides a considerable greenhouse gas, nitrous oxide is currently also the most important ozone-depleting substance emitted (Ravishankara et al., 2009).

Nitrous oxide is produced and emitted during biological nitrogen removal from wastewater through nitrification and denitrification. Schreiber et al. (2012) give an extensive overview of the biological pathways and the chemical reactions that can lead to the formation of nitrous oxide. Nitrous oxide is produced biologically as an intermediate metabolite by heterotrophic denitrifying bacteria and as a side product by ammonia oxidizing bacteria. Allegedly, there are two pathways for nitrous oxide production by ammonia oxidizing bacteria. Either it is produced by the reduction of nitrite (NO_2^-), the so-called nitrifier denitrification pathway, or it is produced as a result of the oxidation of hydroxylamine (NH_2OH) or intermediates of the ammonia oxidation process. The only biological way in which nitrous oxide can be consumed, is by reduction during the denitrification process. Besides these biological pathways, nitrous oxide is also produced during a number of chemical reactions involving nitrite, hydroxylamine and nitroxyl (HNO).

Numerous studies have been dedicated to the identification of the underlying mechanisms of nitrous oxide production and emission during the treatment of municipal wastewater, resulting in a set of process conditions that potentially lead to nitrous oxide emissions (see reviews by Kampschreur et al. (2009), Law et al. (2012b) and Desloover et al. (2012)). The present study reports nitrous oxide emission data from a 16-month, online monitoring campaign. The objective of this study is to identify relationships between the dynamic behaviour of the emission and process conditions in order to verify to what extent commonly measured process variables can explain the seasonal emission of nitrous oxide.

Materials and methods

Field site

The monitoring campaign was performed at Kralingseveer wastewater treatment plant, located near Rotterdam, the Netherlands (51° 54' 30" N 4° 32' 35" E). Under dry weather conditions the plant treats about 80.000 $m^3 d^{-1}$ of domestic wastewater. A comprehensive description of the plant's lay-out can be found in Daelman et al. (2012, chapter 5 in this

thesis). Basically, the plant consists of a plug flow reactor in series with two parallel carrousel reactors (Figure 4.1). After the wastewater has passed through a primary settling tank and an anaerobic selector tank (4800 m³), where it is mixed with part of the return sludge, the mixed liquor enters the plug flow reactor, where the complementary part of the return sludge is added. First, the mixed liquor passes through a non-aerated, anoxic zone for denitrification (3600 m³), followed by an aerated zone (bubble aeration) for nitrification (8000 m³). From the aerated zone, about three quarters of the mixed liquor is recycled to the anoxic zone, while the remainder passes on to the two parallel carrousel reactors (2 x 13.750 m³), each aerated with three surface aerators. After passing through the carrousel reactors, the mixed liquor flows to the secondary settlers, from which part of the sludge is recycled to the selector and another part is waste sludge. The underflow of the primary settler and the secondary sludge are thickened and treated anaerobically. The digestate is dewatered and disposed for incineration. The overflow of the sludge thickening and the reject water from the digestate dewatering are recycled to the primary settler.
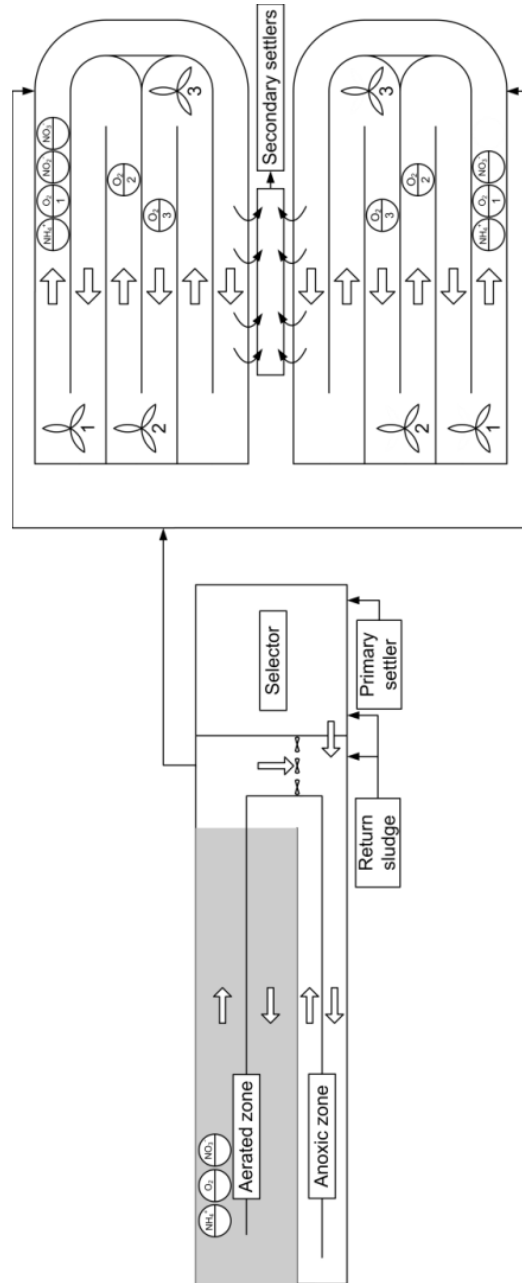
Figure 4.1. Lay-out of the plug flow reactor and the two parallel carrousel reactors, with sensors and aerators indicated. The lower carrousel reactor mirrors the upper one, except for the nitrite sensor which was only available in the upper reactor.

Nitrous oxide monitoring

The plug flow reactor and the two carrousel reactors are covered. The nitrous oxide mass flow rate was calculated from measurement data of the concentration (using a Servomex IR gas analyzer) and the constant volumetric gas flow rate (verified with a Testo 435 hot wire anemometer) of the off-gas coming from the covered activated sludge tanks. The configuration of the activated sludge system and the lay-out of the ventilation system allowed establishing the nitrous oxide mass flow rates from the individual tanks. The monitoring protocol is added as supplementary material. The monitoring period covered 16 months, from October 14, 2010 to January 26, 2012, with a month-long interruption in October 2011 due to a technical failure.

Plant data

Dissolved oxygen concentration, nitrate and ammonium concentrations, mixed liquor temperature, aeration rates, total suspended solids concentration in the activated sludge tanks and influent flow rate were available from the plant's SCADA system at 10 minute intervals. For the online nitrite measurements, an S::CAN spectro::lyzer™ probe was used. The linear calibration curve for this sensor used data pairs of spectral signals and nitrite concentration in mixed liquor samples. The nitrite samples for calibration were taken weekly and analysed immediately using Hach Lange kits. The waterboard provided laboratory data for plant influent and effluent quality, and for the wastewater quality at the outflow of the primary settler.

Calculation of local, specific nitrification activity in the carrousel tank

In the carrousel tank, the nitrite sensor was located near the ammonium and oxygen probes. Using the real-time concentrations of dissolved oxygen, ammonium and nitrite, the local ratio of the specific activity (q) to the maximum specific activity (q_{max}) for the nitrifying bacteria was estimated using a multiplicative Monod-model, as in Yu et al. (2010).

$$\frac{q}{q_{max}} = \frac{S_{NH_4}}{S_{NH_4} + K_{s,NH_4}} \cdot \frac{S_{O_2}}{S_{O_2} + K_{s,O_2}} \cdot \frac{K_{i,NO_2^-}}{S_{NO_2^-} + K_{i,NO_2^-}} \qquad (4.1)$$

With S_{NH_4} the ammonium concentration (g N m^{-3}), K_{s,NH_4} the ammonium half-saturation coefficient (0.5 g N m^{-3}) (Rittmann and McCarty, 2001), S_{O_2} the oxygen concentration (g O$_2$ m^{-3}), K_{s,O_2} the oxygen half-saturation coefficient (0.75 g O$_2$ m^{-3}) (Guisasola et al., 2005), $S_{NO_2^-}$ the nitrite concentration (g N m^{-3}) and K_{i,NO_2^-} the nitrite inhibition coefficient (0.52 g N m^{-3}) (Vadivelu et al., 2006).

Results and discussion

Magnitude and location of the emission

Over the entire period, 2.8 % of the nitrogen entering the plant was emitted as nitrous oxide. As can be seen in Figure 4.2, the emission exhibits a pronounced long-term variability: in the beginning of the monitoring period there was a period with no emission, in December 2010 the emission started to increase, it peaked in March 2011 at about 450 kg N_2O-N d^{-1}, it gradually decreased again to below 100 kg N_2O-N d^{-1} in summer 2011 and in December 2011 there was a short period of no emission at all.
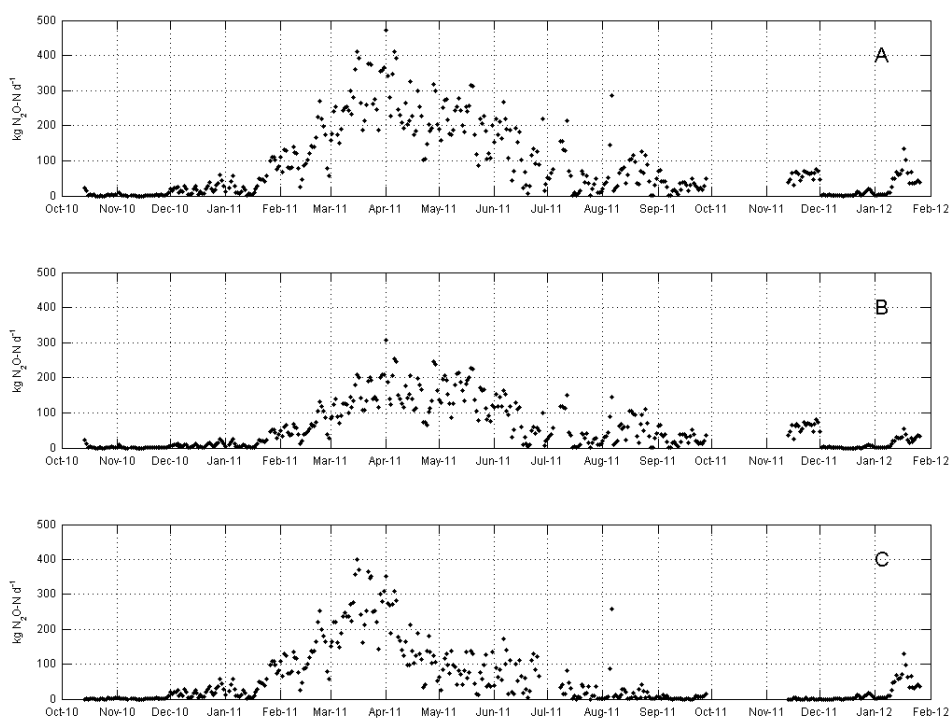
Figure 4.2. Daily nitrous oxide emission from the entire plant (A) and from the plug flow reactor (B) and the carrousel reactor (C) separately. The gap in October 2011 is due to equipment failure.

Because of the high frequency and the long-term coverage of the emission measurements, the emission estimate presented in this study is probably the best estimate so far. At 2.8 % of the incoming nitrogen, the nitrous oxide emission from Kralingseveer WWTP is higher than values reported by a number of other full-scale studies (Czepiel et al., 1995; Sümer et

al., 1995; Kimochi et al., 1998; Sommer et al., 1998; Peu et al., 2006; Ahn et al., 2010b) and within the ranges reported by Foley et al. (2010). Yet, such comparisons are delicate since the present study is the first to report long-term, online data, while the others report results from short-term measurements or low-frequency grab sampling monitoring.

At the peak of the emission, from February until April 2011, it is the carrousel reactor that emits the most nitrous oxide. Yet, at Kralingseveer WWTP, on average about 65 % of the ammonium is converted in the aerated part of the plug flow reactor before the mixed liquor goes to the carrousel reactors, so the latter have in fact a lower nitrogen loading rate than the plug flow reactor. This contradicts the findings of several studies that established a high ammonium loading rate as a cause for the emission of nitrous oxide during nitrification (Burgess et al., 2002a; Ahn et al., 2010b; Chandran et al., 2011; Lotito et al., 2012).

Could the design of the reactors offer an explanation for the higher emission in the carrousel reactors? Foley et al. (2010) suggest that carrousel type reactors are less prone to the production and emission of nitrous oxide, since such reactors approach ideal well-mixed conditions in which inhibitory metabolites such as nitric oxide and nitrite are diluted. Plug flow reactors, on the other hand, are characterized by steep concentration gradients and are therefore supposed to be more susceptible to nitrous oxide emission. This is not supported by the data gathered in the present study.

External influences: influent and temperature
The external disturbances to which a wastewater treatment plant is subjected are atmospheric temperature on the one hand and composition, flow rate and temperature of the wastewater on the other hand. Both atmospheric temperature and influent temperature affect the temperature of the mixed liquor. At Kralingseveer WWTP, the influent is mixed with the reject water from the anaerobic sludge digestion before it passes through a primary settler. The influent of the activated sludge system is therefore the effluent of the primary settler. The mixed liquor temperature, composition of the wastewater at the weir of the primary settler and the influent flow rate are shown in Figure 4.3.

The long-term trend of the emission could not be explained by the long-term variability in the external disturbances to which the WWTP is subject, i.e. wastewater characteristics and atmospheric temperature. It is not possible to discern any long-term trend in the COD and TKN content of the influent to the activated sludge tanks. This is to be expected given that it concern municipal wastewater. As a consequence of the constant TKN and COD concentrations, the long-term variability of the emission cannot be attributed to variations in the COD/N ratio that would influence the denitrification performance (Schulthess, 1995; Itokawa et al., 2001).

The temperature of the mixed liquor shows a seasonal trend, determined by the climatological temperature, with superimposed downward peaks caused by wet weather flow. The production of nitrous oxide could be explained by both high and low temperatures. Ahn et al. (2010b) expect the emission of nitrous oxide from plants that are designed for complete nitrogen removal to be higher at higher temperatures because of the higher overall kinetics of the nitrogen transformations. Nonetheless, in a previous study at Kralingseveer WWTP, the opposite was observed (STOWA, 2010). The plant's emission of nitrous oxide was monitored during one week in October 2008 and another week in February 2009. In October, when the water temperature was ca. 18 °C, the emission amounted to only 0.040 % of the incoming nitrogen, while it went up to 6.1 % in February, when the temperature was as low as 9 °C. Higher emission during colder periods could possibly be explained by increased nitrite concentrations. In WWTPs, nitrite is known to accumulate under low temperatures (Randall and Buth, 1984; Alleman, 1985; Philips et al., 2002) and high nitrite concentrations are commonly recognized as an inducing factor for the production and emission of nitrous oxide (Kampschreur et al., 2009; Wunderlin et al., 2012). Also in the current study at Kralingseveer WWTP, the nitrite concentration in the carrousel tank coincides with colder temperatures in winter. Still, as with temperature, the long-term trend of the emission did not coincide with the seasonal trend of the nitrite concentration. As far as the influent flow rate is concerned, the seasonal emission does not appear to be influenced by increased flow rates during prolonged wet weather flow periods, e.g. in January and July 2011.
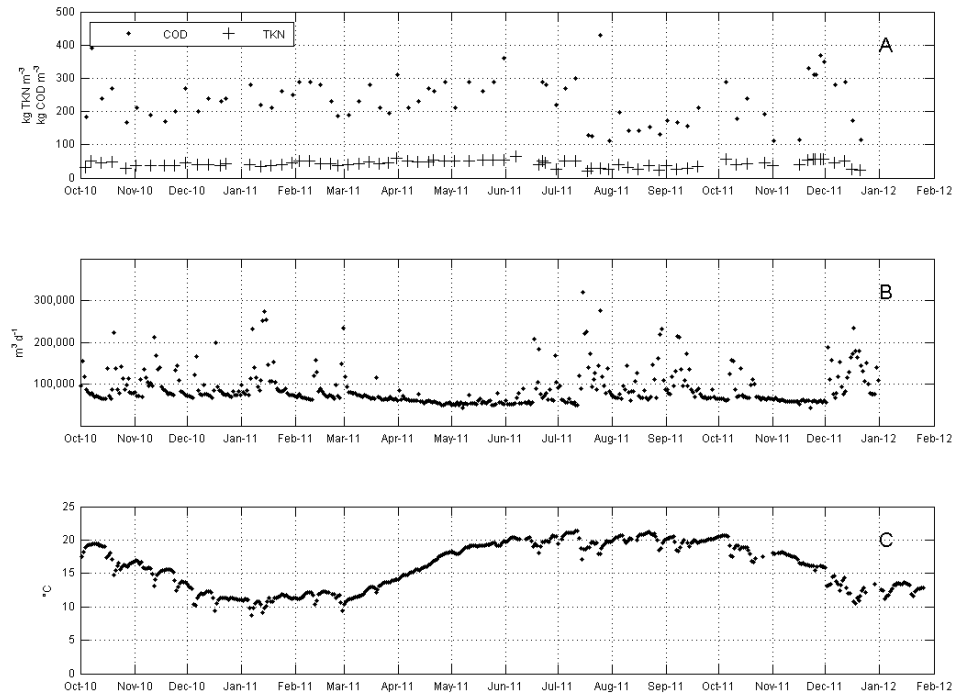
Figure 4.3. COD and TKN concentrations at the weir of the primary settler (A), influent flow rate (B) mixed liquor temperature (C).

Plant performance

Comparing the removal efficiencies of COD, TKN and total nitrogen (Figure 4.4) with the emission (Figure 4.2) does not reveal any relationships. Both the TKN and COD removal efficiencies are rather constant, while the trend in the total nitrogen removal efficiency correlates with temperature, which in its turn was not related to the emission.

A number of researchers suggested to use the emission of nitrous oxide as an early warning for nitrification process failure (Burgess et al., 2002a; Burgess et al., 2002b; Butler et al., 2009) or to control biological ammonia oxidation (Wunderlin et al., 2013b). Yet, the TKN removal efficiency of Kralingseveer WWTP remained adequate and rather constant throughout the entire monitoring period, contradicting any claims that link failing nitrification with the emission of nitrous oxide. The trend of the total nitrogen removal efficiency coincides with seasonal temperature trend, indicating that the denitrification process performed slightly worse during colder periods, but again, this cannot be linked to the long-term trend of the emission.
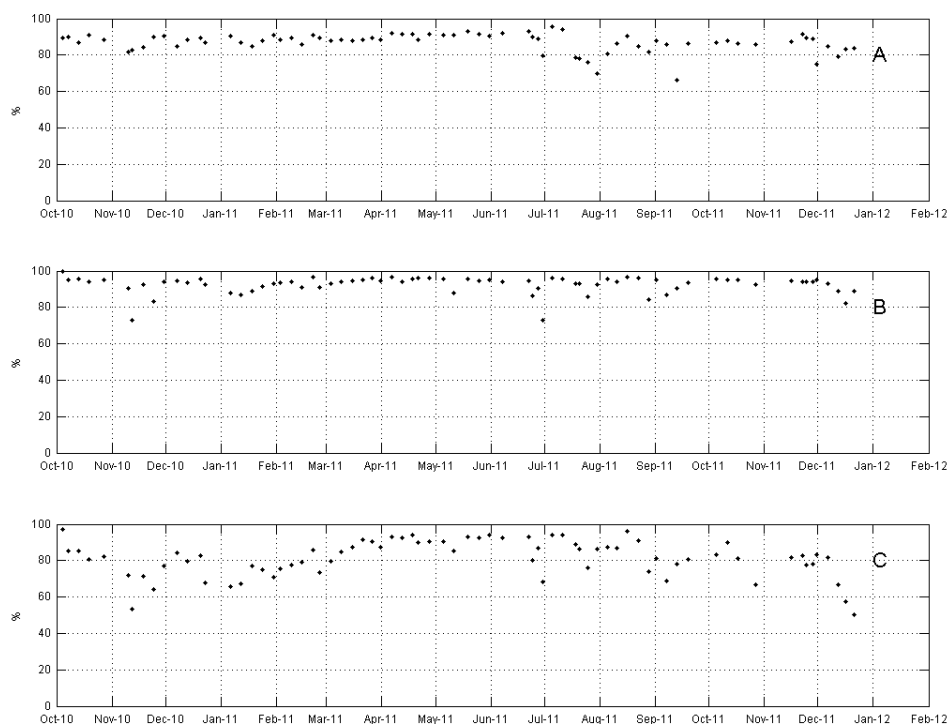
Figure 4.4. Removal efficiencies of COD (A), TKN (B) and total nitrogen (C).

Conditions in the reactors

For both the plug flow reactor and the carrousel reactor, the daily averaged concentrations of ammonium and nitrate are shown in Figure 4.5A and Figure 4.5B, respectively. For the carrousel reactor, the daily averaged concentrations of nitrite are shown in Figure 4.5C. Nor in the plug flow reactor, nor in the carrousel reactor was there any relationship between the emission on the one hand, and concentrations of nitrogen species on the other hand. The production of nitrous oxide has been linked to an increased ammonium concentration (Ahn et al., 2010b; Rassamee et al., 2011; Aboobakar et al., 2013). At Kralingseveer WWTP, the ammonium in the plug flow reactor concentrations was slightly higher during the colder periods, which indicates that during wintertime, the nitrification was slightly hampered in this reactor. Yet, the ammonium concentration in the carrousel reactors, that receive the mixed liquor from the plug flow reactor, was consistently low. This implies that some nitrification capacity was shifted from the plug flow reactor to the carrousel reactor during winter time. Still, this did not coincide with the trend of the nitrous oxide emission. Also the nitrate concentration in the carrousel reactors is slightly higher in

73

winter, indicating that the denitrification process performs slightly worse because of the cold temperatures. This coincides with the lower removal efficiency of total nitrogen. Yet, any link with the nitrous oxide emission cannot be found. Finally, also the nitrite concentration in the carrousel reactor exhibits a seasonal dynamic behaviour. In the beginning of the nitrite measurements, March 2011, the daily averaged nitrite concentration went even up to 5 g $NO_2^- \text{-} N$ m^{-3}. Indeed, at that time, the nitrous oxide emission was also at its highest. When temperature got higher, the nitrite concentration went down but after summer 2011, it went up again but the emission remained low. So, there is no unequivocal relationship between the production and emission of nitrous oxide on the one hand, and nitrite concentration on the other hand, despite ample evidence in literature (Schulthess, 1995; Tallec et al., 2006; Kampschreur et al., 2009; Wunderlin et al., 2012).

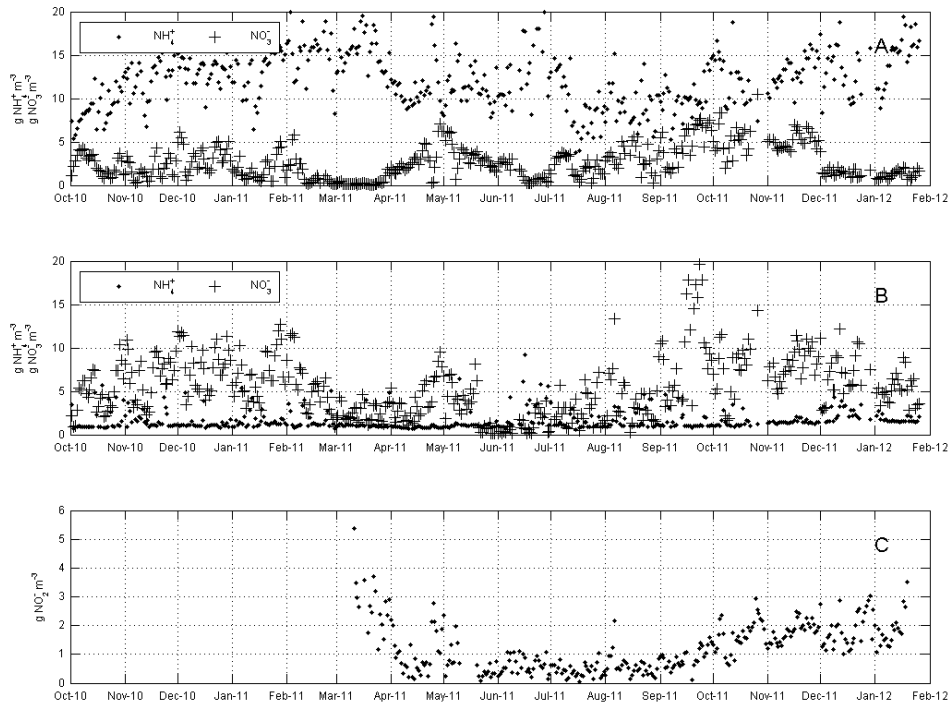**Figure 4.5. Daily average concentrations of nitrate and ammonium in the plug flow reactor (A), nitrate and ammonium in the carrousel reactor (B) and nitrite in the carrousel reactor (C). Nitrite was only measured from March 2011 onwards.**

Figure 4.6 shows the concentration of total suspended solids in the mixed liquor. It remained rather constant throughout the monitoring period at about 4 kg m^{-3}. Combined

with the rather constant TKN concentration of the influent to the activated sludge tanks, shown in Figure 4.3A, this means that also the nitrogen sludge loading rate remained constant. Again, it is not possible to distinguish any relationship between the emission on the one hand and the total suspended solids concentration and sludge loading rates on the other hand. So, on the long-term, the nitrous oxide emission does not correlate to the nitrogen loading rate, as has been suggested in previous research (Burgess et al., 2002a; Chandran et al., 2011; Lotito et al., 2012).
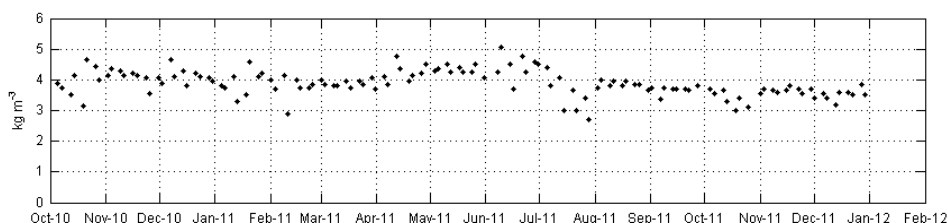
Figure 4.6. Total suspended solids concentration in the activated sludge tanks.

Besides the concentration of the nitrogen species, also the oxygen concentration has been put forward as an important variable with regard to the production and emission of nitrous oxide. An oxygen concentration that is too low during the nitrification process is supposed to induce the nitrifier denitrification pathway (Kampschreur et al., 2008a; Tallec et al., 2008; Rassamee et al., 2011; Wunderlin et al., 2012), while the presence of oxygen during the denitrification process inhibits the reduction of nitrous oxide (Otte et al., 1996; Gong et al., 2012; Wunderlin et al., 2012). Yet, during the entire monitoring period the oxygen setpoints remained the same, so the seasonal variability of the emission cannot be linked to operational changes in aeration at Kralingseveer WWTP.

The concentrations of oxygen and nitrogen species affect the ammonia conversion rate in the reactors. Using the local, real-time concentrations of ammonium, dissolved oxygen and nitrite at the point where the sensors are installed in one of the plug flow reactors, the ratio of the specific activity (q) to the maximum specific activity (q_{max}) for the nitrifying bacteria was calculated according to Eq. 1. The daily maximum values are shown in Figure 4.7. A consistent trend cannot be distinguished, except that the ratio appears to be somewhat lower in spring 2011, when the emission from the carrousel reactor was highest. Yu et al. (2010) attributed the production of nitrous oxide by nitrifying cultures to an increase in their specific activity, in particular when it approaches q_{max}. This was supported by experimental data of Law et al. (2012a) but this was not an explanation for the variability of the emission.
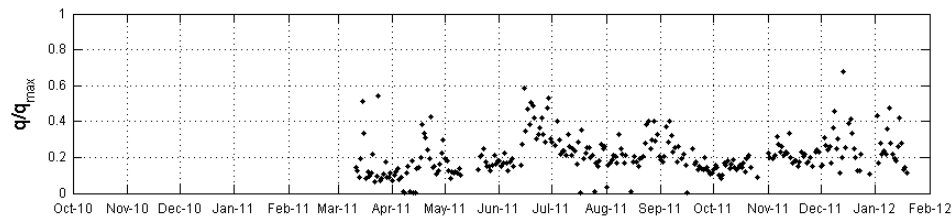
Figure 4.7. Daily maximum ratio of the specific activity (q) to the maximum specific activity (q_{max}). The ratio could only be calculated from March 2011 onwards, since no nitrite measurements were available before that time.

Community dynamics and microbial adaptation as a key?

To summarize, none of the commonly measured process variables at Kralingseveer WWTP was able to explain the seasonal trend of the nitrous oxide emission at Kralingseveer WWTP. This makes it difficult to use standard operational plant data to predict the emission of nitrous oxide.

Any variables that exhibited a seasonal variability varied with temperature, while the emission was highest in spring 2011, when the temperature was intermediate. The time lag between the peak in the emission and the lowest temperatures could possibly be explained by a lagged adaptation of the microorganisms to cope with accumulated metabolites, such as nitrite, during Winter 2010/2011, when the nitrogen conversions are hampered by the colder temperatures. The role of microbial community dynamics and microbial adaptation has been largely neglected up till now. One of the reasons for this blind spot is that most monitoring studies were too short to take seasonal variation into account. Yet, in a lab-scale study Benthum et al. (1998) observed a reduction of nitrous oxide emission by denitrifiers as a result of biomass adaptation to dynamic conditions over 30 days. Similarly, Chandran et al. (2011) saw an adaptive response in nitrous oxide emission from a chemostat pure culture of *Nitrosomonas europaea* that was subjected to pulse feeding over a period of 18 days. Those results cannot be translated directly to full-scale process conditions. Therefore, further research should combine long-term measurements of nitrous oxide emission with a long-term assessment of the microbial community and its adaptation to changing conditions.

Acknowledgements

5

Methane emission during municipal wastewater treatment

Chapter 5

Abstract

Municipal wastewater treatment plants emit methane. Since methane is a potent greenhouse gas that contributes to climate change, the abatement of the emission is necessary to achieve a more sustainable urban water management. This requires thorough knowledge of the amount of methane that is emitted from a plant, but also of the possible sources and sinks of methane on the plant. In this study, the methane emission from a full-scale municipal wastewater facility with sludge digestion was evaluated during one year. At this plant the contribution of methane emissions to the greenhouse gas footprint were slightly higher than the CO_2 emissions related to direct and indirect fossil fuel consumption for energy requirements. By setting up mass balances over the different unit processes, it could be established that three quarters of the total methane emission originated from the anaerobic digestion of primary and secondary sludge. This amount exceeded the carbon dioxide emission that was avoided by utilizing the biogas. About 80 % of the methane entering the activated sludge reactor was biologically oxidized. This knowledge led to the identification of possible measures for the abatement of the methane emission.

Published as

Introduction

During wastewater treatment, the greenhouse gases carbon dioxide (CO_2), methane (CH_4) and nitrous oxide (N_2O) can be emitted to the atmosphere (Hofman et al., 2011). Carbon dioxide is produced indirectly as a result of fossil fuel combustion to generate the energy required for the operation of the wastewater treatment plant, or it is produced directly during the respiration of organic matter. In the latter case it concerns short-cycle carbon dioxide that does not contribute to increased atmospheric carbon dioxide concentrations. Nitrous oxide is expected to be emitted during biological nitrogen removal from wastewater, through nitrification and subsequent denitrification (Kampschreur et al., 2009). Since nitrous oxide has a global warming potential of 300 CO_2-equivalents over a 100 year time horizon (IPCC, 2007a), even a low emission contributes significantly to a WWTP's greenhouse gas footprint. Not in the least due to its high impact, nitrous oxide emission from wastewater treatment processes recently received a lot of attention. Methane, having a global warming potential of 25 CO_2-equivalents over a 100 year time horizon, is expected to be formed in the sewer system (Guisasola et al., 2008) and in those parts of the WWTP where anaerobic conditions prevail. Hitherto, the emission of methane from wastewater treatment received far less attention than the nitrous oxide emission.

Only two peer reviewed studies investigated the methane emissions of municipal wastewater treatment plants with activated sludge. Both studies used grab sampling to monitor the emissions. Czepiel et al. (1993) studied a small (12,500 PE) WWTP in Durnham, New Hampshire, USA; while Wang et al. (2011a) investigated the methane emission from a large plant (1,500,000 PE) in Jinan, China. These WWTPs had no anaerobic digestion facility. The Dutch Foundation for Applied Water Research monitored methane emissions on three wastewater plants: Papendrecht (40,000 PE), Kortenoord (100,000 PE) and Kralingseveer (360,000 PE) (STOWA, 2010). The latter plant - which is also the subject of the present study - had an anaerobic sludge digestion facility, while the former two did not. The reported results from these studies are presented in Table 5.1. The share of methane in the total greenhouse gas emission from wastewater handling can mount up to 75 % expressed as CO_2-equivalents (Foley and Lant, 2008).

Table 5.1. Normalized methane emissions for the present study and the other full-scale studies found in literature, as well as the methane emission factors used in the Netherlands by VROM.

	g CH_4 person^{-1} year^{-1}	kg CH_4 (kg $COD_{influent}$)$^{-1}$	g CH_4 (m^3 influent)$^{-1}$
Present study	*306*	*1.13%*	*3.44*
Czepiel et al. (1993)[1] Durnham WWTP	39	0.16%[2]	0.14
Wang et al. (2011)[1] Jinan WWTP	11	0.08%	0.16
STOWA (2010) Papendrecht	266	0.87%	2.44
STOWA (2010) Kortenoord	140	0.53%	1.56
STOWA (2010) Kralingseveer (October)	310	1.20%	2.73
STOWA (2010) Kralingseveer (February)	230	0.80%	2.03
VROM (2008) WWTP with anaerobic sludge digestion		0.85%	
VROM (2008) WWTP without anaerobic sludge digestion		0.70%	

[1] Based on grab samples

[2] Expressed as kg CH_4 (kg BOD_5)$^{-1}$

Methane is emitted from a WWTP after it enters the plant via stripping from the incoming wastewater, or after it is formed at the plant itself. The influent of a WWTP contains dissolved methane that is formed in the sewer system. Recent studies indicate that methane formation in sewer systems can be substantial (Guisasola et al., 2008; Foley et al., 2009), but actual quantities of methane entering a WWTP have as yet not been reported. As far as methane production at the plant itself is concerned, it can be expected that in anaerobic zones, sludge thickeners and buffer and storage tanks methane is formed. In plants

equipped with a digester for the anaerobic digestion of the surplus sludge, this can be expected to be a major source of methane. The biogas from the digester is usually combusted in a gas engine or flared, resulting in methane emissions with the off-gas (Liebetrau et al., 2010; Woess-Gallasch et al., 2010). Dissolved methane that leaves the digester, sludge thickeners and storage tanks will either be stripped during downstream processing (e.g. dewatering of the digested sludge) or will remain dissolved in the reject water and as such it will end up in the aeration tanks of the WWTP, as does the methane in the influent stream. There it can be stripped during aeration, or it can be biologically oxidized by the microorganisms in the activated sludge. The potential methane oxidation of activated sludge systems has, to the authors' best knowledge, not been reported in the literature.

The objective of this study was to determine the contribution of methane to the greenhouse gas footprint of a wastewater treatment plant and to suggest measures to curb methane emissions. To obtain these goals, a one-year measurement campaign was carried out. The WWTP under study is fully covered, except for the secondary settling tanks, and all ventilation air is discharged through one stack. Gas measurements allowed estimation of total emissions, except for the exhaust of the biogas-based combined heat and power facility. Mass balances were used to reveal the sinks and sources of methane in this WWTP. Therefore, additional gaseous and liquid sampling was performed. To achieve reliable liquid sampling particular attention was paid to the sampling method.

Materials and methods

Wastewater treatment plant process scheme

The measurements and sampling were done at Kralingseveer WWTP, located in the municipality of Capelle aan den IJssel, near Rotterdam, the Netherlands (51° 54' 30" N 4° 32' 35" E). The plant treats the domestic wastewater of 360,000 population equivalents (PE). The excess sludge of the plant is treated in an anaerobic digester, operating at 34 °C. The resulting biogas is used in a combined heat and power installation that fulfills about 60 % of the energy requirements of the plant. The remainder of the plant's energy needs is met by electricity and natural gas from the grid.

Kralingseveer WWTP receives mainly domestic sewage, with an average COD concentration of 339 mg L^{-1}, an average Total Kjeldahl Nitrogen concentration of 41 mg L^{-1} and an average phosphorous concentration of 6 mg L^{-1}. The removal efficiencies are 87 %, 92 % and 77 %, respectively. The average sludge loading rate was 0.21 kg COD.kg VSS^{-1} d^{-1}.

Figure 5.1 displays the WWTP's process scheme, while an aerial picture of the plant with the different unit processes is provided in supplementary material 1. The incoming wastewater first passes through a bar screen and subsequently it goes to a primary settler.

The primary sludge is sent from the primary settler to a gravitary thickener. The understream of the thickener is fed to the anaerobic digester, while the supernatant is returned to the primary settler. The water from the primary settler enters a selector (4,800 m³) and from there it goes to an activated sludge reactor. This tank is a plug flow reactor that consists of an anoxic part for denitrification (3,600 m³) and an aerated part for nitrification (8,000m³). The aeration is achieved with bubble aeration. From the aerated zone, the mixed liquor is recycled to the anoxic zone at a recycle ratio of three. From this plug flow reactor, the mixed liquor flows into two parallel carousel reactors (2 x 13,750m³) that are aerated with surface aerators. From the carousels, the mixed liquor goes to the secondary clarifiers. The secondary sludge from the clarifiers is partially recycled to the selector and the anoxic part of the second activated sludge system, while the waste sludge is fed to a belt thickener and subsequently to the anaerobic digester, together with the thickened primary sludge. Coming from the digester, the digested sludge is stored in a buffer tank with a maximum residence time of five days and from there it goes to a centrifuge. The dewatered sludge is stored in a storage tank, from where it is loaded on a truck for transport to an incineration facility. The reject water from the belt thickener and the centrifuge are returned to the primary settler.
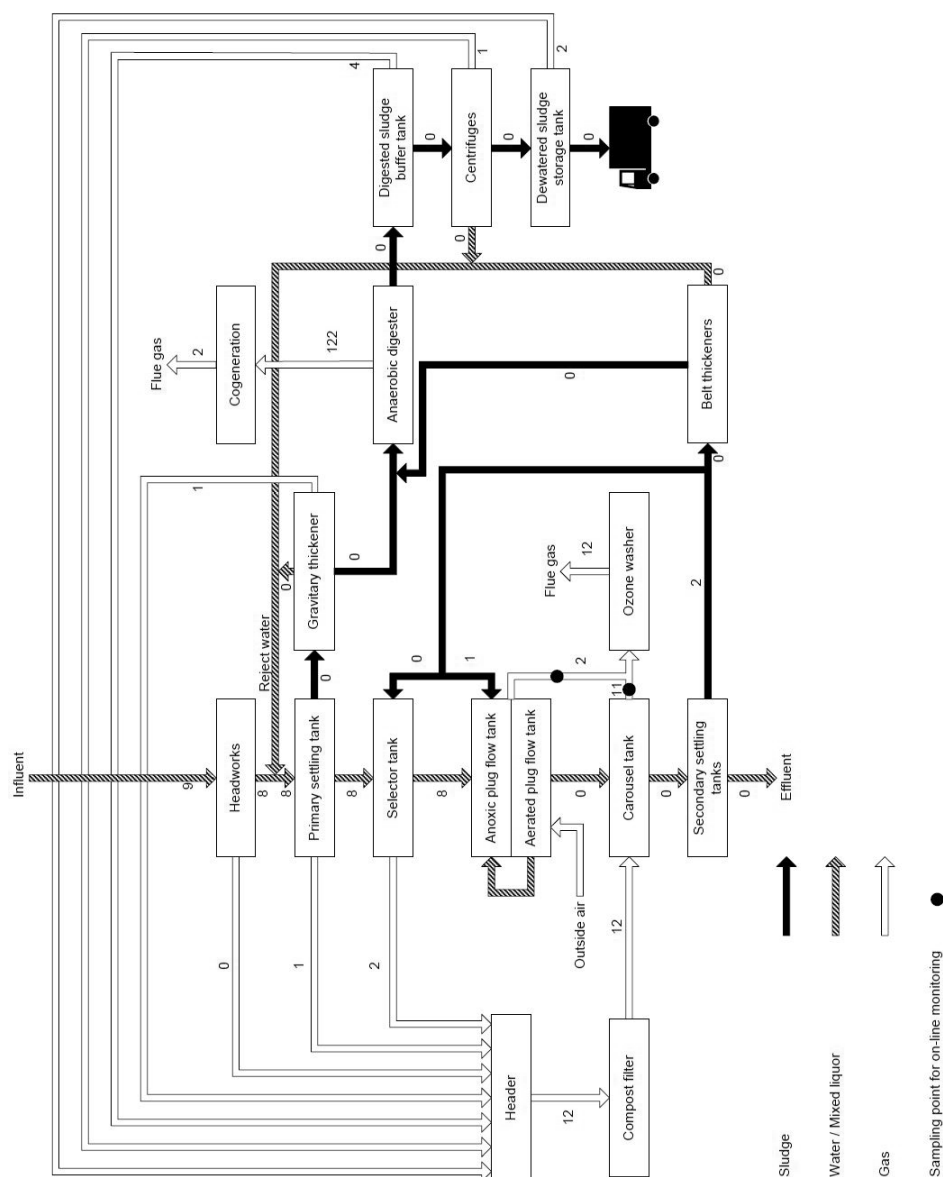
Figure 5.1. Process scheme of the Kralingseveer WWTP with the estimated mass flow rates (kg CH$_4$ h^{-1}) between the different unit processes.

Except for the secondary clarifiers, all process elements of this WWTP are covered in order to collect the off-gas for gas treatment. Apart from the off-gas coming from the plug flow reactor and the carousel, all off-gas is collected and first directed to a compost filter to avoid odor nuisance. The air coming from the compost filter is blown into the headspace of the covered carousel reactor. The off-gas from the plug flow reactor and the carousel are

finally disinfected in an ozone washer before it is released through the flue gas stack. Since the air coming from the compost filter is used to aerate the carousel, the gas flow to the ozone washer makes up the off-gas of the entire plant (except for emissions from the secondary clarifiers).

On-line measurements of the plant's total off-gas

From 14 October 2010 until 28 September 2011, gas was withdrawn from the off-gas pipes going from the carousel and the plug flow reactor to the ozone washer. After passing through a condenser, the gas was directed to an on-line Servomex 4900 infrared gas analyzer, resulting in an estimation of methane in the overall off-gas flow leaving the water line and the sludge line of the plant. The gas flow rates in the off-gas pipes were measured weekly using a Tesco 435 hot wire anemometer. Since the blowers of the off-gas collection system were operated at constant power, the gas flow rates were constant. By multiplying the measured concentrations with the prevailing flow rate in the off-gas pipes, the methane fluxes from the plug flow reactor and the carousel were calculated.

Mass balances over each unit process

In order to identify the sources and sinks of methane on the plant, a mass balance was set up over each unit process. Therefore, the methane load in every single liquid and gas stream had to be calculated from the measured flow rates and corresponding concentrations. A detailed overview of these calculations is provided in supplementary materials 2. The required measurements and sampling took place five times between 4 March and 12 August 2011, except for the exhaust gas of the cogeneration unit, which was measured only once. Flow rates of the gaseous streams were measured using an anemometer, while gas samples were collected with gas bags. The concentration of the content of the gas bags was measured with a Varian 3800 gas chromatograph equipped with a flame ionization detector (GC-FID). Flow rates of liquid streams were either available from the plant's SCADA system, or could be calculated from available data. Dissolved methane concentrations were measured with the salting-out method described below. For each stream, the methane loads determined during the five measurement campaigns were averaged.

For each unit process, the difference between the average methane load coming in and going out is the amount of methane that is produced or converted. In other words, it is possible to identify sources and sinks of methane on the plant, respectively. A unit process was only positively identified as a methane source or sink if the standard deviation of the load was smaller than the methane production or consumption.

Salting-out method for sampling methane in the liquid phase

For sampling dissolved methane, the salting-out method of Gal'chenko et al. (2004) was slightly adapted. The protocol that was used in this study can be found in supplementary material 3. Before the start of each sampling round, serum bottles of 120 mL were filled with 20 g NaCl. At the different sampling locations at the WWTP, samples were collected

with a sampling beaker. From this beaker, 50 mL of sample was added carefully to a serum bottle filled with salt, using a syringe with a catheter tip and a 10 cm silicone tube. While emptying the syringe into the bottle, the silicon tube was held under the rising liquid surface in order to keep the liquid-gas interface as small as possible to avoid stripping. Immediately after adding the syringe content to the bottle, the bottle was sealed with a rubber stopper and an aluminum cap. The sealed bottle was shaken vigorously in order to speed up the dissolving of the salt.

At 20 °C the solubility of NaCl in water is about 360 g L^{-1}, so these samples, containing 400 g NaCl L^{-1}, were over-saturated. As a consequence of the high salt concentration, the microbial activity in the sludge samples is halted, and the dissolved gases are salted out. Gal'chenko et al. (2004) also added potassium hydroxide and/or merthiolate to the sample as a bactericide, but this was omitted in the samples from the WWTP since high salt concentrations (even far below saturation) are known to inhibit microbial activity both in the activated sludge (Zobell et al., 1937; Pernetti and Di Palma, 2005) and in the anaerobic digestion process (Feijoo et al., 1995).

Dissolved methane, but also the other dissolved gases such as carbon dioxide escape from the liquid phase to the headspace of the serum bottles. This results in a pressure build-up in the headspace. Gal'chenko et al. (2004) neglected this pressure build-up, but for the samples of the present study, the pressure build-up was clearly noticeable since they contained substantially higher amounts of dissolved gases. Therefore it was necessary to take into account the pressure build-up due to the salting-out of the dissolved gases. Before sampling the headspace of the samples for analysis with GC-FID, the pressure in the headspace was equilibrated with the atmosphere by allowing the gas in the headspace to expand in a submerged graduated syringe. The increase in gas volume was used to calculate the pressure build-up in the headspace.

After the gas pressure in the headspace was brought to atmospheric pressure, the headspace was sampled with a gas syringe and analyzed. The amount of methane in the headspace before expansion was calculated from the concentration, the measured volume of the headspace of the sealed bottle and the headspace pressure after the pressure build-up that was calculated from the volume expansion of the headspace. Before the sample was saturated with salt, this amount of methane was completely dissolved in the liquid sample. By dividing this amount by the sample volume (50 mL) the original methane concentration in the liquid was established.

In order to compare the salting-out method with another method that had been used to sample dissolved methane, seventeen liquid streams with a solids content that was low enough to allow easy filtering were sampled using both the salting-out method of the present study and the vacuum tube method of Guisasola et al. (2008). According to the latter method, a syringe was filled with the sampled liquid. With a syringe driven filter unit and a hypodermic needle, the liquid was injected in an 11 mL Vacutainer blood serum tube

(BD Diagnostics #367896). With a sample volume of 5 mL, ca. 97 % of the methane is transferred to the headspace (Guisasola et al., 2008). The headspace was sampled with GC-FID. The amount of methane in the Vacutainer was calculated using Henry's law and a mass balance. The volume of the sample in the Vacutainer was determined by weight. This validation was also performed in the laboratory by sampling two prepared solutions of methane dissolved in water with both the salting-out method and the vacuum tube method. The solutions had an approximate concentration of 0.5 and 2.5 mg L^{-1}. For each solution and for each method, sampling was done in triplicate.

It was observed that empty Vacutainers after equilibrating with the atmosphere already contained about 400 ppm of methane. This methane possibly originated from the clot activator coating on the inside of the tube wall. In order to verify this, a number of uncoated Vacutainer urine collection tubes (BD Bioscience #364915) were tested for the presence of methane. Also these uncoated tubes contained about 400 ppm of methane. These measurements were done with GC-FID, and corroborated with the infrared gas analyzer that was used for the online methane measurements at the WWTP. Both in the field and in the laboratory validation, the total amount of methane in the sample tubes was reduced with the average amount of methane that was measured in six empty Vacutainer tubes.

Results

Total methane emission from the WWTP

The daily average methane emission from the entire treatment plant at Kralingseveer during the measuring campaign (from 14 October 2010 until 28 September 2011) was 302 kg CH_4 d^{-1}, with a standard deviation of 83 kg CH_4 d^{-1}. The reported total methane emission comprises all methane in the off-gas that is collected in the plant's ventilation system and sent to the ozone washer, but the plant has two parts of which the off-gas is not collected for disinfection in the ozone washer: the uncovered secondary settlers and the exhaust of the gas engines of the cogeneration plant. The secondary settlers may emit some methane, but from the mass balance over the secondary settlers it appears that this amount will be very low (Table 5.2). The measured methane slip due to incomplete combustion in the gas engines was 1.3 %, resulting in an additional methane emission of 38 kg CH_4 d^{-1}.

The Dutch Ministry of Housing, Spatial Planning and the Environment (VROM, 2008) provided emission factors that are based on the IPCC inventory guidelines (IPCC, 2006). In order to allow comparison with these emission factors and with the results from other studies, the plant's total methane emission can be normalized in several ways: by population served, by wastewater flow or by incoming COD. Table 5.1 summarizes the resulting emission factors, as well as the emission factors from the other reported full-scale studies and the VROM emission factors. Apparently, about 1 % (0.53 - 1.20 %) of the incoming COD is emitted as methane in the Dutch treatment plants. At the Durnham

plant, 0.16 % of the incoming BOD_5 was emitted as methane, while at the Jinan plant, the emission factor was 0.08 % of the incoming COD.

Sinks and sources of methane

All the methane containing streams of the WWTP are summed up in Table 5.2, while Figure 5.1 shows the Kralingseveer WWTP lay-out with the estimated methane mass flow rates between the different unit processes. Using these mass flow rates, mass balances of methane were constructed over every unit process. From these mass balances, sources and sinks of methane could be identified.

For sampling dissolved methane, a method was used that consisted of salting-out the methane and analyzing the headspace of the recipient with gas chromatography. The method was validated by sampling a number of streams with both the salting-out method and with a vacuum tube method. Figure 5.2 shows the result for the validation. The results obtained by both methods correlate extremely well (R^2 = 0.99). The validation in the laboratory also yielded satisfactory results (Table 5.3).
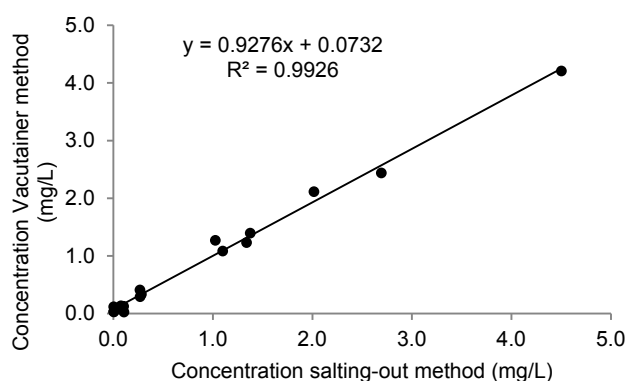
Figure 5.2. Scatter plot of dissolved methane concentrations as determined with the salting-out method and with the vacuum tube method.

Table 5.2. Methane mass balances over the various unit processes(kg CH_4 h^{-1}).

	IN	$\bar{x}$	$\pm$	σ	OUT	$\bar{x}$	$\pm$	σ	BALANCE $\bar{x}$	$\pm$	σ
Headworks	Influent	9	±	3	Water to primary settling tank	8	±	3			
					Off-gas	0	±	0			
	Total	**9**	**±**	**3**	**Total**	**8**	**±**	**3**	**-1**	**±**	**4**
Primary settler	Water from headworks + reject water from centrifuges, belt thickeners and gravitary thickener for primary sludge	8	±	2	Water to selector tank	8	±	3			
					Primary sludge	0	±	0			
					Off-gas	1	±	1			
	Total	**8**	**±**	**2**	**Total**	**9**	**±**	**3**	**2**	**±**	**4**
Selector	Water from primary settling tank	8	±	3	Liquor to plug flow reactor	8	±	3			
	Return sludge	0	±	0	Off-gas	2	±	1			
	Total	**8**	**±**	**3**	**Total**	**9**	**±**	**3**	**1**	**±**	**4**
Plug flow reactor	Liquor from selector	8	±	3	Liquor to carousel reactor	0	±	0			
	Return sludge	1	±	1	Off-gas	2	±	1			
	Total	**9**	**±**	**3**	**Total**	**2**	**±**	**1**	**-7**	**±**	**3**
Carousel reactor	Liquor from plug flow reactor	0	±	0	Liquor to secondary settling tank	0	±	1			
	Air from compost filter	12	±	3	Off-gas	11	±	3			
	Total	**12**	**±**	**3**	**Total**	**11**	**±**	**3**	**-1**	**±**	**5**
Secondary settling tank	Liquor from carousel reactor	0	±	1	Effluent	0	±	0			
					Secondary sludge	2	±	1			
	Total	**0**	**±**	**1**	**Total**	**2**	**±**	**1**	**1**	**±**	**1**
Belt thickeners	Excess sludge supply	0	±	0	Thickened sludge to digester	0	±	0			
					Reject water to primary settling tank	0	±	0			
					Off-gas	0	±	/			
	Total	**0**	**±**	**0**	**Total**	**0**	**±**	**0**	**0**	**±**	**0**

	IN	$\bar{x}$	±	σ	OUT	$\bar{x}$	±	σ	BALANCE $\bar{x}$	±	σ
Gravitary thickener for primary sludge	Primary sludge	0	±	0	Overflow to primary settling tank	0	±	0			
					Thickened primary sludge	0	±	0			
					Off-gas	1	±	1			
	Total	**0**	**±**	**0**	**Total**	**1**	**±**	**1**	**1**	**±**	**1**
Anaerobic digester	Total sludge supply	0	±	0	Effluent to buffer tank	0	±	0			
					Gas to cogeneration	122	±	28			
	Total	**0**	**±**	**0**	**Total**	**122**	**±**	**28**	**122**	**±**	**28**
Digested sludge buffer tank	Effluent from digester	0	±	0	Digested sludge to centrifuges	0	±	0			
					Off-gas	4	±	1			
	Total	**0**	**±**	**0**	**Total**	**5**	**±**	**1**	**4**	**±**	**1**
Centrifuges	Digested sludge from buffer tank	0	±	0	Dewatered sludge to storage tank	0	±	0			
					Reject water to primary settling tank	0	±	0			
					Off-gas	1	±	5			
	Total	**0**	**±**	**0**	**Total**	**0**	**±**	**5**	**0**	**±**	**0**
Dewatered sludge storage tank	Dewatered sludge from centrifuges	0	±	0	Dewatered sludge for incineration	0	±	0			
					Off-gas	2	±	1			
	Total	**0**	**±**	**0**	**Total**	**2**	**±**	**1**	**2**	**±**	**1**
Compost filter	Off-gas to filter	12	±	4	Gas to carousel reactor	12	±	3			
	Total	**12**	**±**	**4**	**Total**	**12**	**±**	**3**	**0**	**±**	**5**
Cogeneration	Biogas from digester	122	±	28	Methane slip	2	±	0			
	Additional natural gas from grid	3	±	/							
	Total	**125**	**±**	**28**	**Total**	**2**	**±**	**0**	**-123**	**±**	**28**

$\bar{x} \pm \sigma$ designates mean ± standard deviation

Table 5.3. Results from laboratory validation of salting-out method and vacuum tube method.

Approximate concentration of prepared solution (mg L^{-1})	Concentration determined by salting-out method (mg L^{-1})	Concentration determined by vacuum tube method (mg L^{-1})
	$\overline{x} \pm \sigma$	$\overline{x} \pm \sigma$
0.5	0.51 ± 0.02	0.48 ± 0.05
2.5	2.78 ± 0.09	2.36 ± 0.21

$\overline{x} \pm \sigma$ designates mean ± standard deviation

Sources of methane at the plant itself are the primary sludge thickener, the exhaust gas of the cogeneration plant, the buffer tank for the digested sludge and the storage tank for the dewatered sludge. The latter two contribute substantially to the methane emission from the plant. From Table 5.2, it can be calculated that the buffer tank is responsible for 40 ± 15 % of the emission from the carousel reactor and 35 ± 13 % in the total emission, while the dewatered sludge storage tank has a share of 17 ± 8 % in the emission from the carousel and 15 ± 6 % in the total emission. Expressed as specific methane production rate, the buffer tank for the digested sludge produced about 3.5 g CH_4 kg^{-1} TSS d^{-1}, while the storage tank for the dewatered sludge produced about 1 g CH_4 kg^{-1} TSS d^{-1}. To compare, the digester had a production rate of 9 g CH_4 kg^{-1} TSS d^{-1}.

Besides the methane produced on the plant itself, methane also enters the plant from outside via the influent. The influent contains methane that has been formed in the sewer. The methane load was estimated as 1 % of the influent COD load. From the measurements it was clear that a significant amount (roughly 80 % of the dissolved methane in the influent, cf. and Figure 5.1) of methane is oxidized in the plug flow reactor. From Figure 5.3 it appears that methane was removed in the aerated part of the plug flow tank only.
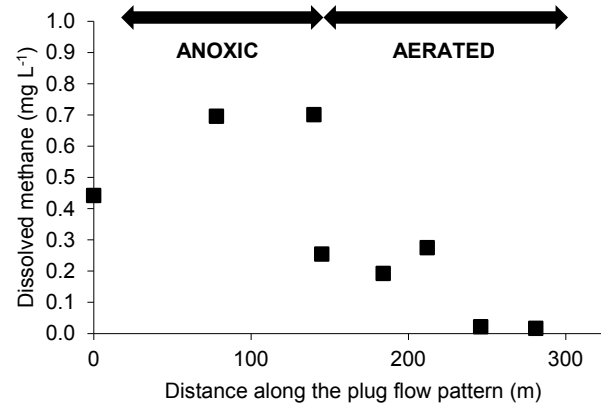
Figure 5.3. Dissolved methane concentration along the path of the plug flow.

Methane emission dynamics

Figure 5.4 shows the variation of the daily average methane emissions from the full treatment plant during the entire measurement period. Of the total emission, about 12 % on average comes from stripping of methane in the plug flow reactor, while the remaining 88 % is coming from the headspace of the carousel reactor. The methane in the off-gas from the plug flow reactor is only methane that is stripped after it enters the tank, since the tank is aerated with fresh air only. The emission from the carousel reactor is higher than the emission from the plug flow reactor, because the carousel is aerated with methane containing air coming from the compost filter. The compost filter treats the off-gas from all covered parts of the plant, except for the plug flow and the carousel reactor. It can reasonably be expected that that most of the methane coming from the carousel reactor is effectively derived from this ventilation air.
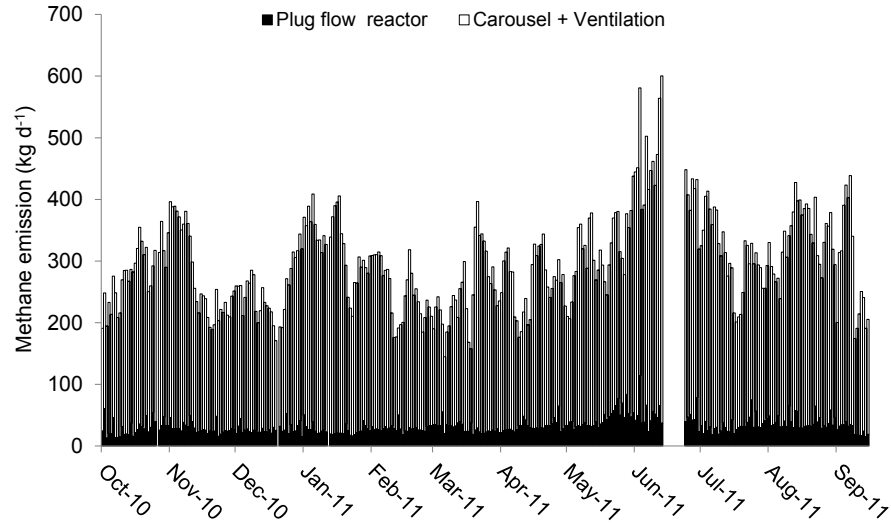
Figure 5.4. Daily methane emission from the plug flow reactor, and from the carousel and the ventilation system.

Figure 5.5 shows the on-line methane emission from the plug flow reactor and the on-line flow rate of the influent. The graph shows the diurnal variation of both variables during one arbitrary week in the measurement period. The coefficient of determination R^2 between influent flow rate and methane emission from the plug flow reactor was 0.20 for the entire measurement period.
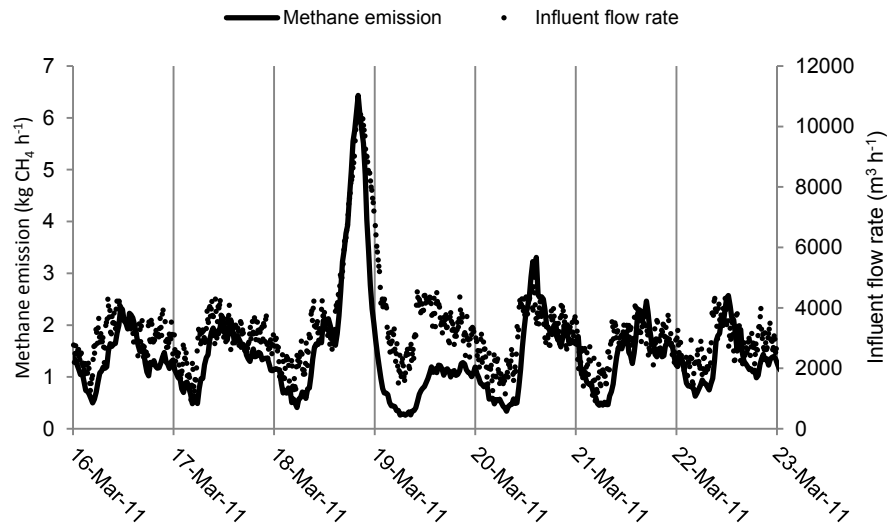
Figure 5.5. On-line methane emission from the plug flow reactor and on-line influent flow rate during one week in March 2011. The vertical gridlines indicate midnight. 18 March 2011 is a wet weather day.

Figure 5.6 compares the on-line methane emission from the carousel reactor, which amounts to the off-gas from the ventilation system, with the on-line sludge content of the dewatered sludge storage tank. Again, the graph shows an arbitrary week in the measurement period. For the entire measurement period, the linear correlation (R^2) between the dewatered sludge content in the storage tank and the emission from the carousel reactor was 0.44.
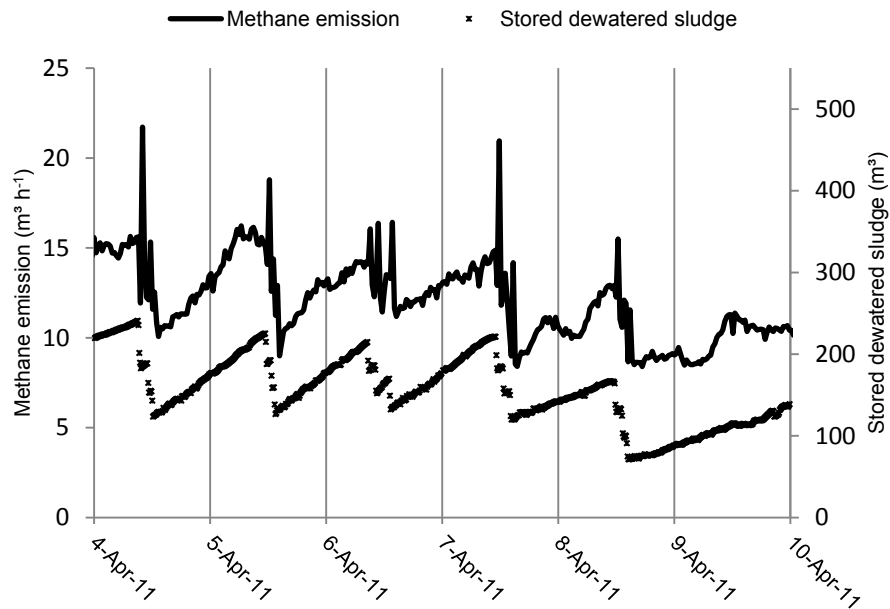
Figure 5.6. On-line methane emission from the carousel reactor and the ventilation system, and on-line volume of the dewatered sludge storage tank content during one week in April 2011. The vertical gridlines indicate midnight.

In order to explain the long-term variation of the methane emission during the measurement period, the possible correlations between the daily emission and the daily values of a number of relevant process variables were checked (Table 5.4). The emission from the plug flow reactor was only slightly correlated with the temperature of the mixed liquor (which ranged from 8.7 to 21.4 °C). For the emission from the carousel reactor and the ventilation system (i.e. after the compost filter), there was only a (weak) correlation with the amount of sludge that was stored in the dewatered sludge storage tank. For the digested sludge buffer tank, data about the stored amount of sludge were not available.

Table 5.4. Determination coefficient (R^2) between daily mean values of emission and relevant process variables. All determination coefficients were found significant at an alpha level of 0.05.

	Emission from the plug flow reactor (kg CH_4 h^{-1})
Influent flow rate (m^3 d^{-1})	0.03
Mixed liquor temperature (°C)	0.17
	Daily emission from the carousel reactor and the ventilation system (kg CH_4 h^{-1})
Atmospheric temperature (°C)	0.08
Biogas production (m^3 d^{-1})	0.00
Residence time of the anaerobic digester (d)	0.08
Sludge supply to the centrifuges (m^3 d^{-1})	0.15
Amount of sludge stored in the dewatered sludge storage tank (m^3)	0.58

During the monitoring period, the anaerobic digester had an average residence time of 26 days. This may cause a time lag between the effect of the anaerobic digestion related process variables on the actual methane emissions. To suppress the effect of this time lag, the relationships between the emission and the variables related to the anaerobic digestion process on the plant were also verified using the moving averages over 26 days. The results are shown in Table 5.5. Indeed, the correlations for the moving averages over 26 days turned out higher than the correlations between the daily values. The emission from the carousel and the ventilation system appears to correlate relatively well with the residence time of the sludge in the anaerobic digester, with the amount of sludge that is fed to the dewatering centrifuges and with the amount of sludge stored in the dewatered sludge storage tank.

Table 5.5. Determination coefficient (R^2) between 26 day moving averages of emission and relevant process variables. All determination coefficients were found significant at an alpha level of 0.05.

	Emission from the carousel reactor and the ventilation system (kg CH_4 h^{-1})
Atmospheric temperature (°C)	0.14
Biogas production (m³ d^{-1})	0.11
Residence time of the anaerobic digester (d)	0.84
Sludge supply to the centrifuges (m³ d^{-1})	0.72
Amount of sludge stored in the dewatered sludge storage tank (m³)	0.70

Discussion

Sampling method for dissolved methane

The validation of the salting-out method by comparing the method with the vacuum tube method yielded very good results, both in the field and in the laboratory. The salting-out method is accurate, and since the standard deviation of the replicas of the salting-out method was smaller than the standard deviation of the replicas of the vacuum tube method, it is in fact even more precise.

The Vacutainers that were used for the validation were blood serum tubes with a clot activator coating (BD Bioscience #367896) similar to the ones used by Foley et al. (2009) (BD Bioscience #367895). It was found out that empty Vacutainers after equilibrating with the atmosphere already contained about 400 ppm methane. The supplier of the Vacutainer tubes could not give any information regarding the presence of methane. Nonetheless, Genge (1991) showed that coated sterilized Vacutainer tubes (Becton Dickinson) indeed contained up to 248 ppm of methane. According to Genge, the gamma sterilization applied to the tubes cross-links the silicone polymers in the coating. During this process, methane is split out causing contamination. However, uncoated Vacutainer urine collection tubes (BD Bioscience #364915) also contained about 400 ppm of methane. Possibly the methane comes from the rubber septum or the plastic of which the tube itself is made instead of from the coating, but that is irrelevant for the present study.

The salting-out method has some practical advantages over other methods. No toxic compounds are used for stopping the biological consumption or production of methane.

In previous studies, this is usually obtained by using inhibiting compounds, such as mercury chloride (Hatamoto et al., 2010; Wang et al., 2011a). However, the use of toxic inhibiting compounds may have a harmful effect on the environment and also puts the scientist at risk for harmful exposure to these chemicals. Another way to inhibit biological activity after taking the sample is by filtering the sample before it is brought into the recipient (Guisasola et al., 2008; Foley et al., 2009; Guisasola et al., 2009), but filtration is only possible for liquids with low solids content, like settled wastewater or treated effluent. On the contrary, the salting-out method can also be applied to slurries like digested sludge or thickened sludge.

Methane emission compared to carbon dioxide emission

The plant's total methane emission, 2,728 ton year $^{-1}$ expressed as CO_2-equivalents, exceeded the carbon dioxide emission related to electricity and natural gas consumption (1,500 ton year^{-1}). In the other two Dutch plants, the methane emission was far lower than the carbon dioxide emission (STOWA, 2010). In the Kortenoord plant, the methane emission amounted to 960 ton CO_2-equivalents year^{-1}, while carbon dioxide was emitted at a rate of 5,820 ton year^{-1}. In Papendrecht the methane emission was 730 ton CO_2-equivalents year^{-1} and the carbon dioxide was 3,458 ton year^{-1}.

Since the normalized methane emissions from the three Dutch plants did not differ that much from each other in comparison with the emission from the Jinan and the Durham plants (Table 5.1), the higher emission of carbon dioxide from Papendrecht and Kortenoord compared to those plants' methane emission was due to their higher indirect carbon dioxide emission. Kortenoord and Papendrecht emitted about 0.41 and 0.46 kg CO_2 m^{-3} wastewater, respectively, while Kralingseveer emitted only 0.05 kg CO_2 m^{-3} wastewater. This difference was due to the presence of the anaerobic digester at Kralingseveer. It produced enough biogas to provide about 60 % of the plants energy requirements, while Kortenoord and Papendrecht took all required energy from the gas and power grid.

For the Durham and Jinan plants, the ratio between the methane and the carbon dioxide emission could not be calculated. Wang et al. (2011a) did not measure carbon dioxide. Czepiel et al. (1993) only measured methane and the biologically produced carbon dioxide that was emitted from the reactors, but not the carbon dioxide that was produced indirectly as a result of fossil fuel combustion to generate the energy required for the operation of the wastewater treatment plant. Only the latter contributes to increased atmospheric carbon dioxide concentrations.

Sinks and sources of methane

The headworks

At the Kralingseveer WWTP, quite some methane entered the plant via the incoming wastewater. The amount that was stripped in the headworks was negligible. Most of the methane that was formed in the sewer went through the headworks to the primary settler, to the selector and finally to the plug flow reactor. The total emission from these four parts amounted to 31 ± 16 % of the total emission going to the ozone washer (Table 5.2 and Figure 1.1). However, the reject water from the belt thickeners and the centrifuges is returned to the primary settler, together with the overflow water of the primary sludge thickener while the return sludge is fed to the selector and the plug flow reactor. These streams also contain some methane, of which a part can be emitted from the primary settler, the selector and the plug flow reactor. This implies that the methane in the influent contributed certainly less than 31 ± 16 % to the total methane emission from the plant.

The amount of methane that was dissolved in the influent was not measured by Czepiel et al. (1993) nor by STOWA (2010) nor by Wang et al. (2011a). However, for Papendrecht and Kortenoord (STOWA, 2010) 86 % and 77 % respectively, of the overall methane emission could be traced back to the influent. This could be concluded from the emissions from the headworks and the aeration tank. Due to the short residence time in the headworks, it was unlikely that the methane was formed there. Rather, it was produced in the pressurized sewer mains and stripped in the headworks. This also holds for the methane emission from the aeration tanks. From the profile of dissolved methane depicted in Figure 5.3 one could conclude that methane is produced in the anoxic part of the plug flow. However, it is likely that the increase in dissolved methane between the start of the plug flow reactor and 80 m further along the plug flow is a sampling artifact due to the configuration of the plug flow reactor. At the start of the plug flow reactor, the mixed liquor entering the tank from the selector tank is mixed with the recycle mixed liquor coming from the end of the plug flow reactor. Since the second part of the plug flow reactor is aerated, the latter stream does not contain any methane anymore, as can be seen on Figure 5.3. Due to non-ideal mixing, it is possible that some of the samples that were taken at the beginning of the plug flow did contain the recycle liquor coming from the aerated part of the plug flow. This explains why the average methane concentration at the beginning of the plug flow is lower than 80 m further along the plug flow. Actual production of methane in aeration tanks is highly improbable because of the anoxic or aerobic conditions in such tanks. So, instead of being produced in the aeration tanks, the methane that was emitted from the Papendrecht and Kortenoord WWTPs must have been produced in the sewer and the part that was not stripped in the headworks was subsequently stripped when it entered the aeration tank. For the Jinan plant, the reported methane emission coming from the influent pump station and the aerated grit chamber, which amounts to the methane from the influent that is stripped upon entering the plant,

was only 7 to 12 % of the plant's total methane emission (Wang et al., 2011a). For the Durham plant, the methane emission at the entrance of the plant was not reported (Czepiel et al., 1993).

When the part of the emission that can be traced back to the methane coming in with the influent is normalized with incoming COD, this part of the emission amounts to 0.0035, 0.0046 and 0.0067 kg CH_4 (kg $COD_{influent}$)$^{-1}$ for the plants of Kralingseveer, Kortenoord and Papendrecht, respectively. A possible explanation for the higher value of Papendrecht is the way in which the raw wastewater enters the WWTP. At Kralingseveer and Kortenoord, the raw wastewater is pumped up by centrifugal pumps, while at Papendrecht, the wastewater is pumped up by screw conveyors. In the latter, there is intense contact between the wastewater and the air, leading to a higher stripping rate of methane. This should be taken into consideration when designing new wastewater treatment plants.

Sludge storage
From the mass balances, it is evident that sludge storage contributes significantly to the methane emissions. Methane is produced both in the digested sludge buffer tank, as well as in the dewatered sludge storage tank.

The digested sludge has a considerable residual methane potential because the conversion of the influent sludge to biogas in a completely mixed anaerobic digester is never complete. For instance when a retention time of 20 days is applied in a digester, 5 % of the fresh incoming sludge is directly discharged from the system again. Consequently, during digested sludge storage a significant amount of methane can still be produced. The buffer tank for the digested sludge can actually be considered as a second completely mixed digester in series with the two parallel anaerobic sludge digesters, albeit with a residence time of maximum five days and a temperature of about 25 °C instead of 35°C. The methane production in this tank is about 3 ± 1 % of the total methane production in both the anaerobic digester and the buffer tank.

Several studies have been dedicated to additional methane production during digested sludge storage. Hansen et al. (2006) investigated the residual methane that was produced during storage of the effluent of a digester that was used for the anaerobic treatment of municipal organic waste. They estimated the residual methane potential at 3% of the CH_4 potential of the organic waste treated in biogas plants with a typical retention time of 15 days. Liebetrau et al. (2010) looked into the additional methane that was produced during storage of digestate from a mix of manure and energy crops. In their study, the residual methane potential was on average 5.03 % of the total methane production (solid retention time not mentioned). Weiland et al. (2009) obtained an average residual methane potential 3.5 % of the total methane production for one-stage biogas installations fed with manure and crops and a solid retention time between 30 and 140 days. So far, the residual methane

potential of digested sewage sludge has received no attention, to the authors' best knowledge.

A valorization of the biogas from the digested sludge buffer tank would result in an additional electricity production of about 3 ± 1 % and a reduction of 35 ± 13 % in the total methane emissions. Normalized by the incoming COD, this would imply a decrease in methane emission of 0.0040 ± 0.0015 kg CH_4 (kg $COD_{influent}$)$^{-1}$. One way to valorize the residual methane that is produced in the buffer tank is to use the ventilation air from the buffer tank as combustion air in the gas engines of the cogeneration plant. The gas engines use on average 1800 m^3 h^{-1} of air, while the flow rate of the ventilation gas coming from the buffer tank is about 1000 m^3 h^{-1}. The remaining 800 m^3 h^{-1} could be taken from the ventilation air from the dewatered sludge storage tank. This stream has the second highest methane concentration, but since its flow rate is 1500 m^3 h^{-1}, only part of this stream could be used. The result would be another 1 % of additional electricity production and another 15 ± 6 % reduction in the total methane emission. Other off-gas streams could be used as well but since their methane concentration is lower, less methane could be recovered. The methane concentration in the ventilation air could of course be increased by using less fresh air for ventilation. This would result in less diluted methane streams, but then the ventilation system should be adapted to handle methane concentrations that exceed the lower explosive limit of methane in air, which is 4.4 % (TNO/VNCI, 2008).

Exhaust of the cogeneration plant
The methane slip of the gas engines consists for 98 % of methane that was produced in the anaerobic digester, while the remainder comes from the external natural gas that complements the biogas. The methane slip was 1.3 %. Although it was based on a single measurement, this value is comparable with other studies that report methane slip from biogas plants. Woess-Gallasch et al. (2010) mention a methane slip of 1.79 % as a representative value for Austrian biogas plants. Liebetrau et al. (2010) measured the methane slip of seventeen cogeneration units and obtained an average methane slip of 1.73 %.

Primary sludge thickener
Primary sludge contains a lot of readily biodegradable matter. Since the gravitary thickener for the primary sludge has a residence time of about one day, since the conditions are anaerobic and since the primary sludge is inoculated with methanogenic bacteria from the sewer, it is perfectly understandable that this is a source of methane, be it less than the other sources (Table 5.2).

Activated sludge as a methane sink
Dissolved methane which enters an activated sludge tank can either be biologically converted to carbon dioxide and water or it can be stripped. Since methane has a global warming potential of 25 CO_2-equivalents, conversion of methane to carbon dioxide leads

to a smaller greenhouse gas footprint. Therefore, efforts should be made to promote conversion over stripping. In the case of Kralingseveer WWTP, 80 % of the dissolved methane entering the plug flow reactor was converted. If this tank would be a CSTR instead of a plug flow, the dissolved methane in the tank would be more diluted. As a result, the driving force for stripping would be smaller, allowing more methane to stay in solution and to be biologically converted. The methane oxidizing capacity of activated sludge could also be applied for the conversion of gaseous methane, provided that the mass transfer of methane from the gas phase to the liquid phase is enhanced, for instance by using the methane containing off-gases in a bubble aeration system instead of surface aeration.

It has been suggested that methane can act as an electron donor during the denitrification process (Raghoebarsing et al., 2006; Ettwig et al., 2010). That would imply a saving in aeration costs, since no oxygen has to be supplied for the oxidation of methane. However, along the length of the anoxic part of the plug flow reactor, the methane concentration did not decrease (Figure 5.3). This indicates that methane is not consumed during the denitrification process. When realizing that already a very significant fraction of the methane is converted aerobically, it is likely that attention to design can further optimize the aerobic methane removal and minimize the emissions.

The role of anaerobic digestion in the plant's methane emission
While the methane emission of the Kortenoord and the Papendrecht WWTP could be mainly attributed to the methane in the influent, the methane emission from the Kralingseveer WWTP was mainly due the anaerobic sludge treatment. This also explains this plant's higher emission in comparison with the Jinan and the Durnham plant, both without anaerobic sludge treatment. 72 ± 23 % of the total methane emissions came from the unit processes that are related to the anaerobic digestion facility: the gravitational thickener for the primary sludge, the centrifuge, the buffer tank for the effluent of the digester, the storage tank that contains the dewatered sludge and the methane slip from the gas engines. Therefore, the anaerobic digestion facilities should certainly be taken into account when determining the greenhouse gas footprint of a WWTP.

Because the biogas is used to provide part of the energy requirement of Kralingseveer WWTP, some fossil fuel consumption and its concomitant carbon dioxide emission is avoided. The International Energy Agency (IEA, 2010) estimates the carbon dioxide emission from energy and heat production in the Netherlands at 0.395 kg CO_2 kWh^{-1} (using the typical Dutch mix of energy resources). Based on the electricity production from biogas in the WWTP's cogeneration unit (13 MWh d^{-1}), the plant's avoided amount of carbon dioxide emission was calculated to be 5.2 ton CO_2d^{-1}. However, the methane emitted by the unit processes related to anaerobic sludge treatment (i.e. the gravitational thickener for the primary sludge, the centrifuge, the buffer tank for the effluent of the digester, the storage tank that contains the dewatered sludge and the methane slip from the

gas engines) amounted to 230 kg CH_4 d^{-1}. Taking into account that methane has a GWP of 25 CO_2-equivalents (IPCC, 2007a), the amount of methane that is emitted from the anaerobic sludge treatment corresponds to an emission of 5.7 ton CO_2 d^{-1}. In other words, the methane emitted from the anaerobic digestion facility exceeds the carbon emission that is avoided by valorizing the biogas. Besides, the methane that is emitted to the atmosphere not only contributes to the greenhouse gas footprint of a WWTP, it also implies a waste of energy since the methane emitted from the unit processes that are related to the anaerobic digestion (7 ± 2 % of the produced methane) could potentially have been used as a fuel for the cogeneration plant.

Although biogas production from waste sludge may be a sustainable technology from an energy point of view, it has in this case no benefits over fossil fuel-derived energy regarding greenhouse gas emissions. Nonetheless it should be emphasized that the emission of methane is not intrinsic for anaerobic digestion, but that a better design and good housekeeping may lead to a drastic mitigation of the emission.

Dynamic behavior of the methane emissions

Diurnal variability

The diurnal pattern of the emission from the plug flow reactor coincided with the diurnal pattern of the influent flow (Figure 5.5). The morning peak of influent flow is closely followed by an increase in methane emission, and on wet weather days, the emission also appeared to be higher than on dry weather days. Despite the similarity between the emission and the influent flow rate patterns, the correlation was not really high ($R^2 = 0.20$). Indeed, Figure 5.7 reveals that a low influent rate corresponds with a low methane emission from the plug flow reactor, but at a high influent flow rate, the emission can be both high and low. This can be explained by taking into account the dynamic behavior of the methane emission during periods with a high influent flow rate. Figure 5.8 shows the pattern of the methane emission and the influent flow rate during a prolonged wet weather period (characterized by an influent flow rate higher than 6,000 m^3 h^{-1}). It is clear that the start of a prolonged rain event coincides with a methane emission peak from the plug flow reactor. However, while the influent flow rate remains high for about two days, the methane emission, after showing an initial peak, drops down to a low level after a few hours. This pattern can be explained by considering the presence of biodegradable material in the sewer system. Only if biodegradable material is present in the sewer, methane can be produced. At the beginning of a rain event, a lot of biodegradable material is still present in the sewer and as a consequence, a lot of methane enters the WWTP via the influent, resulting in an emission peak. However, as the rain persists, biodegradable material is flushed out of the sewer, leaving relatively clean water in the sewer. The lack of biodegradable material results in less methane being formed in the sewer and less methane that enters the plant. This is reflected in the emission pattern during a prolonged rain event and during a short period after the rain event.
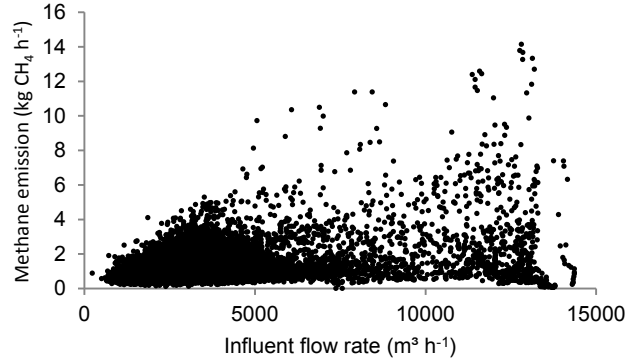
Figure 5.7. Scatter plot of methane emission from the plug flow reactor vs. the influent flow rate.
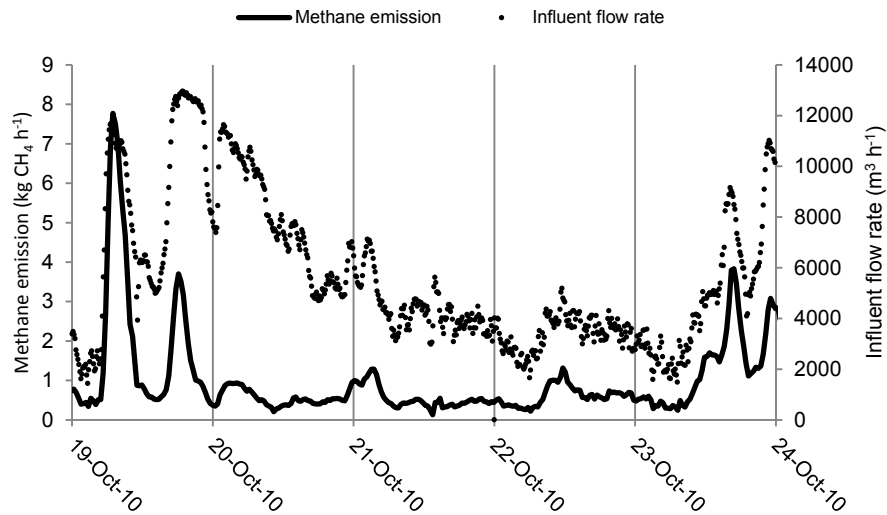
Figure 5.8. On-line methane emission from the plug flow reactor and on-line influent flow rate during a wet weather period. The vertical gridlines indicate midnight.

As can be seen in Figure 5.6, the short-term emission pattern from the carousel, mainly coming from the off-gas from the ventilation system, is in line with the content of the dewatered sludge storage tank ($R^2 = 0.44$). Every day at about 7 AM, except during the weekend, the dewatered sludge is transferred from the storage tank to a truck. The steady increase in the sludge volume over the day parallels the rising methane emission, while the unloading of the sludge into the truck causes a sharp peak. The correlation is not that strong, but that is because the dewatered sludge storage tank contributes only for 17 ± 8 % to the emission from the carousel reactor.

Seasonal variability

As far as daily values are concerned (Table 5.4), the only meaningful correlation was between the daily average amount of sludge stored in the dewatered sludge storage tank and the daily emission from the carousel and the ventilation system ($R^2 = 0.58$). Especially considering the limited contribution of the off-gas from the dewatered sludge storage tank to the emission from the carousel and the ventilation system (17 ± 8 %) this correlation is high. The correlation between the daily values corroborates the correlation between the on-line values.

Regarding the 26-day moving average values (Table 5.5), a relatively high correlation ($R^2 = 0.70$) was found between the moving average of the emission from the carousel and the moving average of the sludge content in the dewatered sludge storage tank. This was also the case for the on-line measurements and the daily averages, so it is obvious that the amount of sludge that is stored here influences the emissions. Keeping less sludge in the dewatered sludge storage tank may be an option to decrease this contribution to the total emissions.

The 26 day moving average of the emission from the carousel and the ventilation system had a strong negative correlation with the moving average of the residence time in the digester ($R^2 = 0.84$). The amount of sludge that is degraded is inversely proportional to the residence time. The less material that is degraded in the digester, the higher the residual methane potential of the digester effluent will be. Since this effluent is stored in the buffer tank, more methane will be produced there, and since the buffer tank contributes for 40 ± 15 % to the emission from the carousel this emission is influenced by the residence time in the digester.

The digester is operated as a CSTR with fixed volume, which implies that the residence time is determined by the flow rate. The effluent of the digester is first sent to the buffer tank with a maximum residence time of 5 days and subsequently to the dewatering centrifuges. The 26 day moving average of the flow rate to the centrifuges is expected to correlate with the average emission from the carousel, because a higher average flow rate to the centrifuges corresponds with a shorter average residence time in the digester and a concomitant higher residual methane potential. This hypothesis was confirmed by the relatively high correlation that was found between the moving average values of the emission from the carousel on the one hand and the flow rate to the centrifuges on the other hand ($R^2 = 0.72$). As a consequence, increasing the sludge residence time in the anaerobic digester will decrease the residual methane potential and the methane emission during storage of the digester effluent.

Conclusions

- The methane emission related to the anaerobic digestion of primary and secondary sludge counts for about three quarters with respect to the WWTPs overall methane emission and causes a slightly larger greenhouse gas footprint than the carbon dioxide emission that is avoided by using the resulting biogas for energy generation.
- Methane emissions can be significantly reduced by better handling of the ventilation air of sludge handling facilities.
- Methane present in the wastewater was for a large part aerobically oxidized in the activated sludge tanks. This could be exploited as a means to further decrease methane emissions from wastewater treatment.
- Dissolved methane can be sampled accurately and precisely with a headspace method based on the salting-out of dissolved gases.

Acknowledgements

Appendix 5A

Google Earth picture of Kralingseveer WWTP, with the different unit processes and sampling points for dissolved methane.
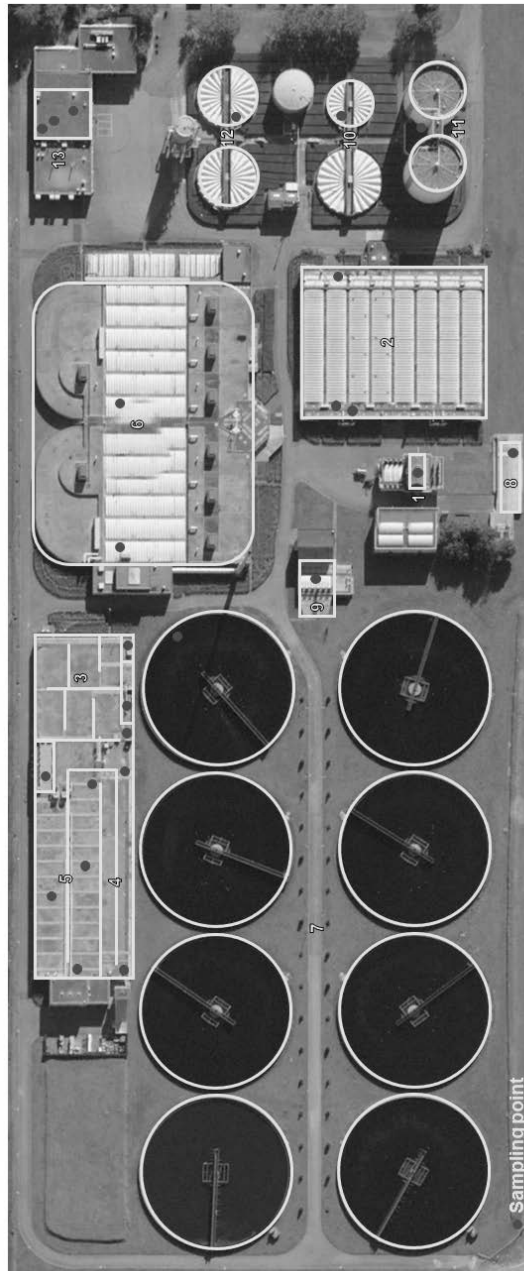
Number	Unit process	Sample point(s)
1	Headworks	Bar screen
2	Primary settlers	Influent PS, effluent PS, primary sludge
3	Selector tank	Influent, return sludge, effluent selector
4	Anoxic plug flow tank	Three sampling points
5	Oxic plug flow tank	Five sampling points in both lanes
6	Carrousels	One sample point per carrousel
7	Secondary clarifiers	Effluent weir

Number	Unit process	Sample point(s)
8	Effluent collector	Exit point of process unit
9	Return sludge pumps	Excess sludge pump
10	Gravitary thickener	Effluent primary sludge thickener
11	Sludge digester	Circulation pump
12	Storage buffer tank	Surface of liquid
13	Sludge treatment	Influent and effluent of belt thickener, reject water of digested sludge dewatering centrifuges

Appendix 5B

Overview of the calculations of the different methane mass flow rates between the unit processes of the WWTP.

Gaseous methane streams

Off-gas from headworks
Concentration: grab sample with gas bag, analysed with GC-FID
Flow rate: measured with TESTO anemometer

Off-gas from primary settling tank
Concentration: grab sample with gas bag, analysed with GC-FID
Flow rate: measured with TESTO anemometer

Off-gas from gravitary thickener for primary sludge
Concentration: grab sample with gas bag, analysed with GC-FID
Flow rate: measured with TESTO anemometer

Off-gas from selector tank
Concentration: grab sample with gas bag, analysed with GC-FID
Flow rate: measured with TESTO anemometer

Off-gas from anoxic and aerated plug flow tank
Concentration: on-line infrared Servomex gas analyser
Flow rate: measured with TESTO anemometer

Off-gas from carousel tank
Concentration: on-line infrared Servomex gas analyser
Flow rate: measured with TESTO anemometer

Gas stream from the header to the compost filter
Concentration: grab sample with gas bag, analysed with GC-FID
Flow rate: measured with TESTO anemometer

Gas stream from the compost filter to the carousel tank
Concentration: grab sample with gas bag, analysed with GC-FID
Flow rate: measured with TESTO anemometer

Off-gas from buffer tank for digested sludge
Concentration: grab sample with gas bag, analysed with GC-FID
Flow rate: measured with TESTO anemometer

Off-gas from storage tank for dewatered sludge
Concentration: grab sample with gas bag, analysed with GC-FID
Flow rate: measured with TESTO anemometer

Off-gas from belt thickeners
Could not be measured separately, but assumed to be zero since both the methane concentration and the flow rate of the waste sludge were low

Off-gas from centrifuges
Could not be measured separately. The methane mass flow rate of the off-gas from the sludge processing building where both the belt thickeners and the centrifuges are located could be calculated from the mass balance over the header, since no methane is converted here. Since the off-gas from the belt thickeners was assumed to be zero, all the methane in the off-gas from the sludge processing building was assumed to come from the centrifuges.

Gas supply to cogeneration unit
Concentration: occasional measurement data were provided by WWTP staff
Flow rate: available from the plant's SCADA system

Flue gas of cogeneration unit
Concentration: grab sample with gas bag, analysed with GC-FID
Flow rate: calculated from gas consumption (available from the plant's SCADA system) and stoichiometric combustion air requirement.

Flue gas of ozone washer
Sum of methane mass flow rate from plug flow reactor and carousel reactor. One measurement showed that methane is not converted in the ozone washer.

Liquid streams

Influent to headworks
Concentration: measured with salting-out method
Flow rate: available from the plant's SCADA system

Sludge supply to centrifuges
Concentration: measured with salting-out method
Flow rate: available from the plant's SCADA system

Reject water from centrifuges
Concentration: measured with salting-out method
Flow rate: could be calculated from solids balance over the centrifuge
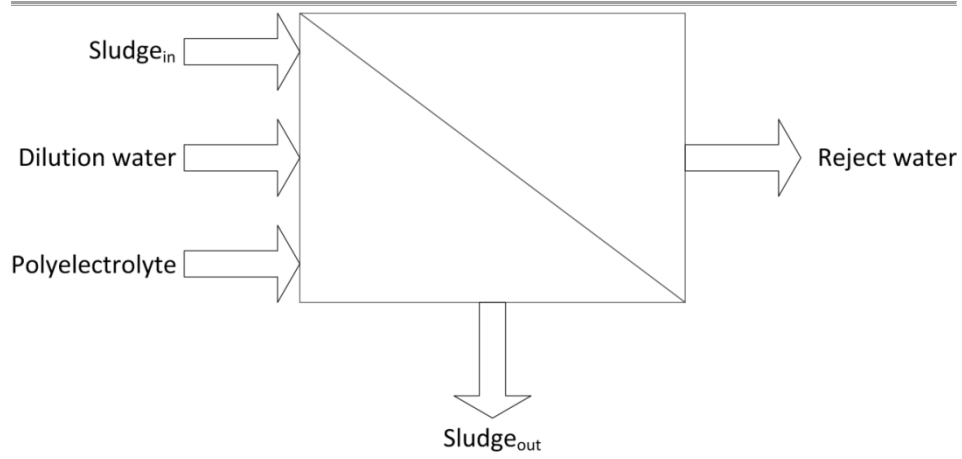
$$Sludge_{in}(m^3h^{-1}) + Polyelectrolyte\ (m^3h^{-1}) + Dilution\ water\ (m^3h^{-1})$$
$$= Sludge_{out}(m^3h^{-1}) + Reject\ water\ (m^3h^{-1})$$

(1)

$$Sludge_{in}(m^3h^{-1}) \cdot Dry\ matter\ content\ of\ sludge_{in}\ (kg\ m^{-3}) + Polyelectrolyte\ (kg\ h^{-1})$$
$$= Sludge_{out}(m^3h^{-1}) \cdot Dry\ matter\ content\ of\ sludge_{out}\ (kg\ m^{-3})$$

(2)

From (1) and (2)

$$Reject\ water\ (m^3h^{-1})$$
$$= Sludge_{in}(m^3h^{-1}) + Polyelectrolyte\ (m^3h^{-1}) + Dilution\ water\ (m^3h^{-1})$$
$$- \frac{Sludge_{in}(m^3h^{-1}) \cdot Dry\ matter\ content\ of\ sludge_{in}\ (kg\ m^{-3}) + Polyelectrolyte\ (kg\ h^{-1})}{Dry\ matter\ content\ of\ sludge_{out}\ (kg\ m^{-3})}$$

Flow rates of sludge$_{in}$, polyelectrolyte and dilution water were available from the plant's SCADA system. Dry matter content of incoming and outgoing sludge was measured in the laboratory.

Dewatered sludge from centrifuges to storage tank
Concentration: measured with salting-out method
Flow rate: could be calculated from solids balance over the centrifuge

From (2)

$$Sludge_{out}(m^3h^{-1})$$
$$= \frac{Sludge_{in}(m^3h^{-1}) \cdot Dry\ matter\ content\ of\ sludge_{in}\ (kg\ m^{-3}) + Polyelectrolyte\ (kg\ h^{-1})}{Dry\ matter\ content\ of\ sludge_{out}\ (kg\ m^{-3})}$$

Sludge supply to belt thickeners
**Concentration:** measured with salting-out method
Flow rate: available from the plant's SCADA system

Reject water from belt thickeners
Concentration: measured with salting-out method
Flow rate: similar to calculation for centrifuges

Thickened secondary sludge from belt thickeners to digester
Concentration: measured with salting-out method
Flow rate: similar to calculation for centrifuges

Reject water from gravitary thickener for primary sludge
Concentration: measured with salting-out method
Flow rate: based on design characteristics

Primary sludge from primary settler to gravitary thickener
Concentration: measured with salting-out method
Flow rate: based on design characteristics

Thickened primary sludge from the gravitary thickener to digester
Concentration: measured with salting-out method
Flow rate: based on design characteristics

Water to primary settling tank
Concentration: measured with salting-out method
Flow rate: sum of influent flow rate of headworks and flow rate of reject water from centrifuges, belt thickeners and gravitary thickener for primary sludge

Effluent from headworks
Calculated by subtracting the methane mass flow rate of the total reject water from the methane mass flow rate of the influent of the primary settler

Effluent of anaerobic digester to buffer tank
Concentration: measured with salting-out method
Flow rate: Sum of flow rates of sludge coming from the belt thickener and the understream of the gravitary thickener for the primary

Water from primary settling tank to selector tank
Concentration: measured with salting-out method
Flow rate: sum of influent flow rate of headworks and flow rate of reject water from centrifuges, belt thickeners and gravitary thickener for primary sludge (= flow rate of influent of primary settling tank), minus the flow rate of the primary sludge to the gravitary thickener for the primary sludge

Return sludge to selector tank
Concentration: measured with salting-out method
Flow rate: 40 % of the return sludge. The flow rate of the return sludge is 1.2 times the influent flow rate

Return sludge to plug flow reactor
Concentration: measured with salting-out method
Flow rate: 60 % of the return sludge. The flow rate of the return sludge is 1.2 times the influent flow rate

Mixed liquor from selector to plug flow reactor
Concentration: measured with salting-out method
Flow rate: Sum of flow rate from primary settling tank and flow rate of return sludge to selector tank

Mixed liquor from plug flow reactor to carousel reactor
Concentration: measured with salting-out method
Flow rate: Sum of flow rate from selector to plug flow reactor and flow rate of return sludge to plug flow reactor

Mixed liquor from carousel reactor to secondary settling tanks
Concentration: measured with salting-out method
Flow rate: Flow rate from plug flow reactor to carousel reactor

Secondary sludge from secondary settling tanks
Concentration: measured with salting-out method
Flow rate: Sum of return sludge flow rate and flow rate of secondary sludge supply to belt thickeners, which is available from the plant's SCADA system

Effluent
Concentration: measured with salting-out method
Flow rate: available from the plant's SCADA system

Appendix 5C
Protocol for the salting-out method for sampling of dissolved methane

Principle
When salt is added to a liquid in a sufficiently high concentration, the dissolved gases escape from the liquid (salting-out effect). If this is done in a closed recipient, the dissolved gases escape to the headspace. By analysing the gas composition in the headspace, it is possible to determine the amount of gas that was dissolved in the liquid. Besides salting-out the dissolved gases, the high salt concentration also cease any microbial activity that may lead to production or consumption of dissolved gases after the sample is taken.

Reference
The method is adapted from Gal'chenko, V.F., Lein, A.Y. and Ivanov, M.V. (2004) Methane content in the bottom sediments and water column of the Black Sea. Microbiology 73(2), 211-223.

Equipment
- Sampling beaker
- Graduated syringe with catheter tip and tube of ca. 15 cm (**Figure**)
- Serum bottle of ca. 120 mL
- Rubber stopper
- Aluminium seal
- Crimper for aluminium seals
- 20 g NaCl
- Beaker
- Graduated syringe with catheter tip and without plunger
- Tube of ca. 30 cm
- Hypodermic needle

Before sampling
Add 20 g NaCl to serum bottle

Sampling procedure
- Take a sample from the liquid surface of the reactor or from the valve of a pipe using a sampling beaker
- Suck 50 mL (V_{sample}) of sample from the sampling beaker into the syringe with catheter tip and tube
- Release the content of the syringe into the serum bottle, while keeping the end of the tube under the liquid surface
- Seal the serum bottle with the rubber stopper and the aluminium seal

- Shake the bottle vigorously

Measurement procedure

Measurement of volume expansion due to pressure build up in the bottle
- Connect the graduated syringe with the catheter tip to the needle with a tube
- Make sure that the open end of the syringe is submerged in the water in the beaker
- Register the headspace volume in the syringe V_0
- Pierce the rubber stopper of the serum bottle with the needle connected to the syringe (**Figure** 2)
- The headspace volume of the syringe will expand
- Bring the water level in the syringe to the water level in the beaker to cancel out the pressure of the water column
- Register the new headspace volume in the syringe V_1
- $V_1 - V_0 = V_s$ with V_s the volume expansion due to the pressure build up in the serum bottle

Measurement of the methane concentration in the headspace
Draw a sample from the headspace of the serum bottle with a gas syringe and measure it with a gas chromatograph equipped with a flame ionization detector according to the appropriate method for measuring methane.

Measurement of the headspace of the serum bottle
- Mark the level of the NaCl saturated sample in the serum bottle
- Mark the lower side of the rubber stopper
- Empty and rinse the bottle
- Fill the bottle with clean water till the mark of the liquid level
- Register the weight of the bottle W_0
- Add clean water to the bottle till the mark of the stopper
- Register the weight of the bottle W_1
- $(W_1 - W_0) \times \varrho = V_{HS}$ with ϱ the density of the water and V_{HS} the volume of the headspace of the serum bottle

Calculations

Volume

$$V = V_s + V_{HS}$$

With

- V the expanded volume of the headspace (m³)

113

- V_s the volume expansion due to the pressure build-up (m³)
- V_{HS} the headspace of the serum bottle before expansion (m³)

Amount of methane

$$n = \frac{P \cdot V}{R \cdot T}$$

With

- n the amount of methane in the expanded headspace of the serum bottle (mol)
- P the atmospheric pressure (Pa)
- V the expanded volume of the headspace (m³)
- R the ideal gas constant: 8.314 m³ Pa mol^{-1} K^{-1}
- T the temperature (K)

Concentration

$$C = \frac{n}{V_{sample}}$$

With

- C the concentration (M)
- N the amount of methane in the expanded headspace of the serum bottle (mol)
- V_{sample} the volume of the sample (L)
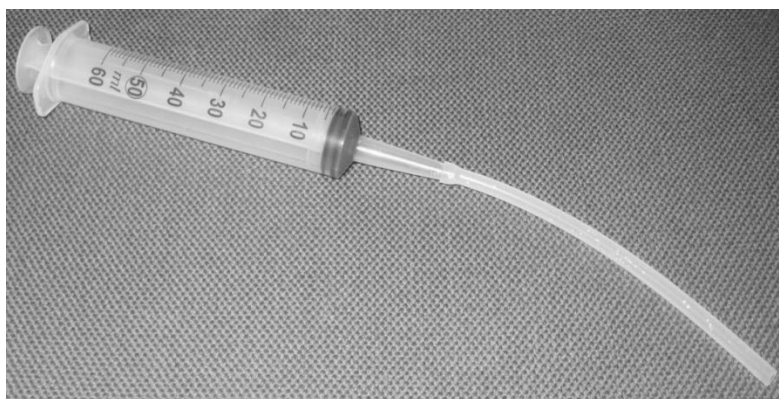
Pictures

Figure 1. Graduated syringe with catheter tip and tube.

Figure 2. Measurement of the volume expansion due to the pressure build-up that is caused by the salting-out of the dissolved gases.

6

Effect of process design and operating parameters on aerobic methane oxidation in municipal WWTPs

Abstract

Methane is a potent greenhouse gas and its emission from municipal wastewater treatment plants (WWTPs) should be prevented. One way to do this is to promote the biological conversion of dissolved methane over stripping in aeration tanks. In this study, the well-established Activated Sludge Model n°1 (ASM1) and Benchmark Simulation Model n°1 (BSM1) were extended to study the influence of process design and operating parameters on biological methane oxidation. The aeration function used in BSM 1 was upgraded to more accurately describe gas-liquid transfer of oxygen and methane in aeration tanks equipped with subsurface aeration. Dissolved methane could be effectively removed in an aeration tank at an aeration rate that is in agreement with optimal effluent quality. Subsurface bubble aeration proved to be better than surface aeration, while a CSTR configuration was superior to plug flow conditions in avoiding methane emissions. The conversion of methane in the activated sludge tank benefits from higher methane concentrations in the WWTP's influent. Finally, if an activated sludge tank is aerated with methane containing off-gas, a limited amount of methane is absorbed and converted in the mixed liquor. This knowledge helps to stimulate the methane oxidizing capacity of activated sludge in order to abate methane emissions from wastewater treatment to the atmosphere.

Published as

Introduction

Municipal wastewater treatment entails the emission of methane (CH_4), a potent greenhouse gas with a global warming potential of 34 CO_2-equivalents (IPCC, 2013a). In a long-term study on a municipal wastewater treatment plant (WWTP) near Rotterdam, the Netherlands, methane was found to make up 13.5 % of the plants greenhouse gas footprint, exceeding the carbon dioxide contribution related to the plant's electricity and natural gas consumption (Daelman et al., 2013, chapter 2 in this thesis). The share of methane in the climate footprint of a WWTP near Gothenburg, Sweden, was estimated at 31 % (Tumlin, 2011). In the US, wastewater treatment is the seventh most important source of methane emission (EPA, 2013), while globally, wastewater treatment accounts for 4 - 5 % of the total methane emission (El-Fadel and Massoud, 2001; Conrad, 2009).

It was recently discovered that about 80 % of the dissolved methane entering an aerobic activated sludge tank was converted, with the remainder being stripped (Daelman et al., 2012, chapter 5 in this thesis). Dissolved methane in sewage or in reject water entering an aerobic activated sludge tank can be biologically converted by methanotrophic bacteria (Ho et al., 2013). These bacteria use methane as their sole source of carbon and energy (Hanson and Hanson, 1996). First, methane is oxidized to methanol (CH_3OH) by particulate or soluble methane monooxygenase. Next, methanol is further oxidized to formaldehyde ($HCHO$), formate ($HCOOH$) and carbon dioxide (CO_2) by methanol dehydrogenase, formaldehyde dehydrogenase and formate dehydrogenase, respectively (Hanson and Hanson, 1996).

Intermediate metabolites of the aerobic methane oxidation pathway (e.g. methanol) can serve as electron donors for denitrifying microorganism. Methane could therefore potentially be used for biological denitrification of wastewater (Harremoës and Henze, 1971; Modin et al., 2007). However, this requires a critical supply of oxygen to the organisms: enough for oxidizing methane but not too much in order to prevent inhibition of denitrification. In a wastewater treatment plant designed for nitrogen removal, the organisms are cycled between anoxic zones, where there is no oxygen to oxidize methane to substrates for denitrification, and aerobic zones, where the high oxygen concentrations ($> 1\ g\ O_2 m^{-3}$) inhibits denitrification, making aerobic methane oxidation coupled to denitrification not likely to happen in wastewater treatment plants. Denitrification with methane is also possible under anoxic conditions by *Methylomirabilis oxyfera* (Ettwig et al., 2010; Kampman et al., 2012), but since the microorganisms in activated sludge are frequently exposed to high oxygen concentrations and given the low growth rate of this organism, anoxic denitrification with methane is unlikely to happen in a wastewater treatment plant. For these reasons, the present study focuses on the complete oxidation of methane to carbon dioxide. Given the frequent exposure of the microorganisms in the activated sludge to aerated conditions and the presence of nitrate in the anoxic reactors,

any methanogenic activity in activated sludge tanks is deemed to be insignificant (Gray et al., 2002).

Since the global warming potential of methane is 34 times that of carbon dioxide, the oxidation of methane to carbon dioxide is beneficial to mitigate climate change. Both lab-scale and full-scale studies have been performed to establish the potential of methanotrophs to curb the emission of methane from gaseous or liquid waste streams. Bio-filtration units were tested for the removal of methane from landfill gas (Nikiema et al., 2007), animal husbandry ventilation (Melse and van der Werf, 2005), manure storage ventilation (Girard et al., 2011) and coal mine ventilation (Sly et al., 1993). As far as liquid streams are concerned, digester effluent received some attention because it can be supersaturated with methane (Pauss et al., 1990; Hartley and Lant, 2006). To avoid that the dissolved methane is emitted to the atmosphere, Hatamoto et al. (2010) and Matsuura et al. (2010) developed a biofilm reactor, while van der Ha et al. (2011) explored a co-culture of methanotrophic bacteria and microalgae to degrade methane in the effluent of anaerobic wastewater treatment plants.

To describe and predict the behaviour and performance of methanotrophic bio-filter systems, a number of models have been developed. Delhomenie et al. (2008) and Yoon et al. (2009) developed models to describe the removal of methane from gas streams using methanotrophs in biofilms, while Oldenhuis et al. (1991), Broholm et al. (1992) and Alvarez-Cohen and McCarty (1991) carried out similar studies for suspended cells. Arcangeli and Arvin (1999) modelled the co-metabolic degradation of dissolved chlorinated aliphatic hydrocarbons in a biofilm by methanotrophic bacteria. To our knowledge, no models for methane degradation in activated sludge have been reported.

The present study investigates the fate of dissolved methane in an activated sludge plant. To this end, the Activated Sludge Model n° 1 (ASM1, Henze et al. (1987)) was extended with aerobic methanotrophic growth. The resulting model, ASM1m, was implemented in the Benchmark Simulation Model n° 1 (BSM1, Copp (2002)). This extended plant model, termed BSM1m, was used to simulate the effect of process design and process conditions on the fate of methane in an activated sludge plant. Taking into account biological methane oxidation on the one hand and stripping of methane on the other hand, BSM1m is the first model that describes biological methane conversion in activated sludge tanks. As such, it complements existing models for the emission of nitrous oxide in estimating greenhouse gas emissions from WWTPs.

Materials and methods

ASM1m model description
The ASM1m model developed in the present study adds two processes to ASM1: aerobic growth and decay of methanotrophs. The two additional state variables are methane as

substrate (S_{CH4}) and methane oxidizing bacteria (X_{MOB}). Since the interest of this study is in the fate of methane in activated sludge systems, methanotrophic bacteria are singled out from the other heterotrophic organisms (X_{BH}) and are therefore described by a separate state variable, X_{MOB}, as in Arcangeli and Arvin (1999). The reaction stoichiometry and kinetics related to the growth and decay of methanotrophic biomass are summarized in Table 6.1.

Table 6.1. Matrix representation of ASM1m showing only the state variables involved in methanotrophic growth and decay.

Component →	i	1	2	3	4	5	6	7	8	Process rate, ρ_j
j	Process ↓	S_{CH_4}	X_S	X_{MOB}	X_P	S_O	S_{NH}	X_{ND}	S_{ALK}	
1	Aerobic growth of methanotrophs	$-\frac{1}{Y_{MOB}}$		1		$-\frac{1-Y_M}{Y_{MO}}$	$-i_{XB}$		$\frac{-i_{XB}}{14}$	$\mu_{MOB}^{max} \cdot \frac{S_{CH4}}{K_{CH4}+S_{CH4}} \cdot \frac{S_O}{K_O^{MOB}+S_O} \cdot X_{MOB}$
2	Decay of methanotrophs		1-f_P	-1	f_P			$i_{XB} - f_p \cdot i_{XP}$		$b_{MOB} \cdot X_{MOB}$
	Conversion rates	$r_i = \sum_j r_{ij} = \nu_{ij}\rho_j$								
		Soluble methane substrate g COD.m^{-3}	Slowly biodegradable substrate g COD.m^{-3}	Active methanotrophic biomass g COD.m^{-3}	Particulate products arising from biomass decay g COD.m^{-3}	Dissolved oxygen g (-COD).m^{-3}	Ammonium ($NH_4^+ - N$) and ammonia ($NH_3 - N$) g N.m^{-3}	Soluble biodegradable organic nitrogen g N.m^{-3}	Alkalinity mol m^{-3}	

In ASM1m, growth of methanotrophs was modelled using Monod kinetics for methane and oxygen. Monod kinetics for methane were also used in Oldenhuis et al. (1991), Alvarez-Cohen and McCarty (1991), Broholm et al. (1992), Arcangeli and Arvin (1999), Oldenhuis et al. (1991) and Yoon et al. (2009). Unlike in Yoon et al. (2009), oxygen was also considered as a limiting substrate.

Ammonia inhibition, as considered by Arcangeli and Arvin (1999), was not included in the model. The effect of the ammonium concentration on the methane oxidation rate by

methanotrophs is ambiguous. A number of studies reported an inhibitory effect of ammonium (Hanson and Hanson, 1996; Begonja and Hrsak, 2001; Nyerges and Stein, 2009), others reported no effect (van der Ha et al., 2010; van der Ha et al., 2011) and Noll et al. (2008) even observed selective stimulation of methanotrophs by ammonium. Whatever the effect may be, the reported ammonium concentrations are at least one order of magnitude higher than the concentration that is commonly encountered in an activated sludge tank and as described in models such as BSM1. Ammonium inhibition is therefore not taken into account in the model.

Decay of methanotrophic biomass was described similarly to the other biomass groups, through the death-regeneration concept with first order reaction kinetics.

The original parameter values of ASM1 were preserved and completed with additional parameters to be used in the equations that describe methanotrophic growth and decay, taken from Arcangeli and Arvin (1999). The latter are shown in Table 6.2. To assess the sensitivity of the model to the values of the newly introduced parameters, each of the parameters was varied between 75 % and 125 % of its assumed value, using the methane conversion rate as the output variable.

Table 6.2. Values for the parameters involved in growth and decay of methanotrophic biomass in ASM1m.

Parameter description	Symbol	Value	Unit
Yield for methanotrophic biomass	Y_{MOB}	0.19	g COD.g COD^{-1}
Maximum specific growth rate for methanotrophic biomass	μ_{MOB}^{max}	1.5	d^{-1}
Methane half saturation concentration for methanotrophic biomass	$K_{CH_4}^{MOB}$	0.24	g COD.m^{-3}
Oxygen half saturation coefficient for methanotrophic biomass	K_O^{MOB}	0.2	g (-COD).m^{-3}
Decay coefficient for methanotrophic biomass	b_{MOB}	0.24	d^{-1}

Plant layout and influent conditions

The ASM1m model was implemented instead of ASM1 as the biological process model in the Benchmark Simulation Model no. 1 (BSM1, Copp (2002)). BSM1 was developed as a standardised simulation and evaluation protocol that serves as a basis to compare control strategies. It describes a WWTP with a Modified Ludzack-Ettinger configuration, consisting of a series of two anoxic reactors of 1000 m³ and three aerobic reactors of 1333

m³, with an internal circulation flow from the last aerobic reactor to the first anoxic reactor, and a sludge circulation flow from the settler to the first anoxic reactor. The basic control strategy of the plant comprises the control of the nitrate level in the second anoxic tank at 1 g N m⁻³ by manipulating the internal recycle flow rate, and oxygen control in the last aerobic tank at 2 g O₂ m⁻³ by manipulating the oxygen transfer coefficient ($k_La_{O_2}$) in this reactor, while $k_La_{O_2}$ in the remaining aerobic reactors is kept at 240 d⁻¹.

For the reference case in this study, the three aerobic tanks of the original BSM1, mimicking plug flow conditions, were replaced by a single continuous stirred-tank reactor (CSTR) with the same volume (3999 m³) as the total volume of the three aerobic tanks of BSM1 and a depth of 4 m. The default nitrate control loop was implemented unless stated otherwise, while the oxygen control loop was implemented as specified in the description of the scenarios. No external carbon was dosed.

Since methane is a volatile compound, its mass balance has to include interphase transport, just like for oxygen. In BSM1 it is assumed that the tank is aerated with porous disks at a depth of 4 m (Alex et al., 2008). Nevertheless, the interphase transport in BSM1 is modelled using Equation 1 (Copp, 2002), disregarding the physical effects taking place in a rising air bubble.

$$TR_i = k_La_i \cdot (S_i^* - S_i) \tag{1}$$

In reality, the partial pressure of dissolved gases (i.c. oxygen and methane) in the bubbles at the reactor bottom is higher than at the water surface due to the hydrostatic pressure of the water column, leading to higher dissolved concentrations and thus enhancing the gas-liquid mass transfer. On the other hand, the gas-liquid mass transfer of oxygen and methane is counteracted by the depletion of oxygen and the enrichment of methane in the bubble as it rises. Both effects are accounted for in Equation 2, which provides a more accurate description of gas-liquid mass transfer in a bubble column. Using Equation 2, the gas-liquid mass transfer rate TR_i of compound i was calculated taking into account the depth H of the aerator in the aeration tank (cf. Supplementary Materials). This equation yields the gas transfer rate in a bubble column with an aspect ratio (height:diameter ratio) lower than 3 and is therefore valid for an aeration tank.

$$TR_i = k_La_i \frac{\dfrac{(p_t + \frac{1}{2} \cdot \rho \cdot g \cdot H) \cdot M_i}{m \cdot R \cdot T^0} \cdot x_{i,in} - S_i}{1 + \dfrac{0.6 \cdot H}{m_i}} \tag{2}$$

In the case of surface aeration, H equals zero and Equation 2 takes the form of Equation 1. In the case of subsurface (bubble) aeration, Equation 2 can be used to verify the effect of the aeration depth on the oxygen transfer rate TR_{O_2} and the methane transfer rate TR_{CH_4} by varying H. Any emission of methane from the anoxic reactors due to passive diffusion or due to mixing was neglected.

During each simulation run, the plant behaviour was simulated for 150 days using the constant (dry weather) influent file of the original BSM1 in order to obtain steady state conditions (Copp, 2002). This influent file was supplemented with a methane concentration of 10 mg COD L^{-1}, in line with methane concentrations in sewage as observed by Foley et al. (2009) and Daelman et al. (2012, chapter 5 in this thesis).

Scenario analysis

The plant performance was compared for several scenarios, in terms of the percentage of incoming methane that was stripped, converted or discharged with the effluent and the waste sludge. When relevant, the plant performance was also assessed using the effluent quality index (kg pollution units d^{-1}, accounting for effluent concentrations of BOD, COD, total nitrogen and total suspended solids) and the consumed aeration energy (kWh d^{-1}) as described in Nopens et al. (2010) (cf. Supplementary materials).

Aeration

Aeration intensity

To verify the effect of aeration intensity on the stripping and conversion of methane in activated sludge, the single CSTR configuration of BSM1m was simulated in open loop mode, i.e. with a fixed internal recycle rate and without controlling the oxygen concentration. The gas-liquid mass transfer coefficient $k_L a_{O_2}$ in the CSTR was varied over the range $0 - 300$ d^{-1}.

Depth of the aerator in the aeration tank

To assess the effect of the aeration depth on the oxygen transfer rate TR_{O_2} and the methane transfer rate TR_{CH_4}, the aeration depth H in Equation 2 was varied between 0 and 8 m. The overall plant performance was evaluated for an aeration depth of 0, 4 and 8 m, while the reactor volume was kept constant at 3999 m^3. This simulates surface aeration, subsurface aeration with a reactor depth of 4 m and subsurface aeration with a reactor depth of 8 m, respectively. In the latter two cases, it is assumed that the bubble aeration equipment is installed on the bottom of the reactor.

Process configuration

The original BSM1 model with three aerobic reactors in series (plug flow) was compared with the configuration with a single CSTR, being the reference case in this study. For the plug flow (standard BSM1) configuration, two aeration modes were considered.

In the first mode, the oxygen concentration in the last of the aerobic tanks was controlled at 2 g m^{-3}, by manipulating the oxygen gas-liquid mass transfer coefficients of the three aerobic reactors, with the constraint that the oxygen gas-liquid mass transfer coefficients is

the same in the three reactors (uniform aeration flow rate). This mimics a plug flow
configuration with an oxygen sensor positioned at the end of the plug flow pattern and the
output signal of this oxygen sensor is used in a feedback loop to manipulate the aeration
rate.

In the second mode, each of the three aerobic reactors had its own control loop with an
oxygen set-point of 2 g m^{-3}, resulting in a different oxygen gas-liquid mass transfer
coefficient in each of the three reactors. This mode mimics a plug flow reactor in which the
aeration rate along the plug flow pattern is adapted to the local oxygen requirement. In a
plug flow reactor, the local oxygen requirement is the highest in the beginning of the
reactor (or in the simulation: in the first aerobic reactor) since the substrate concentrations
are the highest there (Olsson and Andrews, 1978). The result is a so-called tapered aeration
system, with a high aeration rate at the inflow of the reactor and a low aeration rate at the
outflow.

Influent methane concentration
In a final simulation, the concentration of methane in the sewage entering the plant was
varied from 0 to 120 mg COD L^{-1}. The default control strategies for nitrate and oxygen
were applied.

Methane concentration in aeration air
Ventilation of sludge handling and storage facilities can result in off-gas streams that
contain methane. In this study it is investigated to what extent activated sludge can be used
as a bio-scrubber to remove methane from such streams. Two scenarios are considered:
either the methane containing gas stream is added to the main aeration gas stream (diluted),
or the stream is sent as such (undiluted) to a dedicated (part of an) activated sludge reactor
where conditions can be optimized for methane removal. The later scenario is simulated by
using two aerobic reactors, with a total volume of 3999 m^3.

In the first scenario, the concentration of methane in the incoming gas is varied between 0
and 5 %. Since the methane originates from biogas, it is assumed that the foul air also
contains carbon dioxide in a CH_4:CO_2 ratio of 65:35 and that its oxygen content is reduced
accordingly. The oxygen level in the aerobic tank was controlled at 2 g O_2 m^{-3}. This
scenario was simulated without and with methane concentration in the influent.

In the second scenario, a given gas stream with a gas flow rate of 200 m^3 h^{-1} and a methane
concentration of 0.7 % is to be treated undiluted in a dedicated reactor volume. These gas
stream specifications agree with a real waste gas stream observed in a full-scale WWTP
(Daelman et al., 2012, chapter 5 in this thesis). For the dedicated reactor, the optimal gas-
liquid mass transfer coefficient k_La and the optimal reactor (zone) dimensions were
determined. The effect of the aeration depth (H) was assessed by varying the reactor height

over 4, 6 and 8 m. The oxygen level in the aerobic tank that is not used to treat the off-gas is controlled at 2 g O_2 m^{-3}.

Effect of sludge residence time

To assess the effect of sludge residence time on the conversion of methane, the default volumes of the reactors were increased to 1500 m³ for the anoxic reactors and 6000 m³ for the aerobic reactor, as in Nopens et al. (2010). To maintain the same solids concentrations in the reactors, the waste flow rate was changed to 337 $m^3 d^{-1}$ instead of the default 385 $m^3 d^{-1}$. This changed the sludge retention time from 9 to 15 days.

Results and discussion

Parameter sensitivity analysis

The change of the methane conversion rate for a given change in the parameter values compared to the reference case is shown in Figure 6.1. The most influential parameter is the maximum growth rate μ_{MOB}^{max}: when varying μ_{MOB}^{max} between 75 % and 125 % of its default value, the methane conversion rate ranged from 60% to 120% compared to the reference case. The model is also sensitive to the values of the decay rate b_{MOB} and the methane half-saturation constant $K_{CH_4}^{MOB}$, which will also impact the absolute values of the methane conversion rate. Yet, the present study explores the effect of process design and process conditions by comparing different simulated scenarios for the BSM1m plant. A qualitative comparison is aimed at, so the main interest is in the relative difference between the scenarios, rather than in the absolute values of the methane conversion and emission rates.
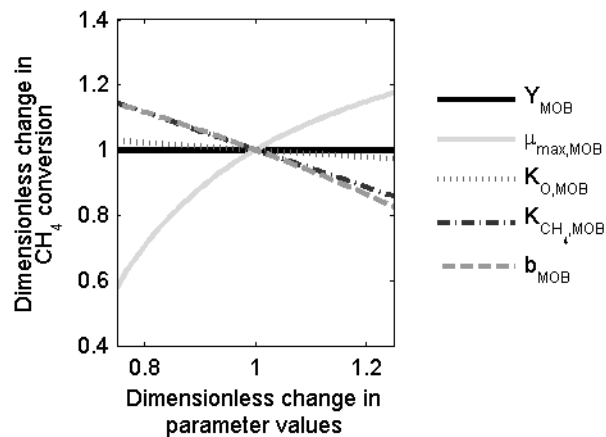

Figure 6.1. Dimensionless change in methane conversion versus the dimensionless change of the values of the parameters involved in growth and decay of methanotrophic biomass.

Aeration

Aeration intensity

In case of no aeration ($k_L a_{O_2}$ equals 0 d^{-1}), all incoming methane leaves with the reactor's effluent (Figure 6.2A). As $k_L a_{O_2}$ increases up to 70 d^{-1}, the oxygen that enters the reactor is consumed by heterotrophic organisms, so the oxygen concentration remains low (Figure 6.2B). For $k_L a_{O_2}$ lower than 70 d^{-1}, autotrophic and methanotrophic organisms are outcompeted for oxygen by heterotrophic organisms (see Supplementary materials for the Monod curves and biomass concentrations). No methane is converted, so all the methane entering the system is stripped or discharged with the influent and as $k_L a_{O_2}$ increases to 70 d^{-1}, the stripping rate increases at the cost of the discharge.

As $k_L a_{O_2}$ reaches 70 d^{-1}, the oxygen supply to the biomass exceeds the oxygen requirement of the heterotrophic biomass, thus allowing for methanotrophic growth (Figure 6.2B). From then on, also conversion contributes to the decrease of the methane concentration with increasing $k_L a_{O_2}$ (Figure 6.2A). At a $k_L a_{O_2}$ of 85 d^{-1} the concentration of methanotrophic biomass peaks, but as $k_L a_{O_2}$ increases further the decline in dissolved methane concentration causes the methanotrophic growth rate to slow down, resulting in a decline of the methanotrophic biomass and therefore the oxygen concentration increases (Figure 6.2B). Since autotrophic organisms have a lower oxygen affinity then methanotrophic biomass ($K_O^{MOB} = 0.2\ g\ O_2 m^{-3}$ and $K_O^{BA} = 0.4\ g\ O_2 m^{-3}$), ammonium conversion by autotrophic bacteria only takes place beyond $k_L a_{O_2} = 85$ d^{-1} (see Supplementary material). Meanwhile, the increase in $k_L a_{O_2}$ causes an increased stripping of methane at the expense of methane conversion (Figure 6.2A). Yet, as the ammonium concentration decreases, a further increase of $k_L a_{O_2}$ will result in an oxygen supply that exceeds the oxygen requirement for autotrophic growth. This will cause a secondary peak of the methane conversion at a $k_L a_{O_2}$ of 150 d^{-1} (Figure 6.2A). Eventually, as $k_L a_{O_2}$ increases beyond 150 d^{-1}, all microbial growth becomes substrate limited. Any further increase in $k_L a_{O_2}$ therefore leads to a higher dissolved oxygen concentration in the tank (Figure 6.2B). As $k_L a_{O_2}$ increases further, also the methane stripping rate will increase, at the expense of the methane conversion in the tank (Figure 6.2A).

The secondary peak of the methane conversion occurs at the $k_L a_{O_2}$ at which the ammonium concentration in the tank drops (see Supplementary materials for substrate concentrations). This implies that optimal methane removal is ensured when the aeration intensity is controlled to obtain optimal nitrogen removal, as is usually the case in plants that are operated for biological nitrogen removal. Assuring optimal methane conversion by optimizing the aeration for nitrogen removal only works if the methanotrophic organisms' affinity for oxygen is at least as high as the autotrophic organisms' affinity for oxygen. In this study, it was assumed that methanotrophic organisms have the same half-saturation

constant for oxygen as the heterotrophic organisms, as in the model of Arcangeli and Arvin (1999). The latter value was thus set at 0.2 $g\ O_2 m^{-3}$ (Henze et al., 1987), while the value for autotrophic organisms is 0.4 $g\ O_2 m^{-3}$. This assumption is supported by other literature indicating that methanotrophic bacteria have a higher affinity for oxygen than autotrophic nitrifying bacteria (Megraw and Knowles, 1987; Ren et al., 1997). Several studies even report K_O^{MOB} values lower than 0.1 $g\ O_2 m^{-3}$ (Nagai et al., 1973; Joergensen, 1985; Van Bodegom et al., 2001).

At the optimal aeration rate about 60 % of the dissolved methane entering the aeration tank is converted (Figure 6.2A). This is the same order of magnitude as the 80 % observed on a full-scale WWTP by Daelman et al. (2012, chapter 5 in this thesis). The biological oxidation of methane requires a stoichiometric amount of oxygen. In the present simulation, with an influent methane concentration of 10 mg COD L^{-1}, the oxidation of methane at the optimal aeration rate accounts for 3.5 % of the total oxygen consumption in the aerobic reactor. So, methane removal in activated sludge contributes to the aeration costs, but it can be done without compromising the effluent quality. Indeed, an aeration rate that is too low to obtain a proper effluent quality will result in a high methane emission because the oxygen concentration in the tank cannot sustain methanotrophic growth. On the other hand, an aeration rate that exceeds the oxygen requirement for proper nitrification will not only be a waste of energy, but it will also result in increased stripping of methane. This proves the need for adequate aeration control.
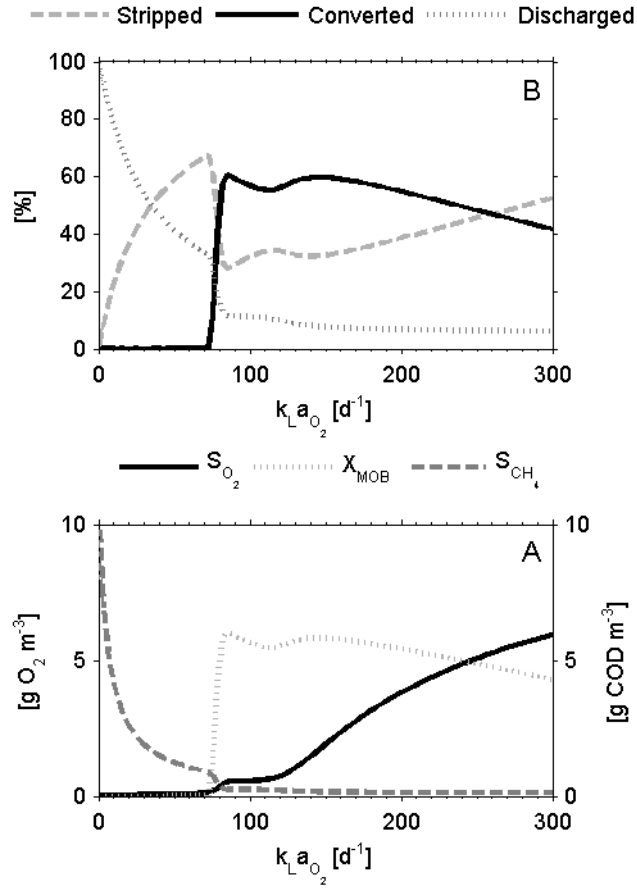
Figure 6.2. Effect of oxygen mass transfer coefficient $k_L a_{O_2}$ on percentages of dissolved methane entering an aeration tank that are stripped, converted and discharged with the effluent (A); and on concentrations of oxygen (S_{O_2}), methane (S_{CH_4}) and methanotrophs (X_{MOB}) (B).

Depth of the aerator in the aeration tank

An aerobic tank can be aerated using surface aeration or subsurface aeration. Furthermore, subsurface aeration can be installed on the bottom of tanks with different depths. The effect of aeration depth on the methane conversion capacity in an aerobic activated sludge tank was verified in simulations for varying aeration depths. By controlling the oxygen concentration S_{O_2} in the aerobic tank at 2 mg L^{-1} for each aeration depth, the oxygen transfer rate TR_{O_2} stays essentially the same for each aeration depth since oxygen consumption for heterotrophic and autotrophic growth is not affected by the aeration depth (Figure 6.3A).

In order to maintain the same oxygen transfer rate (TR_{O_2}) for each aeration depth, $k_L a_{O_2}$ has to decrease as the depth increases (Figure 6.3B). As $k_L a_{O_2}$ decreases, $k_L a_{CH_4}$ decreases as well. This implies a decline in the methane transfer rate TR_{CH_4} (Figure 6.3A), with increasing aeration depth, resulting in less methane stripping in deeper tanks (Figure 6.4). Less stripping of methane results in higher dissolved methane concentrations, which enhances methanotrophic growth for increasing aeration depth.

The constant TR_{O_2} guarantees an equal effluent quality for the different simulations at different aeration depths. Yet, the aeration energy consumption was 3128, 2739, 2469 kWh d^{-1} for an aeration depth of 0, 4 and 8 m, respectively. In sum, the deeper the aeration equipment is installed, the better the performance with regard to methane conversion and aeration energy consumption, without affecting the effluent quality.
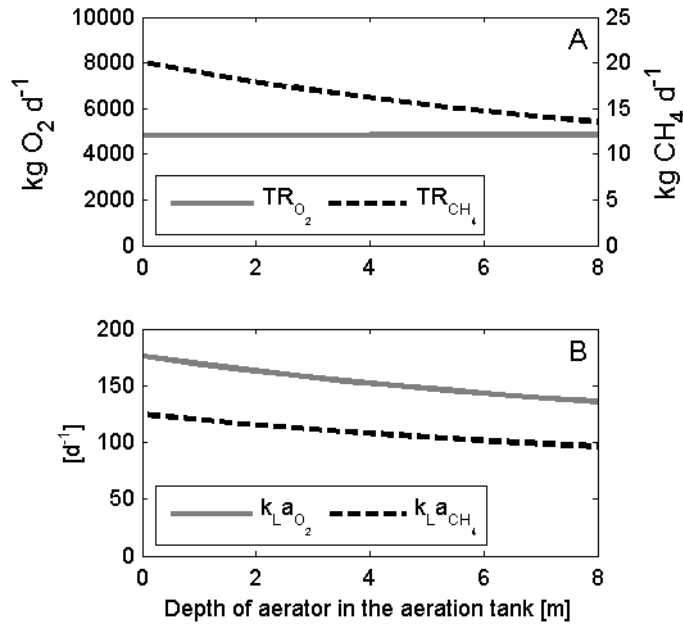

Figure 6.3. Methane transfer rate TR_{CH_4} vs. aeration depth for constant oxygen transfer rate TR_{O_2} (A) and oxygen and methane mass transfer coefficients for constant TR_{O_2} vs. aeration depth (B).
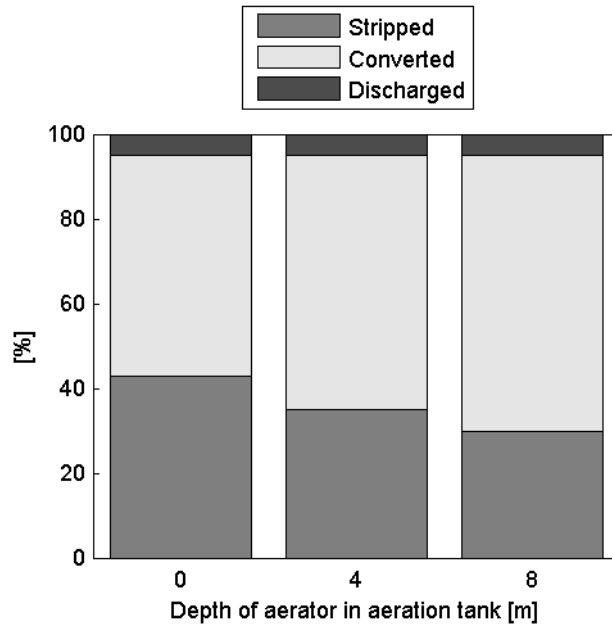
Figure 6.4. Fate of dissolved methane entering an aeration tank for different aeration depths, at constant TR_{O_2}.

Process configuration

The methane conversion capacity of a CSTR configuration was compared with the methane conversion capacity of two plug flow configurations, one with uniform aeration and one with tapered aeration.

The substrate concentration profile in a plug flow reactor results in a decreasing oxygen requirement along the plug flow pattern (Olsson and Andrews, 1978). In a plug flow configuration with tapered aeration, the aeration is adapted to this longitudinal gradient in the oxygen demand: $k_L a_{O_2}$ is high at the inlet and low at the outlet, following the substrate concentration, as can be seen in Figure 6.5. The plug flow reactors exhibit a high methane concentration in the beginning and a low methane concentration at the outflow of the aerobic reactor (Figure 6.5), while the methane concentration in the CSTR, equalling its effluent concentration, is about five times lower than in the first tank of both the plug flow reactors.

The high methane concentration in the first tank of both the plug flow configurations causes a higher driving force for methane transfer to the atmosphere than in the CSTR. Since the gas-liquid mass transfer coefficient $k_L a_{O_2}$ in the uniformly aerated plug flow reactor is only slightly lower than in the CSTR (Figure 6.5), this higher driving force results

in a higher methane emission percentage in the beginning of the uniformly aerated plug flow reactor than in the CSTR configuration, as can be seen in Figure 6.6. For the plug flow configuration with tapered aeration, $k_L a_{O_2}$ in the first aerobic reactor is even higher than $k_L a_{O_2}$ in the CSTR. Together with the higher driving force, this results in even more methane emission from the first tank than in the case of the uniformly aerated plug flow configuration.

Looking at the overall plant performance with regard to the relative importance of methane conversion, the scenario with the CSTR performs better than the plug flow scenarios, while the plug flow reactor with uniform aeration performs slightly better than the plug flow reactor with tapered aeration (Figure 6.6). In the CSTR scenario and in both the plug flow scenarios, the oxygen control ensured that the largest difference in TR_{O_2} between the three configurations was only 3 %, allowing for a fair comparison between the three scenarios. As in section 0, this small difference in TR_{O_2} was due to the difference in methane conversion rate which results in a slight difference in oxygen consumption between the three configurations.

As far as the effluent quality is concerned, the CSTR configuration performs slightly poorer than both plug flow configurations (Figure 6.7), since lower effluent concentrations can be obtained with a plug flow reactor. So, the better performance of a CSTR configuration with regard to the conversion of methane will in practice probably not outweigh its slightly worse performance concerning effluent quality.

Comparing the two plug flow configurations, the effluent quality of the plug flow reactor with tapered aeration is slightly better than the effluent quality of the uniformly aerated plug flow, but this slight improvement in effluent quality comes at the cost of a higher aeration energy consumption (Figure 6.7), which contradicts the rationale of using tapered aeration, i.e. avoiding unnecessary aeration. However, lowering the oxygen set-point at the inlet of the plug flow reactor with tapered aeration results in a decreased $k_L a_{O_2}$ and thus in a decreased aeration energy consumption while safeguarding the effluent quality index (data not shown). At the same time, the lower $k_L a_{O_2}$ will result in less stripping and more conversion of methane. So, when operating a plug flow reactor in tapered aeration mode, it is beneficial to lower the oxygen set-point at the inlet of the reactor.

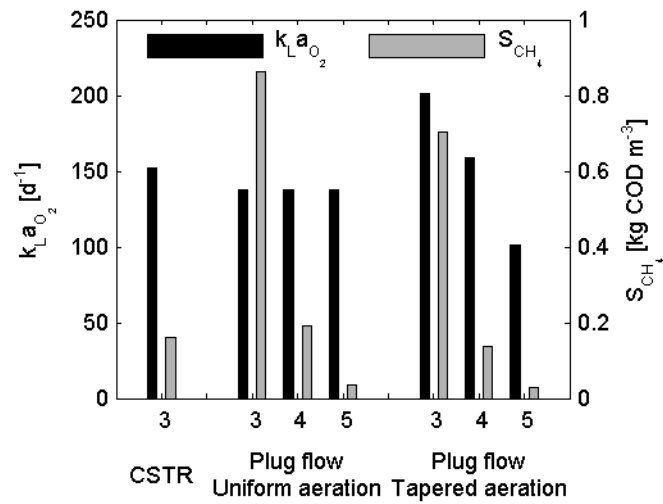**Figure 6.5. Dissolved methane concentration and $k_L a_{O_2}$ values in each aerobic tank for the three configurations.**
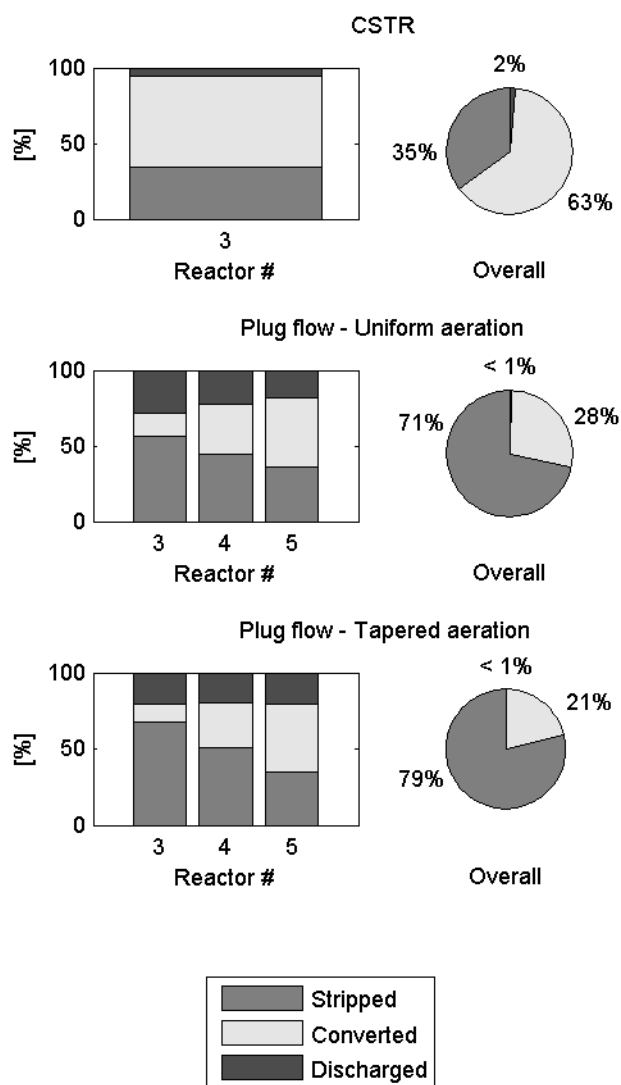
Figure 6.6. The bar charts show the share of incoming methane that is emitted, converted and leaving with the effluent per aerobic reactor for the three scenarios, while the pie charts give the overall amount of influent methane that is emitted, converted or discharged with the effluent.
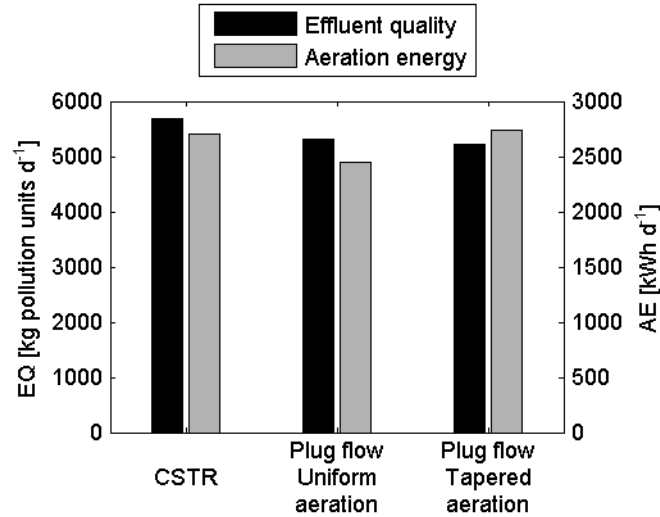
**Figure 6.7. Effluent quality index (EQ) and aeration energy (AE) for the three
configurations.**

Methane concentration in the influent

Figure 6.8 shows the percentage of methane in the influent that is stripped, converted and
discharged with the effluent, respectively, as a function of the methane concentration in the
influent. At methane concentrations < 5 g COD m^{-3} most of the incoming methane is
stripped since the methane concentration in the aeration tank is too low to sustain growth
of methanotrophs, but as the influent methane concentration rises, the amount of methane
that is converted increases rapidly at the expense of the amount of methane that is
stripped. At an influent methane concentration of 40 g COD m^{-3} about 90 % of the
incoming methane is converted.

Supersaturated methane concentrations as high as 120 mg COD L^{-1}, equal to
30 mg CH_4 L^{-1}, have been observed in rising main sewers (Guisasola et al., 2008). Options
to mitigate the production of methane in sewers have been investigated (Mohanakrishnan
et al., 2009; Zhang et al., 2009; Jiang et al., 2010), but still, the concentration of methane in
the influent is difficult to control. Yet, the configuration of the headworks can determine
the concentration of methane in the stream entering the activated sludge tanks. For
instance, if the incoming sewage is pumped up with centrifugal pumps, less methane may
be stripped than when screw conveyors are used since the latter cause more intense contact
between the methane containing wastewater and the atmosphere (Daelman et al., 2012,
chapter 5 in this thesis).

High methane concentrations in the influent entering the activated sludge system benefit
the conversion of methane. It may therefore be unnecessary to prevent methane
production in rising mains going to a WWTP, since high methane concentrations in the

135

influent will result in a higher methane conversion in the activated sludge tanks, provided that the methane is not stripped before the sewage reaches the aeration tank.
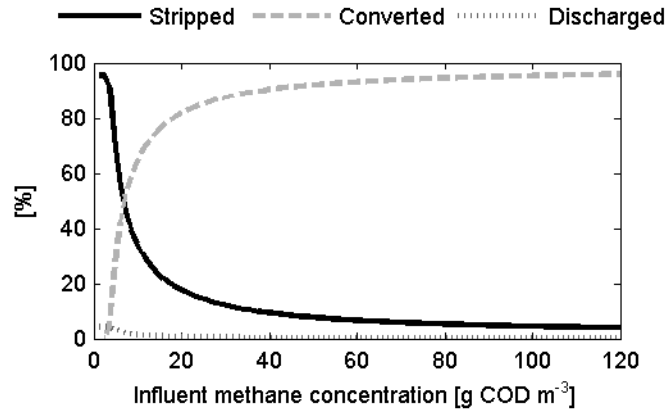
Figure 6.8. Fate of dissolved methane entering the WWTP as function of methane concentration in the plant's influent.

Methane concentration in aeration air

An activated sludge tank could be used as a bio-scrubber to remove odorous compounds (such as H₂S) from foul air generated by several unit processes on a wastewater treatment plant (Burgess et al., 2001; Estrada et al., 2011; Lebrero et al., 2011). In such a system, the foul air is sparged into the aeration tank to meet the biological oxygen demand in the reactor; the targeted compounds absorb in the liquid and are subsequently degraded by the microorganisms in the activated sludge. Considering the methane oxidizing capacity of activated sludge, it is verified to what extent this technique can be applied to remove methane from gaseous waste streams, such as ventilation air from sludge dewatering or storage facilities.

In a first scenario, the methane containing off-gas is diluted with the main aeration stream. The effect of the methane concentration in the aeration gas on the removal efficiency was verified (Figure 6.9). The methane removal efficiency rises steeply with an increasing methane concentration in the aeration gas, but at a methane concentration in the aeration air of about 0.5 %, the removal efficiency levels off.

With an increasing methane concentration in the gas stream the methane transfer rate TR_{CH_4} increases according to Equation 2, causing an increase in the methane removal efficiency. However, this increasing methane concentration implies a decreasing oxygen concentration in the gas stream. Yet, the biological oxygen demand increases due to the growth of methanotrophs. To meet this increasing oxygen demand with an air mixture that is increasingly leaner in oxygen, the flow rate of the methane containing aeration gas has to

increase. Together with the increasing methane concentration in the gas stream, this causes more gaseous methane to enter the system. So, despite that TR_{CH_4} and the absolute methane conversion rate increase with the increasing methane concentration in the gas stream, the initial increase of the methane removal efficiency levels off.

Comparing the above mentioned simulation results obtained for the first scenario without methane in the influent with those obtained in case the influent contained 10 g COD m^{-3} of methane in the influent, it was found that the removal efficiency of gaseous methane was not influenced by the methane concentration in the influent (data not shown).
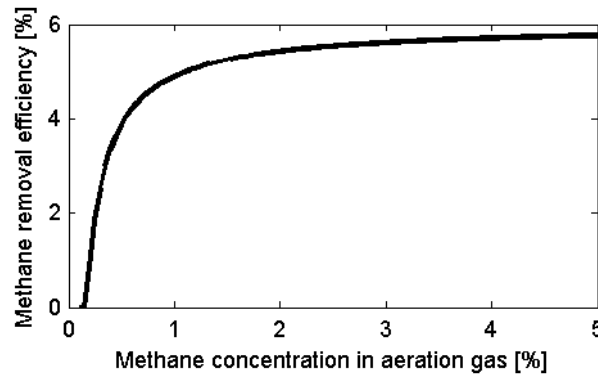
Figure 6.9. Methane removal efficiency as function of methane concentration in aeration gas stream.

In a second scenario, a given methane containing off-gas stream with a gas flow rate of 200 m^3 h^{-1} and a methane concentration of 0.7 % is sent undiluted to a dedicated aerobic reactor volume, in which the aeration intensity and the aeration depth can be optimized to obtain maximum methane removal. In this scenario, the methane removal efficiency is simulated for an oxygen mass transfer coefficient $k_L a_{O_2}$ ranging from 35 to 350 d^{-1} (Figure 6.10A). After a steep increase with $k_L a_{O_2}$ increasing from 35 d^{-1} to 50 d^{-1}, the methane removal efficiency levels off for each of the simulated aeration depths, despite that the volume specific methane transfer rate TR_{CH_4} (kg CH$_4$ m^{-3} d^{-1}) increases with $k_L a_{O_2}$. Yet, for each aeration depth the increasing $k_L a_{O_2}$ implies an increasing superficial gas velocity v_{Gs}^c, but since the gas flow rate is fixed, this can only be achieved by decreasing the reactor volume dedicated to methane removal, as shown in Figure 6.10B. As a consequence, the amount of methane transferred (kg CH$_4$ d^{-1}) levels off with increasing $k_L a_{O_2}$.

As far as the aeration depth is concerned, a better removal efficiency is achieved with deeper aeration (Figure 6.10A). Since $k_L a_{O_2}$ and the superficial gas velocity are assumed linearly dependent (see Supplementary material), an equal aeration intensity requires an equal reactor surface area, resulting in a larger reactor volume for deeper aeration. Once

$k_L a_{O_2}$ exceeds 50 d^{-1}, the methane removal efficiency remains essentially constant when $k_L a_{O_2}$ increases further, but the dedicated reactor volume decreases. This results in a trade-off between aeration costs and investment cost.

In practice, the methane concentration in the gaseous waste stream should be lower than 5%, i.e. the lower explosion limit of methane, to avoid hazardous situations. Taking into account a safety margin, this leaves only a narrow concentration window in which methane removal from foul air is optimal, but even in the extreme case of an 8 m high reactor, the optimal methane removal efficiency is only about 12 % when the oxygen level is controlled at 2 mg L^{-1}. This is very low in comparison with biofilter systems where a methane removal efficiency higher than 50% is common (Sly et al., 1993; Melse and van der Werf, 2005; Girard et al., 2011). Yet, if there is no alternative besides emitting all the methane to the atmosphere, it should still be evaluated if these methane removal efficiencies could warrant any additional investment cost required to aerate the activated sludge tank with methane containing off-gas.
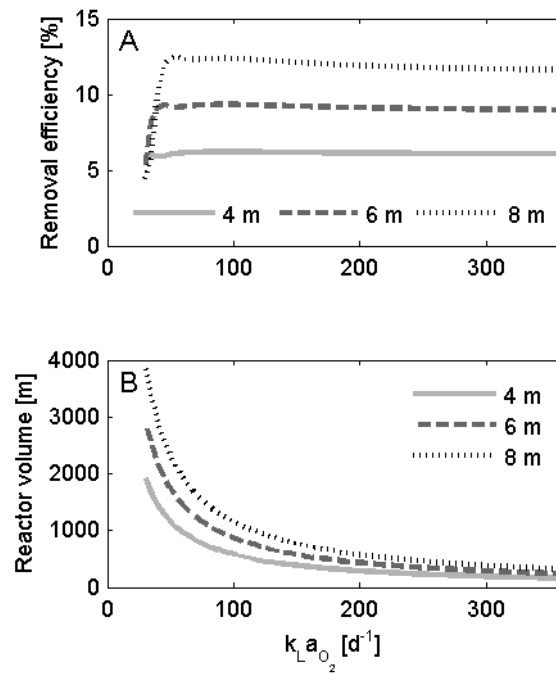
Figure 6.10. Methane removal efficiency (A) and dedicated reactor volume (B) for removal of methane from a given gas stream (0.7 % methane, 200 m³h⁻¹) as function of $k_L a_{O_2}$ for different aeration depths.

Sludge residence time

The default BSM1 plant is overloaded (Nopens et al., 2010), which results in incomplete nitrification process (effluent ammonium concentration is 2.0 $g\ NH_4^+ - N\ m^{-3}$). To improve the performance of the plant, the volume of the reactors was increased, resulting in a longer sludge residence time. The effect of this intervention on the fate of incoming methane is shown in Figure 6.11. With the longer sludge residence time, the plant's nitrification rate increased, resulting in a decreased effluent ammonium concentration (0.9 $g\ NH_4^+ - N\ m^{-3}$). Yet, this did not impact the methane conversion rate since ammonium was not considered as a substrate or as an inhibiting agent for this process in ASM1m.

The larger reactor volume that is required for a longer sludge residence time results in a decrease in a lower volume specific oxygen requirement. So, for the larger reactors, the oxygen transfer rate TR_{O_2} that is required to keep the oxygen concentration at 2 g O₂ m⁻³ is lower. The lower TR_{O_2} implies a lower oxygen mass transfer coefficient $k_L a_{O_2}$ (111 instead of 152 d⁻¹), resulting in less stripping of methane and more conversion (Figure 6.11).
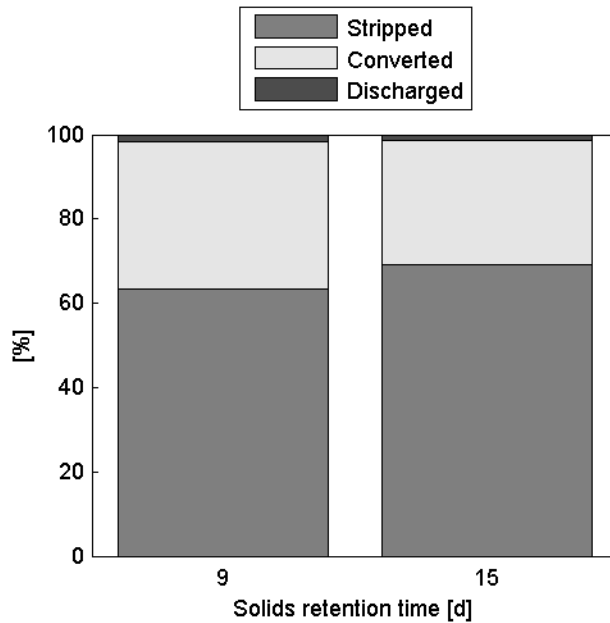
Figure 6.11. Effect of sludge residence time on the fate of influent methane.

Balancing methane conversion with effluent quality and aeration costs

The obtained simulation results clearly show that the conversion of dissolved methane can be enhanced by using deeper aeration and by using a CSTR configuration instead of a plug flow reactor. For removing methane from gaseous waste streams using activated sludge as

a bio-scrubber, it is beneficial to have deep aeration, and an optimal balance between aeration intensity and reactor volume. However, these measures can potentially lead to poorer effluent quality and they can entail increased operational and capital costs. Therefore, it requires a cost-benefit analysis to verify whether the potential deterioration of the effluent quality is compensated by the avoided emission, or whether the additional costs are warranted by any economic benefits.

As far as the environmental impact is concerned, there is not consensual way to compare the impact of methane emission with the impact of the effluent quality. This would require a common currency that is currently not available. An economic cost-benefit analysis could be based on the price of carbon credits in a carbon trading scheme. Wang et al. (2011b) suggested using carbon credits garnered by reducing the emissions of nitrous oxide from wastewater treatment to offset the costs incurred by additional nitrogen removal. This approach could also work with methane emissions, but currently the wastewater treatment sector is not subject to any emission trading scheme. So, for the time being, there is no economic incentive whatsoever to invest in the mitigation of methane emissions.

Conclusions

This study assessed to what extent the methane oxidizing capacity of activated sludge can be exploited to mitigate methane emissions from municipal wastewater treatment plants. For this purpose, the well-established Activated Sludge Model nr. 1 was extended with aerobic methanotrophic growth. This model was implemented in Benchmark Simulation Model nr. 1, in order to simulate the emission and conversion of methane.

From the simulations, the following conclusions were obtained:

Accurate aeration control should ensure a sufficient supply of oxygen. If the oxygen level is too low to sustain methanotrophic growth, methane will only be stripped without being converted, while aerating too much will benefit stripping at the expense of conversion.

- Dissolved methane can be removed in activated sludge at an aeration rate that is in agreement with optimal effluent quality.
- Aiming at the same effluent quality in terms of COD and nitrogen, more dissolved methane is converted as the aerator equipment is installed deeper below the liquid surface.
- A continuous stirred-tank reactor performs better than a plug flow reactor with regard to methane conversion. In case of a plug flow reactor, excessive aeration in the first part of the aeration tank should be avoided.
- A high methane concentration in the plant's influent benefits the conversion of methane.

- Activated sludge has limited potential as a bio-scrubber for the removal of methane from foul off-gas.

The obtained results are valid for the virtual BSM1m plant. Any extrapolation to real wastewater treatment plants would require calibration and validation of the model with real plant data. Yet, these results contain valuable information about potential differences between operation or design modes of wastewater treatment plants in general.

Acknowledgements

Nomenclature

c_G	concentration of compound i in gas	kg m^{-3}
g	gravitational field constant	m s^{-2}
H	height of the bubble column	m
$k_L a_i$	gas-liquid mass transfer coefficient of compound i	s^{-1}
m_i	partitioning coefficient gas-liquid for compound i $m_i = \frac{c_G}{s_i^*}$	-
M_i	molecular weight of compound i	kg mol^{-1}
p_t	pressure at the water surface	Pa
S_i	concentration of compound i in the mixed liquor	kg m^{-3}
S_i^*	equilibrium concentration of compound i in the mixed liquor corresponding with the given gas phase concentration	kg m^{-3}
TR_i	transfer rate of compound i	kg . m^{-3} . d^{-1}
$x_{i,in}$	concentration of compound i in the ingoing aeration gas flow (mole fraction)	-
ρ	density of the mixed liquor	kg m^{-3}

Appendix 6A

ASM1m: Activated Sludge Model with aerobic methane oxidation
This supplementary material offers a description of ASM1m, an adaptation of ASM1 that accommodates for aerobic oxidation of methane in activated sludge.

- Table 1: state variables for ASM1m.
- Table 2: matrix representation of ASM1m
- Table 3: process rates of ASM1m
- Table 4: stoichiometric parameter values for ASM1m
- Table 5: kinetic parameter values for ASM1m.

Table 1. State variables for ASM1m. The state variables that were added to the original ASM1 are in bold.

State variable	Symbol	Unit
Soluble inert organic matter	S_I	g COD.m^{-3}
Readily biodegradable substrate	S_S	g COD.m^{-3}
Soluble methane substrate	$\mathbf{S_{CH4}}$	**g COD.m^{-3}**
Particulate inert organic matter	X_I	g COD.m^{-3}
Slowly biodegradable substrate	X_S	g COD.m^{-3}
Active heterotrophic biomass	X_{BH}	g COD.m^{-3}
Active autotrophic biomass	X_{BA}	g COD.m^{-3}
Active methanotrophic biomass	$\mathbf{X_{MOB}}$	**g COD.m^{-3}**
Particulate products arising from biomass decay	X_P	g COD.m^{-3}
Dissolved oxygen	S_O	g (-COD).m^{-3}
Nitrate (NO_3^--N) and nitrite (NO_2^--N)	S_{NO}	g N.m^{-3}
Ammonium (NH_4^+-N) and ammonia (NH_3-N)	S_{NH}	g N.m^{-3}
Soluble biodegradable organic nitrogen	S_{ND}	g N.m^{-3}
Particulate biodegradable organic nitrogen	X_{ND}	g N.m^{-3}
Alkalinity	S_{ALK}	mol.m^{-3}

Table 2. Matrix representation of ASM1m. The processes and reactions added to the original ASM1 are shaded (table continues on opposite page).

A_{ij}	S_I [gCOD.m^{-3}]	S_S [gCOD.m^{-3}]	S_{CH4} [gCOD.m^{-3}]	X_I [gCOD.m^{-3}]	X_S [gCOD.m^{-3}]	X_{BH} [gCOD.m^{-3}]
PROCESS						
1. Aerobic growth of heterotrophs		$-1/Y_H$				1
2. Anoxic growth of heterotrophs		$-1/Y_H$				1
3. Aerobic growth of autotrophs						
4. Aerobic growth of methanotrophs			$-1/Y_{MOB}$			
5. Decay of heterotrophs					$1-f_P$	-1
6. Decay of autotrophs					$1-f_P$	
7. Decay of methanotrophs					$1-f_P$	
8. Ammonific. of soluble organic nitrogen						
9. Hydrolysis of entrapped organics		1			-1	
10. Hydrolysis of entrapped organic nitrogen						
CONSERVATIVES						
COD	1	1	1	1	1	1
N						i_{XB}
Charge						

X_{BA} [gCOD.m-3]	X_{MOB} [gCOD.m-3]	X_P [gCOD.m-3]	S_O [gO2. m-3]	S_{NO} [gN. m-3]	S_{NH} [gN. m-3]	S_{ND} [gN. m-3]	X_{ND} [gN. m-3]	S_{ALK} [mole HCO3-. m-3]
			$-(1-Y_H)/Y_H$		$-i_{XB}$			$-i_{XB}/14$
				$-(1-Y_H)/(2.86Y_H)$	$-i_{XB}$			$(1-Y_H)/(14*2.86*Y_H) -i_{XB}/14$
1			$-(4.57-Y_A)/Y_A$	$1/Y_A$	$-i_{XB} -1/Y_A$			$-i_{XB}/14- 1/(7*Y_A)$
	1		$-(1-Y_{MOB})/Y_{MOB}$		$-i_{XB}$			$-i_{XB}/14$
		f_P					$i_{XB}-f_P* i_{XP}$	
-1		f_P					$i_{XB}-f_P* i_{XP}$	
	-1	f_P					$i_{XB}-f_P* i_{XP}$	
					1	-1		1/14
						1	-1	

X_{BA}	X_{MOB}	X_P	S_O	S_{NO}	S_{NH}	S_{ND}	X_{ND}	S_{ALK}
1	1	1	-1	-4.57	0			
i_{XB}	i_{XB}	i_{XP}	0	1	1	1	1	
				-1/14	1/14			-1

Table 3. Process rates for ASM1m. The rates for the processes added to the original ASM1 are shaded.

j process	ϱ_j
1. Aerobic growth of heterotrophs	$\mu_H^{max} \cdot \dfrac{S_S}{K_S + S_S} \cdot \dfrac{S_O}{K_O^H + S_O} \cdot X_{BH}$
2. Anoxic growth of heterotrophs	$\mu_H^{max} \cdot \dfrac{S_S}{K_S + S_S} \cdot \dfrac{K_O^H}{K_O^H + S_O} \cdot \dfrac{S_{NO}}{K_{NO} + S_{NO}} \cdot \eta_{y,g} \cdot X_{BH}$
3. Aerobic growth of autotrophs	$\mu_A^{max} \cdot \dfrac{S_{NH}}{K_{NH}^A + S_{NH}} \cdot \dfrac{S_O}{K_O^A + S_O} \cdot X_{BA}$
4. Aerobic growth of methanotrophs	$\mu_{MOB}^{max} \cdot \dfrac{S_{CH4}}{K_{CH4} + S_{CH4}} \cdot \dfrac{S_O}{K_O^{MOB} + S_O} \cdot X_{MOB}$
5. Decay of heterotrophs	$b_H \cdot X_{BH}$
6. Decay of autotrophs	$b_A \cdot X_{BA}$
7. Decay of methanotrophs	$b_{MOB} \cdot X_{MOB}$
8. Ammonification of soluble organic nitrogen	$k_a \cdot S_{ND} \cdot X_{BH}$
9. Hydrolysis of entrapped organics	$k_H \cdot \dfrac{\frac{X_S}{X_{BH}}}{K_X + \frac{X_S}{X_{BH}}} \cdot \left[\dfrac{S_O}{K_O^H + S_O} + \eta_{y,h} \cdot \dfrac{K_O^H}{K_O^H + S_O} \cdot \dfrac{S_{NO}}{K_{NO} + S_{NO}} \right] \cdot X_{BH}$
10. Hydrolysis of entrapped organic nitrogen	$k_H \cdot \dfrac{\frac{X_S}{X_{BH}}}{K_X + \frac{X_S}{X_{BH}}} \cdot \left[\dfrac{S_O}{K_O^H + S_O} + \eta_{y,h} \cdot \dfrac{K_O^H}{K_O^H + S_O} \cdot \dfrac{S_{NO}}{K_{NO} + S_{NO}} \right] \cdot X_{BH} \cdot \dfrac{X_{ND}}{X_S}$

Table 4. Stoichiometric parameter values for ASM1m. The parameters that were added to the original ASM1 are in bold. All parameter values were taken from Henze et al. (1987), except when indicated differently.

Parameter description	Symbol	Value	Unit
Yield for heterotrophic biomass	Y_H	0.67	g COD.g COD^{-1}
Yield for autotrophic biomass	Y_A	0.24	g COD.g N^{-1}
Yield for methanotrophic biomass	**Y_{MOB}**	**0.19[a]**	**g COD.g COD^{-1}**
Fraction of biomass leading to particulate products	f_P	0.08	-
Fraction of nitrogen in biomass	i_{XB}	0.086	g N.g COD^{-1}
Mass of nitrogen in particulate products	i_{XP}	0.06	g N.g COD^{-1}

[a] Methanotrophic yield is 0.57 g biomass **(Arcangeli and Arvin, 1999)**. g CH$_4^{-1}$. This value was converted to the desired units using a conversion factor of 0.75 g biomass. g COD^{-1} (Henze et al., 1987).

Chapter 6

Table 5. Kinetic parameter values for ASM1m. The parameters that were added to the original ASM1 are in bold.

Parameter description	Symbol	Value	Unit	Reference
Maximum specific growth rate for heterotrophic biomass	$\mu_{max,H}$	6.0	d^{-1}	[1]
Half saturation concentration for heterotrophic biomass	K_s	20.0	$g\ COD.m^{-3}$	[1]
Oxygen half saturation coefficient for heterotrophic biomass	$K_{O,H}$	0.20	$g\ (-COD).m^{-3}$	[1]
Nitrate half saturation coefficient for denitrifying heterotrophic biomass	K_{NO}	0.50	$g\ N.m^{-3}$	[1]
Decay coefficient for heterotrophic biomass	b_H	0.62	d^{-1}	[1]
Correction factor for μ_H under anoxic conditions	$\eta_{y,g}$	0.8	-	[1]
Correction factor for hydrolysis under anoxic conditions	$\eta_{y,h}$	0.4	-	[1]
Maximum specific hydrolysis rate	k_h	3.0	$g\ COD.\ g\ COD^{-1}.d^{-1}$	[1]
Half saturation coefficient for hydrolysis of SBCOD	K_X	0.03	$g\ COD.\ g\ COD^{-1}$	[1]
Maximum specific growth rate for autotrophic biomass	$\mu_{max,A}$	0.80	d^{-1}	[1]
Ammonia half saturation coefficient for autotrophic biomass	$K_{NH,A}$	1.0	$g\ N.m^{-3}$	[1]
Decay coefficient for autotrophic biomass	b_A	0.20	d^{-1}	[1]
Oxygen half saturation coefficient for autotrophic biomass	$K_{O,A}$	0.4	$g\ (-COD).m^{-3}$	[1]
Ammonification rate	k_a	0.08	$m^3.g\ COD^{-1}.d^{-1}$	[1]
Maximum specific growth rate for methanotrophic biomass	$\mu_{max,MOB}$	1.5	d^{-1}	[2]
Half saturation concentration for methanotrophic biomass	K_{CH4}	0.24	$g\ COD.m^{-3}$	[2]
Oxygen half saturation coefficient for methanotrophic biomass	$K_{O,MOB}$	0.2	$g\ (-COD).m^{-3}$	[2]
Decay coefficient for methanotrophic biomass	b_{MOB}	0.24	d^{-1}	[2]

[1] Henze, M., Grady, C.P.L.J., Gujer, W., Marais, G.v.R. and Matsuo, T. (1987) Activated Sludge Model No. 1., IAWQ Scientific and Technical Report No. 1, IAWQ, London.
[2] Arcangeli, J.P. and Arvin, E. (1999) Modelling the growth of a methanotrophic biofilm: Estimation of parameters and variability. Biodegradation 10(3), 177-191.

Gas-liquid mass transfer

Derivation of Equation 1 according to van der Lans (2011)

According to the two-film theory concerning gas-liquid transfer (Lewis and Whitman, 1924), the interphase transfer rate of a compound i, TR_i [kg m^{-3} s^{-1}], is proportional to its gas-liquid mass transfer coefficient $k_L a$ [s^{-1}] and to the driving force between the concentration S_i [kg m^3] of the compound and its solubility S_i^* [kg m^3] at a certain partial pressure. The gas-liquid mass transfer coefficient $k_L a$ lumps the resistance to mass transfer at the interface k_L [m s^{-1}] and the specific interfacial area a [m^{-1}].

$$TR_i = k_L a_i \cdot (S_i^* - S_i) \tag{1}$$

The steady state gas phase mass balance is expressed as to calculate the depletion in the gas phase:

$$\begin{aligned} k_L a_i \cdot V \cdot (S_i^* - S_i) &= \phi_G^0 \cdot \left(c_{G,in}^0 - c_{G,out}^0 \right) \\ &= \phi_G^0 \cdot \frac{p^0 \cdot M_i}{R \cdot T^0} \cdot \left(x_{i,in} - x_{i,out} \right) \end{aligned} \tag{2}$$

Note that it is reasonably assumed that no reactions take place in the gas phase. The solubility S_i^* is proportional to pressure and dependent on depletion and thus varies with the location in the reactor.

To calculate the global (average) oxygen transfer rate from Eq. 1, a system characteristic value for S_i^* should be used, which depends on the gas phase mixing behaviour. For low aspect ratio's (column height over diameter less than 3) the assumption of an ideally mixed gas phase is reasonable, so the solubility corresponding with the gas outlet concentrations and corrected for the mean pressure in the column is chosen as its characteristic value:

$$S_i^* = \frac{c_{G,out}^0}{m_i} \cdot \frac{p_t + \frac{1}{2} \cdot \rho \cdot g \cdot H}{p^0} = \frac{(p_t + \frac{1}{2} \cdot \rho \cdot g \cdot H) \cdot M_i}{m_i \cdot R \cdot T^0} \cdot x_{i,out} \tag{3}$$

Calculation of $c_{G,out}^0$ from Eq. 2, followed by substitution in (3) yields:

$$S_i^* = \frac{\dfrac{c_{G,in}^0}{m_i} + \dfrac{k_L a_i \cdot V}{\phi_G^0 \cdot m_i} S_i}{1 + \dfrac{k_L a_i \cdot V}{\phi_G^0 \cdot m_i} \cdot \dfrac{p_t + \frac{1}{2}\cdot \rho \cdot g \cdot H}{p^0}} \cdot \frac{p_t + \frac{1}{2}\cdot \rho \cdot g \cdot H}{p^0} \tag{4}$$

In its turn, Eq. 4 is substituted in Eq. 1 to calculate the interphase transfer rate:

$$
\begin{aligned}
TR_i &= \frac{k_L a_i \cdot \left(\dfrac{c_{G,in}^0}{m_i} \cdot \dfrac{p_t + \frac{1}{2}\cdot \rho \cdot g \cdot H}{p^0} - S_i \right)}{1 + \dfrac{k_L a_i \cdot V}{\phi_G^0 \cdot m_i} \cdot \dfrac{p_t + \frac{1}{2}\cdot \rho \cdot g \cdot H}{p^0}} \\[2em]
&= \frac{k_L a_i \cdot \left(\dfrac{(p_t + \frac{1}{2}\cdot \rho \cdot g \cdot H)\cdot M_i}{m_i \cdot R \cdot T^0} \cdot x_{i,in} - S_i \right)}{1 + \dfrac{k_L a_i \cdot V}{\phi_G^0 \cdot m_i} \cdot \dfrac{p_t + \frac{1}{2}\cdot \rho \cdot g \cdot H}{p^0}}
\end{aligned}
\tag{5}
$$

The gas flow rate ϕ_G^0 can be substituted in terms of the characteristic (height-averaged) superficial gas flow velocity v_{Gs}^c through the relationship

$$\phi_G^0 = v_{Gs}^c \cdot A \cdot \frac{p_t + \frac{1}{2}\cdot \rho \cdot g \cdot H}{p^0} \tag{6}$$

resulting in

$$
\begin{aligned}
TR_i &= \frac{k_L a_i \cdot \left(\dfrac{c_{G,in}^0}{m_i} \cdot \dfrac{p_t + \frac{1}{2}\cdot \rho \cdot g \cdot H}{p^0} - S_i \right)}{1 + \dfrac{k_L a_i \cdot H}{v_{Gs}^c \cdot m_i}} \\[2em]
&= \frac{k_L a_i \cdot \left(\dfrac{(p_t + \frac{1}{2}\cdot \rho \cdot g \cdot H)\cdot M_i}{m_i \cdot R \cdot T^0} \cdot x_{i,in} - S_i \right)}{1 + \dfrac{k_L a_i \cdot H}{v_{Gs}^c \cdot m_i}}
\end{aligned}
\tag{7}
$$

For $v_{Gs}^c < 0.1$ m s^{-1}, the relationship between $k_L a_i$ and the characteristic (height-averaged) superficial gas flow velocity is given by (Heijnen and Van 't Riet, 1984):

$$k_L a_i [s^{-1}] = 0.6 \cdot v_{Gs}^c [m \ s^{-1}] \tag{8}$$

Eq. 8 is used to eliminate the superficial gas flow velocity from Eq. 7, which finally yields

$$TR_i = k_L a_i \cdot \frac{\dfrac{(p_t + \frac{1}{2} \cdot \rho \cdot g \cdot H) \cdot M_i}{m_i \cdot R \cdot T^0} \cdot x_{i,in} - S_i}{1 + \dfrac{0.6 \cdot H}{m_i}} \tag{9}$$

Eq. 9 gives the gas-liquid mass transfer of compound i as a function of the height H of the water column above the aeration equipment. For surface aeration, $H = 0$, and Eq. 9 equals Eq. 1.

The mass transfer coefficient $k_L a_i$ for methane is related to the mass transfer coefficient of oxygen by the ratio of their respective diffusion coefficients according to Equation 10 (based on van Suijdam et al. (1978)).

$$k_L a_{CH_4} = k_L a_{O_2} \cdot \sqrt{\frac{D_{CH_4}}{D_{O_2}}} \tag{10}$$

Nomenclature

$c_{G,in}^0$	Concentration of compound i in the ingoing aeration gas flow at reference conditions	kg m^{-3}
$c_{G,out}^0$	Concentration of compound i in the outgoing aeration gas flow at reference conditions	kg m^{-3}
g	Gravitational field constant	m s^{-2}
H	Height of the bubble column	m
$k_L a_i$	Gas-liquid mass transfer coefficient of compound i	s^{-1}
m_i	Partition coefficient gas-liquid $\frac{c_G}{S_i^*}$	-
M_i	Molecular weight of compound i	kg mol^{-1}
p^0	Atmospheric pressure	Pa
p^c	Characteristic pressure	Pa
p_t	Pressure at the water surface	Pa
R	Ideal gas constant	Pa m^3 mol^{-1} K^{-1}
S_i	Concentration of compound i in the mixed liquor	kg m^{-3}
S_i^*	Equilibrium concentration of compound i in the mixed liquor corresponding with the given gas phase concentration	kg m^{-3}
T^0	Temperature at reference conditions	K
TR_i	Transfer rate of compound i	kg m^{-3} d^{-1}
V	Volume	m^3
v_{Gs}^c	Characteristic superficial gas velocity	m s^{-1}
$x_{i,in}$	Concentration of compound i in the ingoing aeration gas flow (mole fraction)	-
$x_{i,out}$	Concentration of compound i in the outgoing aeration gas flow (mole fraction)	-
ρ	Density of the mixed liquor	kg m^{-3}
ϕ_G^0	Volumetric gas flow rate at 1 bar	m^3 s^{-1}

Effluent quality index and aeration energy

The effluent quality index (EQI) is calculated according to Nopens et al. (2010). It represents the weighted average of the effluent loads of Total Suspended Solids, COD, BOD$_5$, Total Kjeldahl Nitrogen and nitrite + nitrate.

$$EQI = \frac{1}{1000 \cdot t_{obs}} \int_{t_{start}}^{t_{end}} [\beta_{TSS}TSS(t) + \beta_{TSS}COD(t) + \beta_{TSS}BOD(t) + \beta_{TSS}TKN(t) + \beta_{TSS}TSS(t)]Q_e(t)dt$$

where t_{obs} represents the observed time between t_{start} and t_{end}. The symbols are explained in Table 6.

Table 6. Compounds taken into account for the calculation of the Effluent Quality Index.

Symbol	Compound	Weights β	Units
TSS	Total suspended solids	2	g.m^{-3}
COD	Chemical oxygen demand	1	g COD.m^{-3}
BOD	Biological oxygen demand	2	g COD.m^{-3}
TKN	Total Kjeldahl Nitrogen	30	g N.m^{-3}
NO	Nitrite + Nitrate	10	g N.m^{-3}

The aeration energy [kWh.d^{-1}] was calculated with an assumed transfer efficiency of 1.8 kg O^2 kWh^{-1} (Nopens et al., 2010):

$$AE = \frac{S_{O,sat}}{t_{obs} \cdot 1.8 \cdot 1000} \int_{t_{start}}^{t_{end}} \sum_{i=1}^{5} V_i \cdot k_L a_i(t)\, dt$$

with

t_{obs}	between t_{start} and t_{end} [d];
$S_{O,sat}$	the saturated oxygen concentration [gO$_2$. m^{-3}];
V_i	the volume of tank i [m^{-3}];
$k_L a_i$	the oxygen mass transfer coefficient in tank i [d^{-1}].

In steady state, as in the present study, this equation is reduced to

$$AE = \frac{S_{O,sat} \cdot V_i \cdot k_L a_i}{t_{obs} \cdot 1.8 \cdot 1000}$$

Influence of aeration intensity (section 3.3.1) - supporting graphs

The following graphs support the discussion of the effect of aeration intensity. Figure 1 shows the Monod terms for the respective substrates and oxygen for heterotrophic, autotrophic and methanotrophic organisms. This helps understanding the effect of the concentrations on the growth rates. The biomass concentrations of the three biomass groups is shown in Figure 2. The presence of heterotrophic biomass when there is no aeration can be explained by their presence in the influent. The inlfuent does not contain autotrophic nor methanotrophic organisms. Figure 3 shows the concentrations of the respective substrates. The increase in ammonium concentration as $k_L a_{O_2}$ increases to 80 d^{-1} is due to the hydrolysis and ammonification of the nitrogen that is set free as biomass decays. Finally, Figure 4 gives the effluent quality and consumed aeration energy.
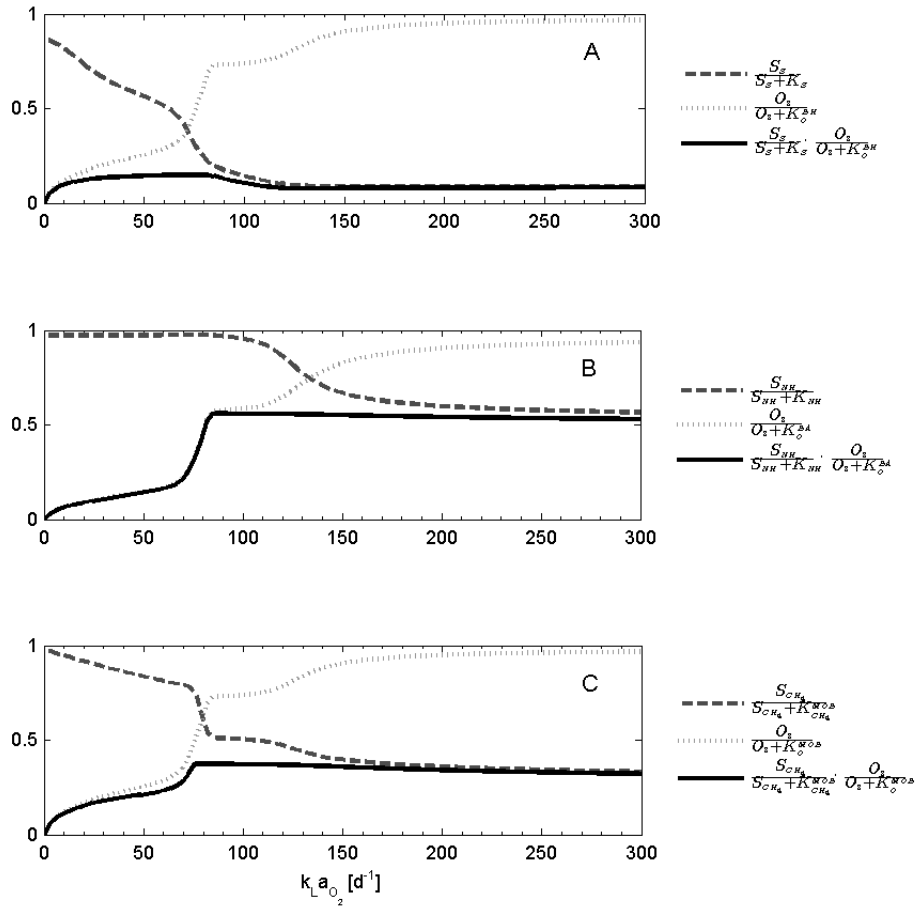

Figure 1. Monod terms for heterotrophic (A), autotrophic (B) and methanotrophic (C) biomass over the range of the oxygen mass transfer coefficient $k_L a_{O_2}$. The dashed line is the

curve for the Monod term for the substrate, the dotted line is the curve for the Monod term
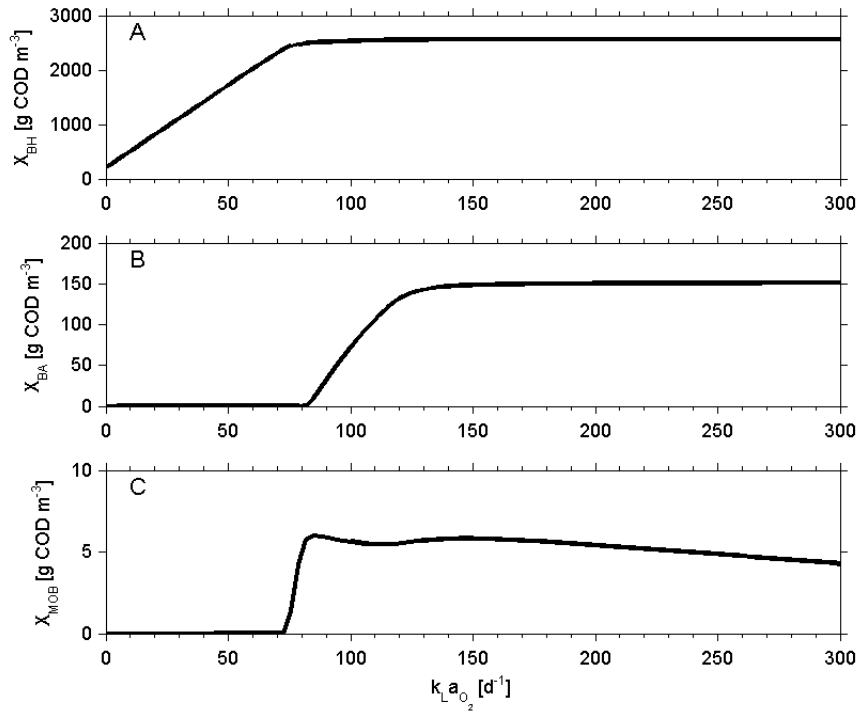for oxygen, and the full line is the product of the two Monod curves.

Figure 2. Biomass concentrations as function of the oxygen mass transfer coefficient $k_L a_{O_2}$.
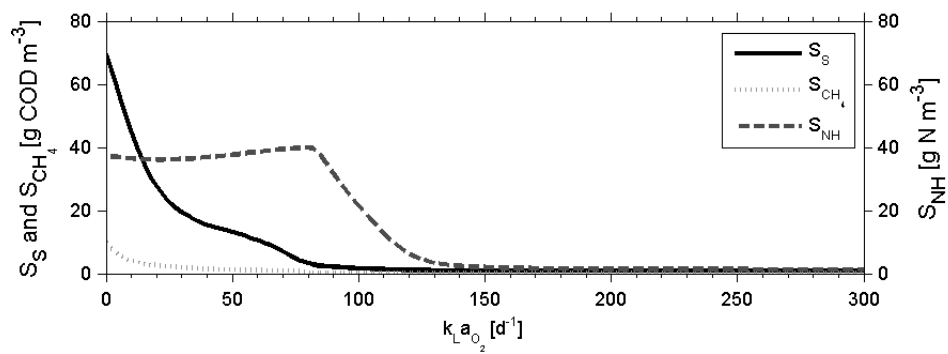

Figure 3. Substrate concentrations as function of the oxygen mass transfer coefficient $k_L a_{O_2}$.
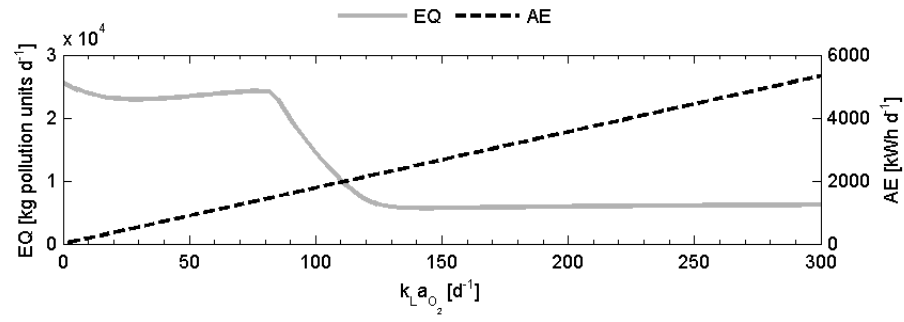
Figure 4. Effluent quality (EQ) and aeration energy consumption (AE) as function of the oxygen mass transfer coefficient $k_L a_{O_2}$.

7

Concluding remarks

The objective of this thesis was to advance insight in the extent of methane and nitrous oxide emissions from municipal wastewater treatment and to gain understanding of the process conditions leading to methane and nitrous oxide emissions from municipal wastewater treatment. This knowledge is required to come up with design and operation guidelines to mitigate the emissions.

Significance of greenhouse gas emissions

At the core of this study is a comprehensive dataset from the high-frequency, long-term monitoring of nitrous oxide and methane emissions on a covered municipal wastewater treatment plant. This study arguably led to the most accurate estimate of a plant's greenhouse gas emissions to date. Together with the indirect emission of carbon dioxide related to the plant's electricity and natural gas consumption, these data showed that the emission of nitrous oxide from this particular plant largely surpasses the emission of carbon dioxide with respect to greenhouse gas footprint. The emission of methane is also slightly higher than the plant's indirect carbon dioxide emission. The methane that is emitted from anaerobic sludge treatment should be compared with the carbon dioxide emission that is avoided by using the resulting biogas as fossil fuel replacement. As long as the methane emission, expressed as CO_2-equivalents, is lower than the avoided emission of carbon dioxide, the net contribution of anaerobic sludge digestion to the wastewater treatment sector's climate footprint is negative. This was, however, not the case in the present study: using a global warming potential of 25 CO_2-equivalents (IPCC, 2007a), the emission of methane originating from anaerobic sludge treatment amounted to 110 % of the avoided carbon dioxide emission. Using the revised global warming potential of 34 CO_2-equivalents (IPCC, 2013a), this value is as high as 150 %.

Extrapolation of this study's greenhouse gas emission estimate to the entire wastewater treatment sector is not warranted, considering the wide variability between wastewater treatment plants that has been found in previous studies (see Kampschreur et al. (2009) and Law et al. (2012b) for nitrous oxide and Aboobakar et al. (2014) for methane). Not until many more monitoring results are published, will it be possible to obtain an accurate estimate of the global emission of greenhouse gases of wastewater treatment. Such a bottom-up approach could eventually lead to an estimate of the share of wastewater treatment in a country's total anthropogenic climate footprint that is more accurate than the current use of fixed assumed emission factors, as prescribed by the International Panel for Climate Change.

Monitoring

Rather than establishing the amount of greenhouse gas that is emitted from wastewater treatment in general, this study describes the dynamics of methane and nitrous oxide emissions of a specific plant, Kralingseveer WWTP. This required an extensive monitoring effort that is to date unprecedented and that can therefore serve as a reference case for

future monitoring efforts. Hence, this study also deals with a number of methodological aspects related to monitoring of methane and nitrous oxide emissions. Especially regarding nitrous oxide, the present work exposed the temporal variability that can be encountered on a full-scale plant, and how to deal with it when monitoring emissions from activated sludge tanks. In contrast to nitrous oxide, the emission of methane was not limited to activated sludge tanks. A rigorous mass balance approach was set up in order to identify sinks and sources of methane on the WWTP. This required measurements of all methane mass flow rates between the different unit processes of the plant. For sampling methane that is dissolved in liquid streams, a salting-out method was developed.

The WWTP of Kralingseveer lent itself very well for this monitoring campaign, since it was covered. This allowed for an accurate estimate of the amount of methane and nitrous oxide that is emitted from the various parts of the plant to the atmosphere. In contrast, the emission from uncovered plants, as most plants in the world, can only be measured from a small surface and those measurements may therefore not be representative of the total emission of an entire reactor, given the emission's high spatial variability. The amount of greenhouse gases emitted from an uncovered plant can therefore not be established as accurate as e.g. nitrogen, COD and suspended solids leaving the plant with the effluent. While the effluent leaves the plant through a channel that can be monitored relatively easy, nitrous oxide emissions are dispersed across the surface of the activated sludge tank, while methane emissions are even spread across several unit processes. This spatial variability forms an additional impediment, besides the temporal variability, to obtain an accurate emission estimate.

The difficulties involved in measuring the amount of methane and nitrous oxide emitted to the atmosphere have serious consequences for a possible greenhouse gas mitigation policy. Without being able to account for the emissions in a sufficiently accurate way, imposing levies on greenhouse gases or the introduction of a greenhouse gas crediting system as proposed by Wang et al. (2011b) is impossible. This precludes any financial incentive for a wastewater treatment utility to curb the emission of greenhouse gases.

Implications for modelling

Given the difficulties related to monitoring methane and nitrous oxide emissions from wastewater treatment, it would be helpful to have a model that predicts the emission of methane and nitrous oxide based on one or more input variables that are easy to monitor, e.g. mixed liquor inorganic nitrogen concentrations in the case of nitrous oxide emissions.

Although there are models that predict the production of methane during the anaerobic treatment of sewage and sewage sludge (e.g. Batstone et al. (2002)), the emission of methane from full-scale wastewater treatment plants has not yet been predicted using such models. In principle, this should be rather straightforward since methanogenesis from

organic matter is well understood. The difficulty is finding out how much of the organic matter ending up in a plant is degraded anaerobically and, in the case of biogas production, to what extent the produced methane is recovered for producing heat and/or power. For methane emissions from sewer systems, a model was developed by Guisasola et al. (2009).

Much more attention has been given to the modelling of nitrous oxide emissions (e.g. Hiatt and Grady (2008), Guo et al. (2010), Mampaey et al. (2011), Ni et al. (2011), Ni et al. (2013)). Either such models attempt at predicting the dynamic behaviour or they are used as a tool to gain insight into the mechanisms behind the production and emission of nitrous oxide. Eventually, these models are to be implemented in the design and control of real plants with the aim of reducing greenhouse gas emissions. As yet, no model has been able to describe the long-term dynamic behaviour of the nitrous oxide emission from a full-scale wastewater treatment plant. If that will ever be possible, remains to be seen, since the modelling efforts are thwarted by several obstacles.

First, there is no consensus yet about the microbial pathways that are responsible for the production of nitrous oxide, nor about the relative significance of the proposed pathways. Especially the pathways in ammonia oxidizing bacteria are subject to debate (Schreiber et al., 2012). This knowledge gap causes uncertainty about the equations that should be included in the model. This uncertainty in the model structure is exacerbated by a number of other unexplained phenomena in the data. As suggested in Chapter 4, the seasonal trend in the emission may be related to adaptation of the biomass community in the activated sludge. This may cause seasonal variability of the rates of the different proposed pathways and their mutual significance. So, over time, different production and emission mechanisms may be happening with various time constants.

So far, no model has yet taken into account all these considerations, but it is imperative that such a model would live up to the required levels of precision and accuracy. So, once the model structure has been established, the second hurdle is the reduction of the error on the predicted nitrous oxide emission. This is particularly relevant because of the high global warming potential of nitrous oxide in comparison with methane and carbon dioxide. The uncertainty on the predicted outcome is the result of the error propagation of all errors in model parameter estimates and model inputs, and both are subject to significant uncertainties themselves. Measurements on a full-scale WWTP are not always reliable and together with the large process flows this results in inaccurate data of operational conditions and inaccurate model inputs as a consequence (Meijer et al., 2002). The sensitivity of nitrous oxide models to model parameters can be particularly high when their higher order interaction effects are taken into account (Sweetapple et al., 2013). This effect of parameter interaction may be related with the present study's observation that none of the investigated process conditions correlated with the long-term emission trend.

Mitigating methane and nitrous oxide emissions

The emission of methane could be traced back either to methane formed in the sewer or to storage and manipulation of sludge during anaerobic treatment. Mitigation of methane emissions can often be achieved pre-emptively, by good housekeeping practices in WWTP operations, such as avoiding leakages during sludge storage and good combustion management to avoid methane slip from the gas engine. Methane formation in sewers could possibly be counteracted by dosing alkali (Gutierrez et al., 2009), free nitrous acid (Jiang et al., 2011a; Jiang et al., 2011b), free nitrous acid (Jiang et al., 2011a; Jiang et al., 2011b), nitrite (Mohanakrishnan et al., 2008; Jiang et al., 2010), nitrate (Mohanakrishnan et al., 2009) or ferric iron (Zhang et al., 2009). Although dosing nitrite may prevent the formation of methane, it can give rise to the emission of nitrous oxide, since nitrite is known to induce its production during nitrification and denitrification processes. Since nitrous oxide has a global warming potential of 298 CO_2-equivalents and methane has a global warming potential of 25 CO_2-equivalents, the resulting nitrous oxide may even cause more harm than the avoided methane emission.

If methane formation cannot be avoided, e.g. in sludge storage tanks, gaseous methane could be combusted by using the ventilation air from the tank as combustion air in a combined heat and power system, while the methane oxidizing capacity of activated sludge could be exploited to respire dissolved methane, e.g. in the influent or in reject water. To promote microbial conversion of methane in an aeration tank over stripping, subsurface bubble aeration and a CSTR configuration proved to be better to avoid emissions than surface aeration and plug flow conditions.

The prevention of the emission of nitrous oxide from municipal wastewater treatment is still hampered by the limited knowledge about the several nitrous oxide production pathways and their mutual relevancies. The results presented in this thesis do not allow establishing unequivocally which operational conditions actually contribute to the production and emission of nitrous oxide, nor was it possible to assess to what extent denitrification is a sink for nitrous oxide.

Recommendations for further research

The mechanisms behind the production and emission of methane are well known and mitigation is rather straightforward. Still, the contribution of methane to climate footprint of the wastewater treatment sector and the contribution of methane from wastewater treatment to the total anthropogenic greenhouse gas emissions is unclear. Monitoring of the methane emission from more and different plants may eventually lead to a more accurate estimate, but further development of methane emission models could contribute to this aim as well.

As with methane, a better estimate of the significance of nitrous oxide emissions from wastewater treatment is yet something to achieve, but in contrast to the emission of methane, the mechanisms leading to the emission of nitrous oxide are still unclear. The identification of the nitrous oxide production pathways and their mutual significance is important for developing mitigation strategies.

The production of nitrous oxide during nitrification, and via the hydroxylamine pathway in particular, is still under debate. Unravelling this pathway is something that can only be done in lab-scale tests, since full-scale data are usually too cluttered and not accurate enough. Also the mutual significance of the different pathways, both during nitrification and denitrification, could be determined with lab-work, but translating those findings to conditions in a full-scale is delicate. Furthermore, the high seasonal variability of the nitrous oxide emission, which appeared unrelated to temperature, suggests that the level of the emission may be influenced by a change in the microbial community. This seasonal trend also leaves the possibility that different nitrous oxide production pathways may dominate during different periods of the year. Future attempts to unravel the mechanisms of nitrous oxide production from wastewater treatment plants should therefore look into the dynamics of the relative balance of production and consumption of nitrous oxide. For those reasons, as well as for obtaining better estimates of the emissions' magnitude, full-scale measurements remain a necessity.

Especially for the majority of plants that are uncovered, off-gas measurements are cumbersome and can be unreliable. As mentioned earlier, off-gases can only be measured from a limited surface area of the aeration tank, raising concerns about representativeness. For nitrous oxide, a sensor exists that can measure dissolved nitrous oxide. Monitoring dissolved nitrous oxide could be a way to overcome the drawbacks of off-gas measurements. If dissolved nitrous oxide measurements are combined with knowledge about the gas-liquid mass transfer rate of the reactor, it may be possible to obtain an accurate estimate of the nitrous oxide emission. Of course, this method has its own sources of uncertainty: it requires a good estimation of the gas-liquid mass transfer rate and its dynamics, and incomplete mixing or plug flow conditions in the activated sludge tanks raises concerns about the extent to which a local nitrous oxide measurement is representative of the concentration in the entire tank.

Another drawback of off-gas measurements is that it blurs the distinction between production and emission of nitrous oxide. In most WWTPs designed for biological nitrogen removal via nitrification and denitrification, the mixed liquor cycles between aerobic and anoxic reactors (e.g. in the Modified Ludzack-Ettinger configuration). Nitrous oxide can be produced in anoxic or in aerobic reactors, but even if it is produced in an anoxic reactor, most of it will only be emitted after the mixed liquor enters an aerobic reactor because of the high gas-liquid mass transfer. So, emission measurements do not show whether the nitrous oxide was produced in the anoxic or in the aerobic reactor. By

measuring dissolved nitrous oxide instead of emitted nitrous oxide, it can be established whether nitrous oxide is produced in anoxic or aerobic conditions. Yet, this knowledge does not provide a decisive answer as to what pathway(s) dominate(s) the production of nitrous oxide on a plant, since heterotrophic denitrification can go on in aerobic tanks (e.g. when the inner part of a sludge floc becomes anoxic) and autotrophic nitrification can go on in anoxic tanks (e.g. if oxygen enters this tank with the internal recycle flow).

The identification of different nitrous oxide pathways has also been attempted by using fractionation data of stable nitrogen isotopes (Wunderlin et al., 2013a). The $^{15}N/^{14}N$ ratio of nitrous oxide and its site preference (i.e. the difference of the $^{15}N/^{14}N$ ratio on the central and the terminal nitrogen atom of nitrous oxide) differs according to the enzymatic reaction by which the nitrous oxide is formed. By comparing fractionation data from mixed cultures with available fractionation data from pure culture studies, it is possible to trace the pathway by which the nitrous oxide is formed. Yet, when the three nitrous oxide production pathways and heterotrophic nitrous oxide reduction can all happen at the same time, e.g. under low oxygen conditions, the partitioning of the production pathways is difficult (Wunderlin et al., 2013a). Furthermore, these techniques cannot be used to estimate the amount of nitrous oxide that is emitted. So, in the end, adequate monitoring remains a necessity.

Future perspectives

As the world population keeps on growing and as more and more people get access to sanitation, the amount of nitrogen that ends up in wastewater treatment plants is increasing. At the same time, ever more stringent effluent standards require more nitrogen to be removed from sewage. The increasing importance of biological nitrogen removal could probably result in an increase of nitrous oxide emissions. Yet, emerging technologies focusing on source separation of urine and recovery of nitrogen from concentrated streams such as source separated urine by ion exchange (Sutton et al., 2011), struvite precipitation (Zeeman and Kujawa-Roeleveld, 2011) or stripping (Maurer et al., 2006) can decrease the nitrogen load to wastewater treatment. As a result, less nitrogen has to be treated biologically, which in its turn diminishes the risk of nitrous oxide emission. Obviously, the additional energy and chemicals required by these emerging nitrogen recovery technologies should not lead to indirect greenhouse gas emissions that exceed the avoided nitrous oxide emissions.

Technologies for nutrient recovery instead of removal are often integrated in novel process schemes where anaerobic digestion is used to recover energy from sewage in the form of biogas, as an alternative to the energy intensive conventional activated sludge technology (Verstraete and Vlaeminck, 2011). Of course, an increasing use of anaerobic digestion instead of aerated activated sludge raises concerns about methane emissions, especially dissolved methane that is stripped from the digester effluent (Cakir and Stenstrom, 2005;

Hartley and Lant, 2006), but also emissions during storage and thickening of sludge. Several new technologies for the removal of dissolved methane are currently being investigated. Among these are aerobic methane oxidation (Hatamoto et al., 2010; Matsuura et al., 2010; van der Ha et al., 2011), anaerobic methane oxidation (Ettwig et al., 2010; Kampman et al., 2012) and membrane degassing (Bandara et al., 2011). Yet, a lot of methane emission can already be avoided by good housekeeping, such as avoiding dispersed emissions from leakages and proper treatment of ventilation air from storage of digester effluent. In brief, while new wastewater treatment technologies focus on the recovery of nutrients and the decrease in energy consumption with the concomitant decrease of indirect carbon dioxide emissions, these technologies will also result in a decrease of direct nitrous oxide emissions, while good housekeeping together with emerging methane oxidation and recovery technologies can curb methane emissions.
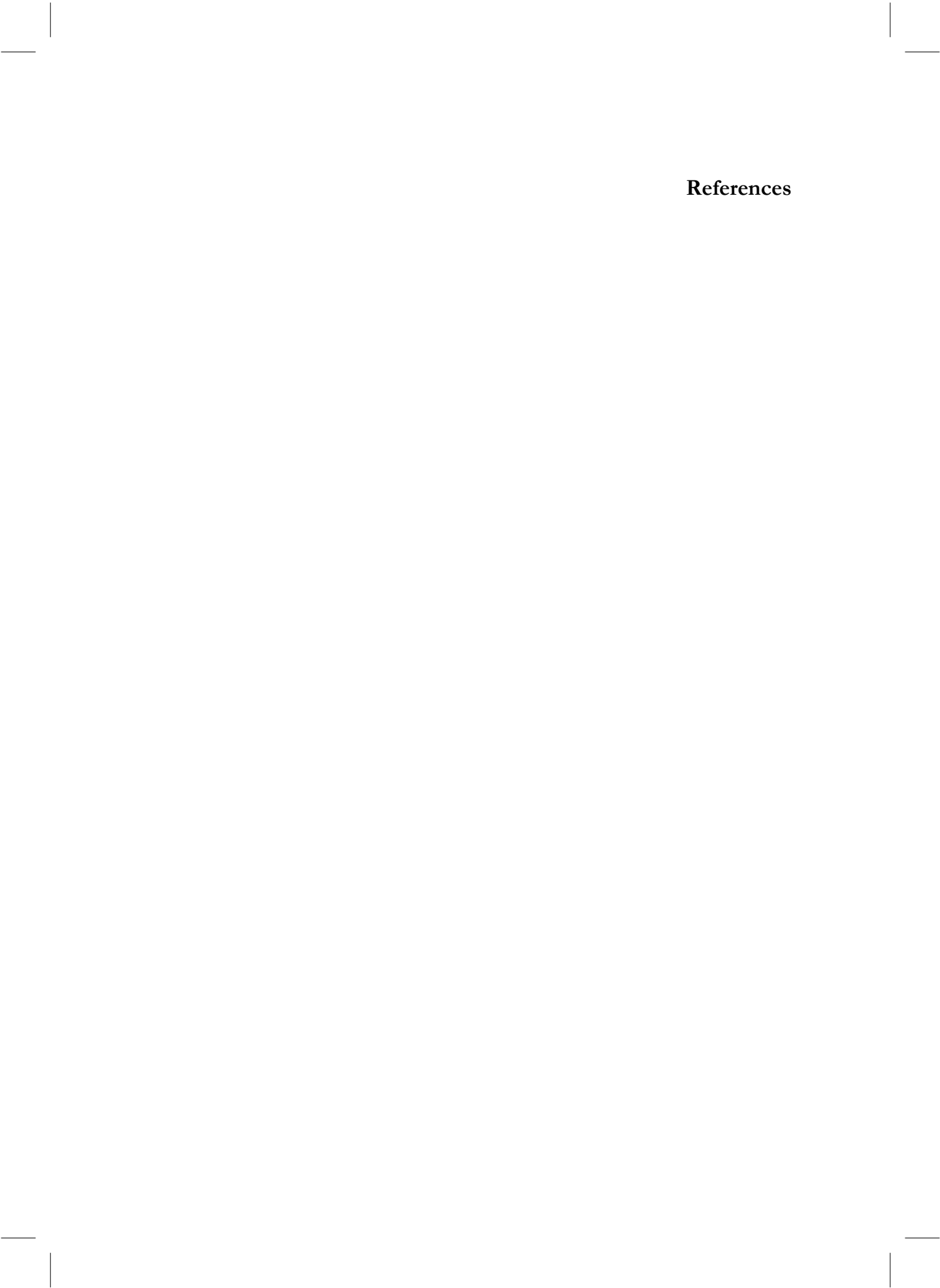
References

References

Aboobakar, A., Cartmell, E., Stephenson, T., Jones, M., Vale, P. and Dotro, G. (2013) Nitrous oxide emissions and dissolved oxygen profiling in a full-scale nitrifying activated sludge treatment plant. Water Research 47(2), 524-534.

Aboobakar, A., Jones, M., Vale, P., Cartmell, E. and Dotro, G. (2014) Methane Emissions from Aerated Zones in a Full-Scale Nitrifying Activated Sludge Treatment Plant. Water Air and Soil Pollution 225(1).

Ahn, J.H., Kim, S., Park, H., Katehis, D., Pagilla, K. and Chandran, K. (2010a) Spatial and temporal variability in atmospheric nitrous oxide generation and emission from full-scale biological nitrogen removal and non-BNR processes. Water Environment Research 82(12), 2362-2372.

Ahn, J.H., Kim, S., Park, H., Rahm, B., Pagilla, K. and Chandran, K. (2010b) N_2O emissions from activated sludge processes, 2008-2009: results of a national monitoring survey in the United States. Environmental science and technology 44(12), 4505-4511.

Alex, J., Benedetti, L., Copp, J.B., Gernaey, K.V., Jeppsson, U., Nopens, I., Pons, M.N., Steyer, J.P. and Vanrolleghem, P. (2008) Benchmark Simulation Model no. 1 (BSM1).

Alleman, J.E. (1985) Elevated nitrite occurrence in biological wastewater treatment systems. Water Science and Technology 17(2-3 -3 pt 1), 409-419.

Alvarez-Cohen, L. and McCarty, P.L. (1991) Product toxicity and cometabolic competitive-inhibition modeling of chloroform and trichloroethylene transformation by methanotrophic resting cells. Applied and Environmental Microbiology 57(4), 1031-1037.

Arcangeli, J.P. and Arvin, E. (1999) Modelling the growth of a methanotrophic biofilm: Estimation of parameters and variability. Biodegradation 10(3), 177-191.

Bandara, W.M.K.R.T.W., Satoh, H., Sasakawa, M., Nakahara, Y., Takahashi, M. and Okabe, S. (2011) Removal of residual dissolved methane gas in an upflow anaerobic sludge blanket reactor treating low-strength wastewater at low temperature with degassing membrane. Water Research 45(11), 3533-3540.

Batstone, D.J., Keller, J., Angelidaki, I., Kalyuzhnyi, S.V., Pavlostathis, S.G., Rozzi, A., Sanders, W.T.M., Siegrist, H. and Vavilin, V.A. (2002) The IWA Anaerobic Digestion Model No 1(ADM 1). Water Science & Technology 45(10), 65-73.

Begonja, A. and Hrsak, D. (2001) Effect of growth conditions on the expression of soluble methane monooxygenase. Food Technology and Biotechnology 39(1), 29-35.

Benthum, W.A.J.v., Garrido, J.M., Mathijssen, J.P.M., Sunde, J., Loosdrecht, M.C.M.v. and Heijnen, J.J. (1998) Nitrogen Removal in Intermittently Aerated Biofilm Airlift Reactor. Journal of Environmental Engineering 124(3), 239-248.

Broholm, K., Christensen, T.H. and Jensen, B.K. (1992) Modeling TCE degradation by a mixed culture of methane-oxidizing bacteria. Water Research 26(9), 1177-1185.

Burgess, J.E., Parsons, S.A. and Stuetz, R.M. (2001) Developments in odour control and waste gas treatment biotechnology: a review. Biotechnology Advances 19(1), 35-63.

Burgess, J.E., Colliver, B.B., Stuetz, R.M. and Stephenson, T. (2002a) Dinitrogen oxide production by a mixed culture of nitrifying bacteria during ammonia shock loading and aeration failure. Journal of industrial microbiology & biotechnology 29(6), 309-313.

Burgess, J.E., Stuetz, R.M., Morton, S. and Stephenson, T. (2002b) Dinitrogen oxide detection for process failure early warning systems. Water Science and Technology 45(4-5), 247-254.

Butler, M.D., Wang, Y.Y., Cartmell, E. and Stephenson, T. (2009) Nitrous oxide emissions for early warning of biological nitrification failure in activated sludge. Water Research 43(5), 1265-1272.

Cakir, F.Y. and Stenstrom, M.K. (2005) Greenhouse gas production: A comparison between aerobic and anaerobic wastewater treatment technology. Water Research 39(17), 4197-4203.

Chandran, K., Stein, L.Y., Klotz, M.G. and van Loosdrecht, M.C.M. (2011) Nitrous oxide production by lithotrophic ammonia-oxidizing bacteria and implications for engineered nitrogen-removal systems. Biochemical Society transactions 39, 1832-1837.

Colliver, B.B. and Stephenson, T. (2000) Production of nitrogen oxide and dinitrogen oxide by autotrophic nitrifiers. Biotechnology Advances 18(3), 219-232.

Conrad, R. (2009) The global methane cycle: recent advances in understanding the microbial processes involved. Environmental Microbiology Reports 1(5), 285-292.

Copp, J.B. (2002) The COST simulation benchmark: description and simulator manual, Office for Official Publications of the European Communities, Luxembourg.

Czepiel, P., Crill, P. and Harriss, R. (1995) Nitrous oxide emissions from municipal wastewater treatment. Environmental Science and Technology 29(9), 2352-2356.

Czepiel, P.M., Crill, P.M. and Harriss, R.C. (1993) Methane emissions from municipal wastewater treatment processes. Environmental Science and Technology 27(12), 2472-2477.

Daelman, M.R.J., van Voorthuizen, E.M., van Dongen, U.G.J.M., Volcke, E.I.P. and van Loosdrecht, M.C.M. (2012) Methane emission during municipal wastewater treatment. Water Research 46(11), 3657-3670.

Daelman, M.R.J., van Voorthuizen, E.M., van Dongen, L.G.J.M., Volcke, E.I.P. and van Loosdrecht, M. (2013) Methane and nitrous oxide emissions from municipal wastewater treatment – results from a long-term study. Water Science and Technology 67(10), 2350–2355.

Delhomenie, M.-C., Nikiema, J., Bibeau, L. and Heitz, M. (2008) A new method to determine the microbial kinetic parameters in biological air filters. Chemical Engineering Science 63(16), 4126-4134.

Desloover, J., De Clippeleir, H., Boeckx, P., Du Laing, G., Colsen, J., Verstraete, W. and Vlaeminck, S.E. (2011) Floc-based sequential partial nitritation and anammox at full scale with contrasting N_2O emissions. Water Research 45(9), 2811-2821.

Desloover, J., Vlaeminck, S.E., Clauwaert, P., Verstraete, W. and Boon, N. (2012) Strategies to mitigate N_2O emissions from biological nitrogen removal systems. Current Opinion in Biotechnology 23(3), 474-482.

El-Fadel, M. and Massoud, M. (2001) Methane emissions from wastewater management. Environmental Pollution 114(2), 177-185.

EPA (2013) Inventory of U.S. Greenhouse Gas Emissions and Sinks: 1990 - 2011, U.S. Environmental Protection Agency, Washington DC, USA.

Estrada, J.M., Kraakman, N.J.R.B., Munoz, R. and Lebrero, R. (2011) A Comparative Analysis of Odour Treatment Technologies in Wastewater Treatment Plants. Environmental Science & Technology 45(3), 1100-1106.

Ettwig, K.F., Butler, M.K., Le Paslier, D., Pelletier, E., Mangenot, S., Kuypers, M.M.M., Schreiber, F., Dutilh, B.E., Zedelius, J., de Beer, D., Gloerich, J., Wessels, H.J.C.T., van Alen, T., Luesken, F., Wu, M.L., van de Pas-Schoonen, K.T., Op den Camp, H.J.M., Janssen-Megens, E.M., Francoijs, K.-J., Stunnenberg, H., Weissenbach, J., Jetten, M.S.M. and Strous, M. (2010) Nitrite-driven anaerobic methane oxidation by oxygenic bacteria. Nature 464(7288), 543-548.

Feijoo, G., Soto, M., Mendez, R. and Lema, J.M. (1995) Sodium inhibition in the anaerobic-digestion process: Antagonism and adaptation phenomena. Enzyme and Microbial Technology 17(2), 180-188.

References

Foley, J. and Lant, P. (2008) Fugitive greenhouse gas emissions from wastewater systems - WSAA Literature Review No.01, Water Services Association of Australia, Melbourne and Sydney, Australia.

Foley, J., Yuan, Z. and Lant, P. (2009) Dissolved methane in rising main sewer systems: field measurements and simple model development for estimating greenhouse gas emissions. Water Science and Technology 60(11), 2963-2971.

Foley, J., de Haas, D., Yuan, Z. and Lant, P. (2010) Nitrous oxide generation in full-scale biological nutrient removal wastewater treatment plants. Water Research 44(3), 831-844.

Fred, T., Heinonen, M., Sundell, L. and Toivikko, S. (2009) Air emissions at large municipal wastewater treatment plants in Finland for national E-PRTR reporting register. Water Practice & Technology 4(2).

Freitag, A., Rudert, M. and Bock, E. (1987) Growth of Nitrobacter by dissimilatoric nitrate reduction. Fems Microbiology Letters 48(1-2), 105-109.

Gal'chenko, V.F., Lein, A.Y. and Ivanov, M.V. (2004) Methane content in the bottom sediments and water column of the Black Sea. Microbiology 73(2), 211-223.

Genge, J.R. (1991) Contamination of breath methane samples in sterilized vacutainer tubes. Clinical Chemistry 37(11), 2019-2020.

Gevaert, V., Verdonck, F., Benedetti, L., De Keyser, W. and De Baets, B. (2009) Evaluating the usefulness of dynamic pollutant fate models for implementing the EU Water Framework Directive. Chemosphere 76(1), 27-35.

Girard, M., Ramirez, A.A., Buelna, G. and Heitz, M. (2011) Biofiltration of methane at low concentrations representative of the piggery industry--Influence of the methane and nitrogen concentrations. Chemical Engineering Journal 168(1), 151-158.

Gong, Y.-K., Peng, Y.-Z., Yang, Q., Wu, W.-M. and Wang, S.-Y. (2012) Formation of nitrous oxide in a gradient of oxygenation and nitrogen loading rate during denitrification of nitrite and nitrate. Journal of Hazardous Materials 227, 453-460.

Gray, N.D., Miskin, I.P., Kornilova, O., Curtis, T.P. and Head, I.M. (2002) Occurrence and activity of Archaea in aerated activated sludge wastewater treatment plants. Environmental Microbiology 4(3), 158-168.

Gresch, M., Braun, D. and Gujer, W. (2010) The role of the flow pattern in wastewater aeration tanks. Water Science and Technology 61(2), 407-414.

Guisasola, A., Jubany, I., Baeza, J.A., Carrera, J. and Lafuente, J. (2005) Respirometric estimation of the oxygen affinity constants for biological ammonium and nitrite oxidation. Journal of Chemical Technology & Biotechnology 80(4), 388-396.

Guisasola, A., de Haas, D., Keller, J. and Yuan, Z. (2008) Methane formation in sewer systems. Water Research 42(6-7), 1421-1430.

Guisasola, A., Sharma, K.R., Keller, J. and Yuan, Z. (2009) Development of a model for assessing methane formation in rising main sewers. Water Research 43(11), 2874-2884.

Guo, J., Peng, Y., Huang, H., Wang, S., Ge, S., Zhang, J. and Wang, Z. (2010) Short- and long-term effects of temperature on partial nitrification in a sequencing batch reactor treating domestic wastewater. Journal of Hazardous Materials 179(1-3), 471-479.

Gutierrez, O., Park, D., Sharma, K.R. and Yuan, Z. (2009) Effects of long-term pH elevation on the sulfate-reducing and methanogenic activities of anaerobic sewer biofilms. Water Research 43(9), 2549-2557.

Hanaki, K., Hong, Z. and Matsuo, T. (1992) Production of nitrous oxide gas during denitrification of wastewater. Water Science and Technology 26(5-6), 1027-1036.

Hansen, T.L., Sommer, S.G., Gabriel, S. and Christensen, T.H. (2006) Methane production during storage of anaerobically digested municipal organic waste. Journal of Environment Quality 35(3), 830-836.

Hanson, R.S. and Hanson, T.E. (1996) Methanotrophic bacteria. Microbiological reviews 60(2), 439-471.

Harremoës, P. and Henze, M. (1971) Denitrifikation med methan. Vand 1, 7-11.

Hartley, K. and Lant, P. (2006) Eliminating non-renewable CO_2 emissions from sewage treatment: An anaerobic migrating bed reactor pilot plant study. Biotechnology and Bioengineering 95(3), 384-398.

Hatamoto, M., Yamamoto, H., Kindaichi, T., Ozaki, N. and Ohashi, A. (2010) Biological oxidation of dissolved methane in effluents from anaerobic reactors using a down-flow hanging sponge reactor. Water Research 44(5), 1409-1418.

Henze, M., Grady, C.P.L.J., Gujer, W., Marais, G.v.R. and Matsuo, T. (1987) Activated Sludge Model No. 1. (IAWQ Scientific and Technical Report No. 1), IAWQ, London.

Heslinga, D.C. and van Harmelen, A.K. (2006) Vaststellingsmethodieken voor CO_2-emissiefactoren van aardgas in Nederland, TNO, Apeldoorn, Netherlands.

Hiatt, W.C. and Grady, C.P.L. (2008) An updated process model for carbon oxidation, nitrification, and denitrification. Water environment research : a research publication of the Water Environment Federation 80(11), 2145-2156.

Ho, A., Vlaeminck, S.E., Ettwig, K.F., Schneider, B., Frenzel, P. and Boon, N. (2013) Revisiting Methanotrophic Communities in Sewage Treatment Plants. Applied and Environmental Microbiology 79(8), 2841-2846.

Hofman, J., Hofman-Caris, R., Nederlof, M., Frijns, J. and van Loosdrecht, M. (2011) Water and energy as inseparable twins for sustainable solutions. Water Science and Technology 63(1), 88-92.

IEA (2010) CO_2 emissions from fuel combustion. Highlights, International Energy Agency, Paris, France.

IPCC (2006) 2006 IPCC Guidelines for National Greenhouse Gas Inventories, Prepared by the National Greenhouse Gas Inventories Programme, Eggleston H.S., Buendia L., Miwa K., Ngara T. and Tanabe K. (eds), IPCC, Hayama, Japan.

IPCC (2007a) Climate Change 2007: The Physical Science Basis. Contribution of Working Group I to the Fourth Assessment Report of the Intergovernmental Panel on Climate Change, IPCC, Cambridge, United Kingdom and New York, NY, USA.

IPCC (2007b) Climate Change 2007: Mitigation. Contribution of Working Group III to the Fourth Assessment Report of the Intergovernmental Panel on Climate Change, IPCC, Cambridge, United Kingdom and New York, NY, USA.

IPCC (2007c) Climate Change 2007: Impacts, Adaptation and Vulnerability. Contribution of Working Group II to the Fourth Assessment Report of the Intergovernmental Panel on Climate Change, IPCC, Cambridge, United Kingdom and New York, NY, USA.

IPCC (2013a) Climate Change 2013: The Physical Science Basis. Working Group I Contribution to the IPCC 5th Assessment Report - Changes to the underlying Scientific/Technical Assessment, IPCC, Cambridge, United Kingdom and New York, NY, USA.

IPCC (2013b) Climate Change 2013: The Physical Science Basis. Working Group I Contribution to the IPCC 5th Assessment Report, IPCC, Cambridge, United Kingdom and New York, NY, USA.

Itokawa, H., Hanaki, K. and Matsuo, T. (2001) Nitrous oxide production in high-loading biological nitrogen removal process under low COD/N ratio condition. Water research 35(3), 657-664.

References

Jiang, G., Gutierrez, O., Sharma, K.R. and Yuan, Z. (2010) Effects of nitrite concentration and exposure time on sulfide and methane production in sewer systems. Water Research 44(14), 4241-4251.

Jiang, G., Gutierrez, O., Sharma, K.R., Keller, J. and Yuan, Z. (2011a) Optimization of intermittent, simultaneous dosage of nitrite and hydrochloric acid to control sulfide and methane productions in sewers. Water Research 45(18), 6163-6172.

Jiang, G., Gutierrez, O. and Yuan, Z. (2011b) The strong biocidal effect of free nitrous acid on anaerobic sewer biofilms. Water Research 45(12), 3735-3743.

Joergensen, L. (1985) The methane mono-oxygenase reaction system studied invivo by membrane-inlet mass-spectrometry. Biochemical Journal 225(2), 441-448.

Kampman, C., Hendrickx, T.L.G., Luesken, F.A., van Alen, T.A., Op den Camp, H.J.M., Jetten, M.S.M., Zeeman, G., Buisman, C.J.N. and Temmink, H. (2012) Enrichment of denitrifying methanotrophic bacteria for application after direct low-temperature anaerobic sewage treatment. Journal of Hazardous Materials 227–228(0), 164-171.

Kampschreur, M.J., Tan, N.C.G., Kleerebezem, R., Picioreanu, C., Jetten, M.S.M. and van Loosdrecht, M.C.M. (2008a) Effect of dynamic process conditions on nitrogen oxides emission from a nitrifying culture. Environmental Science & Technology 42(2), 429-435.

Kampschreur, M.J., van der Star, W.R.L., Wielders, H.A., Mulder, J.W., Jetten, M.S.M. and van Loosdrecht, M.C.M. (2008b) Dynamics of nitric oxide and nitrous oxide emission during full-scale reject water treatment. Water Research 42(3), 812-826.

Kampschreur, M.J., Temmink, H., Kleerebezem, R., Jetten, M.S.M. and van Loosdrecht, M.C.M. (2009) Nitrous oxide emission during wastewater treatment. Water Research 43(17), 4093-4103.

Kampschreur, M.J., Kleerebezem, R., de Vet, W.W.J.M. and van Loosdrecht, M.C.M. (2011) Reduced iron induced nitric oxide and nitrous oxide emission. Water Research 45(18), 5945-5952.

Kimochi, Y., Inamori, Y., Mizuochi, M., Xu, K.-Q. and Matsumura, M. (1998) Nitrogen removal and N2O emission in a full-scale domestic wastewater treatment plant with intermittent aeration. Journal of Fermentation and Bioengineering 86(2), 202-206.

Lammel, G. and Cape, J.N. (1996) Nitrous acid and nitrite in the atmosphere. Chemical Society Reviews 25(5), 361-369.

Law, Y., Ni, B.-J., Lant, P. and Yuan, Z. (2012a) N_2O production rate of an enriched ammonia-oxidising bacteria culture exponentially correlates to its ammonia oxidation rate. Water Research 46(10), 3409-3419.

Law, Y., Jacobsen, G.E., Smith, A.M., Yuan, Z. and Lant, P. (2013) Fossil organic carbon in wastewater and its fate in treatment plants. Water Research 47(14), 5270-5281.

Law, Y.Y., Ye, L., Pan, Y.T. and Yuan, Z.G. (2012b) Nitrous oxide emissions from wastewater treatment processes. Philosophical Transactions of the Royal Society B-Biological Sciences 367(1593), 1265-1277.

Le Moullec, Y., Potier, O., Gentric, C. and Leclerc, J.P. (2011) Activated sludge pilot plant: Comparison between experimental and predicted concentration profiles using three different modelling approaches. Water Research 45(10), 3085-3097.

Lebrero, R., Rodriguez, E., Garcia-Encina, P.A. and Munoz, R. (2011) A comparative assessment of biofiltration and activated sludge diffusion for odour abatement. Journal of Hazardous Materials 190(1-3), 622-630.

Liebetrau, J., Clemens, J., Cuhls, C., Hafermann, C., Friehe, J., Weiland, P. and Daniel-Gromke, J. (2010) Methane emissions from biogas-producing facilities within the agricultural sector. Engineering in Life Sciences 10(6), 595-599.

Lotito, A.M., Wunderlin, P., Joss, A., Kipf, M. and Siegrist, H. (2012) Nitrous oxide emissions from the oxidation tank of a pilot activated sludge plant. Water Research 46(11), 3563-3573.

Mampaey, K.E., Beuckels, B., Kampschreur, M.J. and Kleerebezem, R. (2011) Modelling nitrous and nitric oxide emissions by autotrophic ammonium oxidizing bacteria. Environment.

Matsuura, N., Hatamoto, M., Sumino, H., Syutsubo, K., Yamaguchi, T. and Ohashi, A. (2010) Closed DHS system to prevent dissolved methane emissions as greenhouse gas in anaerobic wastewater treatment by its recovery and biological oxidation. Water Science & Technology 61(9), 2407.

Maurer, M., Pronk, W. and Larsen, T.A. (2006) Treatment processes for source-separated urine. Water Research 40(17), 3151-3166.

Megraw, S.R. and Knowles, R. (1987) Active methanotrophs suppress nitrifidation in a humisol. Biology and Fertility of Soils 4(4), 205-212.

Meijer, S., van der Spoel, H., Susanti, S., Heijnen, J. and van Loosdrecht, M. (2002) Error diagnostics and data reconciliation for activated sludge modelling using mass balances.

Melse, R.W. and van der Werf, A.W. (2005) Biofiltration for Mitigation of Methane Emission from Animal Husbandry. Environmental Science & Technology 39(14), 5460-5468.

Modin, O., Fukushi, K. and Yamamoto, K. (2007) Denitrification with methane as external carbon source. Water Research 41(12), 2726-2738.

Mohanakrishnan, J., Gutierrez, O., Meyer, R.L. and Yuan, Z. (2008) Nitrite effectively inhibits sulfide and methane production in a laboratory scale sewer reactor. Water Research 42(14), 3961-3971.

Mohanakrishnan, J., Gutierrez, O., Sharma, K.R., Guisasola, A., Werner, U., Meyer, R.L., Keller, J. and Yuan, Z. (2009) Impact of nitrate addition on biofilm properties and activities in rising main sewers. Water Research 43(17), 4225-4237.

Nagai, S., Mori, T. and Aiba, S. (1973) Investigation of energetics of methane-utilizing bacteria in methane-limited and oxygen-limited chemostat cultures. Journal of Applied Chemistry and Biotechnology 23(7), 549-562.

Ni, B.-J., Yuan, Z., Chandran, K., Vanrolleghem, P.A. and Murthy, S. (2013) Evaluating four mathematical models for nitrous oxide production by autotrophic ammonia-oxidizing bacteria. Biotechnology and Bioengineering 110(1), 153-163.

Ni, B.J., Ruscalleda, M., Pellicer-Nacher, C. and Smets, B.F. (2011) Modeling Nitrous Oxide Production during Biological Nitrogen Removal via Nitrification and Denitrification: Extensions to the General ASM Models. Environmental Science & Technology 45(18), 7768-7776.

Nikiema, J., Brzezinski, R. and Heitz, M. (2007) Elimination of methane generated from landfills by biofiltration: a review. Reviews in Environmental Science and Bio/Technology 6(4), 261-284.

Noll, M., Frenzel, P. and Conrad, R. (2008) Selective stimulation of type I methanotrophs in a rice paddy soil by urea fertilization revealed by RNA-based stable isotope probing. Fems microbiology ecology 65(1), 125-132.

Nopens, I., Benedetti, L., Jeppsson, U., Pons, M.N., Alex, J., Copp, J.B., Gernaey, K.V., Rosen, C., Steyer, J.P. and Vanrolleghem, P.A. (2010) Benchmark Simulation Model No 2: finalisation of plant layout and default control strategy. Water Science and Technology 62(9), 1967-1974.

References

Nyerges, G. and Stein, L.Y. (2009) Ammonia cometabolism and product inhibition vary considerably among species of methanotrophic bacteria. FEMS Microbiology Letters 297(1), 131-136.

Oldenhuis, R., Oedzes, J.Y., Vanderwaarde, J.J. and Janssen, D.B. (1991) Kinetics of chlorinated hydrocarbon degradation by Methylosinus trichosporium OB3B and toxicity of trichloroethylene. Applied and Environmental Microbiology 57(1), 7-14.

Olsson, G. and Andrews, J.F. (1978) Dissolved-oxygen profile - valuable tool for control of activated-sludge process. Water Research 12(11), 985-1004.

Ort, C. and Gujer, W. (2006) Sampling for representative micropollutant loads in sewer systems. Water Science and Technology 54(6-7), 169-176.

Ort, C., Lawrence, M.G., Reungoat, J. and Mueller, J.F. (2010a) Sampling for PPCPs in wastewater systems: comparison of fifferent sampling modes and optimization strategies. Environmental Science & Technology 44(16), 6289-6296.

Ort, C., Lawrence, M.G., Rieckermann, J. and Joss, A. (2010b) Sampling for pharmaceuticals and personal care products (PPCPs) and illicit drugs in wastewater systems: are your conclusions valid? A critical review. Environmental Science & Technology 44(16), 6024-6035.

Otte, S., Grobben, N.G., Robertson, L.a., Jetten, M.S. and Kuenen, J.G. (1996) Nitrous oxide production by Alcaligenes faecalis under transient and dynamic aerobic and anaerobic conditions. Applied and environmental microbiology 62(7), 2421-2426.

Pauss, A., Andre, G., Perrier, M. and Guiot, S.R. (1990) Liquid-to-Gas Mass Transfer in Anaerobic Processes: Inevitable Transfer Limitations of Methane and Hydrogen in the Biomethanation Process. Applied and Environmental Microbiology 56(6), 1636-1644.

Pernetti, M. and Di Palma, L. (2005) Experimental evaluation of inhibition effects of saline wastewater on activated sludge. Environmental Technology 26(6), 695-703.

Peu, P., Béline, F., Picard, S. and Héduit, A. (2006) Quantification des émissions de protoxyde d'azote issues du traitement biologique d'eaux usées par boues activées. Journées Techniques Nationales INSA 2006, Progrès techniques appliqués aux domaines Air, Eau, Sol et Déchets, 8 - 9 June 2006, Toulouse, France.

Philips, S., Laanbroek, H.J. and Verstraete, W. (2002) Origin, causes and effects of increased nitrite concentrations in aquatic environments. Reviews in environmental science and biotechnology 1(2), 115-141.

Portmann, R.W., Daniel, J.S. and Ravishankara, A.R. (2012) Stratospheric ozone depletion due to nitrous oxide: influences of other gases. Philosophical Transactions of the Royal Society B-Biological Sciences 367(1593), 1256-1264.

Raghoebarsing, A.A., Pol, A., van de Pas-Schoonen, K.T., Smolders, A.J.P., Ettwig, K.F., Rijpstra, W.I.C., Schouten, S., Damste, J.S.S., Op den Camp, H.J.M., Jetten, M.S.M. and Strous, M. (2006) A microbial consortium couples anaerobic methane oxidation to denitrification. Nature 440(7086), 918-921.

Randall, C.W. and Buth, D. (1984) Nitrite buildup in activated sludge resulting from temperature effects. Journal Water Pollution Control Federation 56(9), 1039-1044.

Rassamee, V., Sattayatewa, C., Pagilla, K. and Chandran, K. (2011) Effect of Oxic and Anoxic Conditions on Nitrous Oxide Emissions from Nitrification and Denitrification Processes. Biotechnology and Bioengineering 108(9), 2036-2045.

Ravishankara, A.R., Daniel, J.S. and Portmann, R.W. (2009) Nitrous Oxide (N_2O): The Dominant Ozone-Depleting Substance Emitted in the 21st Century. Science 326(5949), 123-125.

Ren, T., Amaral, J.A. and Knowles, R. (1997) The response of methane consumption by pure cultures of methanotrophic bacteria to oxygen. Canadian Journal of Microbiology 43(10), 925-928.

Rittmann, B.E. and McCarty, P.L. (2001) Environmental biotechnology, McGraw Hill New York.

Schreiber, F., Wunderlin, P., Udert, K.M. and Wells, G.F. (2012) Nitric oxide and nitrous oxide turnover in natural and engineered microbial communities: biological pathways, chemical reactions and novel technologies. Frontiers in microbiology 3.

Schulthess, R. (1995) Release of nitric and nitrous oxides from denitrifying activated sludge. Water Research 29(1), 215-226.

Short, M.D., Daikeler, A., Peters, G.M., Mann, K., Ashbolt, N.J., Stuetz, R.M. and Peirson, W.L. (2014) Municipal gravity sewers: An unrecognised source of nitrous oxide. Science of The Total Environment 468–469(0), 211-218.

Sivret, E.C., Peirson, W.L. and Stuetz, R.M. (2008) Nitrous oxide monitoring for nitrifying activated sludge aeration control: A simulation study. Biotechnology and Bioengineering 101(1), 109-118.

Sly, L.I., Bryant, L.J., Cox, J.M. and Anderson, J.M. (1993) Development of a biofilter for the removal of methane from coal mine ventilation atmospheres. Applied Microbiology and Biotechnology 39(3).

Sommer, J., Ciplak, G., Linn, A., Sumer, E., Benckiser, G. and Ottow, J.C.G. (1998) Quantification of emitted and retained N_2O in a municipal waste water treatment plant with activated sludge and nitrifying-denitrifying units. Agribiological research 51(1), 59-73.

STOWA (2010) Emissies van broeikasgassen van RWZI's, Amersfoort, the Netherlands.

Sümer, E., Weiske, A., Benckiser, G. and Ottow, J.C.G. (1995) Influence of environmental conditions on the amount of N_2O released from activated sludge in a domestic waste water treatment plant. Cellular and Molecular Life Sciences 51(4), 419-422.

Sutton, P.M., Melcer, H., Schraa, O.J. and Togna, A.P. (2011) Treating municipal wastewater with the goal of resource recovery. Water Science and Technology 63(1), 25-31.

Sweetapple, C., Fu, G. and Butler, D. (2013) Identifying key sources of uncertainty in the modelling of greenhouse gas emissions from wastewater treatment. Water Research 47(13), 4652-4665.

Tallec, G., Garnier, J., Billen, G. and Gousailles, M. (2006) Nitrous oxide emissions from secondary activated sludge in nitrifying conditions of urban wastewater treatment plants: Effect of oxygenation level. Water Research 40(15), 2972-2980.

Tallec, G., Garnier, J., Billen, G. and Gousailles, M. (2008) Nitrous oxide emissions from denitrifying activated sludge of urban wastewater treatment plants, under anoxia and low oxygenation. Bioresource Technology 99(7), 2200-2209.

TNO/VNCI (2008) Chemiekaarten, ten Hagen & Stam, Den Haag, Netherlands.

Tumlin, S. (2011) Carbon Footprint för Ryaverket 2010. Rapport 2011:9. Gryaab (ed), p. 39, Göteborg.

Vadivelu, V.M., Keller, J. and Yuan, Z. (2006) Effect of free ammonia and free nitrous acid concentration on the anabolic and catabolic processes of an enriched Nitrosomonas culture. Biotechnology and Bioengineering 95(5), 830-839.

Van Bodegom, P., Goudriaan, J. and Leffelaar, P. (2001) A mechanistic model on methane oxidation in a rice rhizosphere. Biogeochemistry 55(2), 145-177.

Van Cleemput, O. (1998) Subsoils : chemo- and biological denitrification , N_2O and N_2 emissions. Nutrient Cycling in Agroecosystems, 187-194.

References

van der Ha, D., Hoefman, S., Boeckx, P., Verstraete, W. and Boon, N. (2010) Copper enhances the activity and salt resistance of mixed methane-oxidizing communities. Applied Microbiology and Biotechnology 87(6), 2355-2363.

van der Ha, D., Bundervoet, B., Verstraete, W. and Boon, N. (2011) A sustainable, carbon neutral methane oxidation by a partnership of methane oxidizing communities and microalgae. Water Research 45(9), 2845-2854.

van der Lans, R. (2011) Advanced Course in Environmental Biotechnology. Chapter 12 Gas-liquid interphase transport.

Verstraete, W. and Vlaeminck, S.E. (2011) ZeroWasteWater: short-cycling of wastewater resources for sustainable cities of the future. International Journal of Sustainable Development and World Ecology 18(3), 253-264.

VROM (2008) Protocol 8136 Afvalwater, t.b.v NIR 2008 uitgave maart 2008 6B: CH_4 en N_2O uit Afvalwater, The Hague, Netherlands.

Wang, J., Zhang, J., Xie, H., Qi, P., Ren, Y. and Hu, Z. (2011a) Methane emissions from a full-scale A/A/O wastewater treatment plant. Bioresource Technology 102(9), 5479-5485.

Wang, J.S., Hamburg, S.P., Pryor, D.E., Chandran, K. and Daigger, G.T. (2011b) Emissions Credits: Opportunity To Promote Integrated Nitrogen Management in the Wastewater Sector. Environmental Science & Technology 45(15), 6239-6246.

Weiland, P., Gemmeke, B. and Rieger, C. (2009) Biogas-Messprogramm II–61 Biogasanlagen im Vergleich, Fachagentur Nachwachsende Rohstoffe e.V., Gülzow, Germany.

Wicht, H. and Beier, M. (1995) N_2O-Emissionen aus nitrifizierenden und denitrifizierenden Kläranlagen. Korrespondenz Abwasser 42(3), 404-406.

Wiesen, P., Kleffmann, J., Kurtenbach, R. and Becker, K.H. (1995) Mechanistic study of the heterogeneous conversion of NO2 into HONO and N2O on acid surfaces. Faraday Discussions 100, 121-127.

Woess-Gallasch, S., Bird, N., Enzinger, P., Jungmeier, G., Padinger, R., Pena, N. and Zanchi, G. (2010) Greenhouse Gas Benefits of a Biogas Plant in Austria, Joanneum Research Forschungsgesellschaft mbH. Resources - Institute of Water, Energy and Sustainability, Graz, Austria.

Wunderlin, P., Mohn, J., Joss, A., Emmenegger, L. and Siegrist, H. (2012) Mechanisms of N_2O production in biological wastewater treatment under nitrifying and denitrifying conditions. Water Research 46(4), 1027-1037.

Wunderlin, P., Lehmann, M.F., Siegrist, H., Tuzson, B., Joss, A., Emmenegger, L. and Mohn, J. (2013a) Isotope Signatures of N2O in a Mixed Microbial Population System: Constraints on N2O Producing Pathways in Wastewater Treatment. Environmental Science & Technology 47(3), 1339-1348.

Wunderlin, P., Siegrist, H. and Joss, A. (2013b) Online N_2O Measurement: The Next Standard for Controlling Biological Ammonia Oxidation? Environmental Science & Technology 47(17), 9567-9568.

Ye, L., Ni, B.-J., Law, Y., Byers, C. and Yuan, Z. (2014) A novel methodology to quantify nitrous oxide emissions from full-scale wastewater treatment systems with surface aerators. Water Research 48, 257-268.

Yoon, S., Carey, J.N. and Semrau, J.D. (2009) Feasibility of atmospheric methane removal using methanotrophic biotrickling filters. Applied Microbiology and Biotechnology 83(5), 949-956.

Yu, R., Kampschreur, M.J., Loosdrecht, M.C.M.v. and Chandran, K. (2010) Mechanisms and Specific Directionality of Autotrophic Nitrous Oxide and Nitric Oxide Generation during Transient Anoxia. Environmental Science & Technology 44(4), 1313-1319.

Zeeman, G. and Kujawa-Roeleveld, K. (2011) Resource recovery from source separated domestic waste(water) streams; full scale results. Water Science and Technology 64(10), 1987-1992.

Zhang, L., Keller, J. and Yuan, Z. (2009) Inhibition of sulfate-reducing and methanogenic activities of anaerobic sewer biofilms by ferric iron dosing. Water Research 43(17), 4123-4132.

Zobell, C.E., Anderson, D.Q. and Smith, W.W. (1937) The bacteriostatic and bactericidal action of Great Salt Lake water. Journal of Bacteriology 33(3), 253-262.

Curriculum vitae

Curriculum vitae

Personal data

Name	Matthijs Roger Juliette DAELMAN
Date and place of birth	30 January 1982, Lokeren, Belgium
Address	Patrijzenlaan 6 9180 Moerbeke Belgium
Nationality	Belgian
Telephone	+31653874028
E-mail	m.r.j.daelman@tudelft.nl

Education

Master of bioscience engineering: environmental technology
Ghent University, 2010

Master in linguistics and literature: Germanic languages
Ghent University, 2005

General secondary education: Greek - sciences
Sint-Lodewijkscollege, Lokeren, 2000

Work experience

February 2014 - …	Researcher at Delft University of Technology
	Topic: alkaline bioconversions for biofuel production from sunlight
August 2010 - January 2014	Doctoral researcher at Delft University of Technology and at Ghent University (joint PhD)
	Topic: greenhouse gas emissions from fullscale municipal wastewater treatment plants

August 2013 - January 2014	Delft University of Technology
February 2012 - July 2013	Ghent University
August 2010 - January 2012	Delft University of Technology

List of publications

Journal articles

Daelman, M.R.J., van Voorthuizen, E.M., van Dongen, L.G.J.M, Volcke, E.I.P., van Loosdrecht, M.C.M. (2014). Seasonality of nitrous oxide emissions from full-scale municipal wastewater treatment. Submitted.

Daelman, M.R.J., van Eynde, T., van Loosdrecht, M.C.M., Volcke, E.I.P. (2014). Effect of process design and operating parameters on aerobic methane oxidation in municipal WWTPs. Water Research 66: 308-319.

Castro Barros, C.M., **Daelman, M.R.J.**, Mampaey, K.E., van Loosdrecht, M.C.M, Volcke, E.I.P. (2013) Dynamics of N2O emission from partial nitritation-anammox in a full-scale granular sludge reactor. Submitted.

Daelman, M.R.J., De Baets, B., van Loosdrecht, M.C.M., Volcke, E.I.P. (2013). Influence of sampling strategies on the estimated nitrous oxide emission from wastewater treatment plants. Water Research 47(9): 3120-3130.

Daelman, M.R.J., van Voorthuizen, E.M., van Dongen, L.G.J.M, Volcke, E.I.P., van Loosdrecht, M.C.M. (2013). Methane and nitrous oxide emissions from municipal wastewater treatment - results from a long-term study. Water Science and Technology 67(11): 2350–2355.

Daelman, M.R.J., van Voorthuizen, E.M., van Dongen, L.G.J.M, Volcke, E.I.P., van Loosdrecht, M.C.M. (2012). Methane emission during municipal wastewater treatment. Water Research 46(11): 3657-3670.

Other publications

van Voorthuizen, E.M., IJpelaar, G., **Daelman, M.R.J.**, van Dongen, L.G.J.M., van Loosdrecht, M.C.M. (2012). Emissie Broeikasgassen uit RWZI's. STOWA. Rapport 2012 – 20. 126 pp.

Conference contributions

Oral presentations

Daelman, M.R.J., van Eynde, T., van Loosdrecht, M.C.M., Volcke, E.I.P. (2014). Effect of process design and operating parameters on aerobic methane oxidation in municipal WWTPs. IWA World Water Congress & Exhibition, 21-26 September 2014, Lisbon, Portugal.

Daelman, M.R.J., van Voorthuizen, E.M., van Dongen, L.G.J.M., Volcke, E.I.P. and van Loosdrecht, M.C.M. (2013) Full-scale evaluation of process conditions leading to nitrous oxide emissions from municipal wastewater treatment plants.

Young Water Professionals Benelux 3rd Regional Conference, 2 - 4 October, 2013, Esch-sur-Alzette, Luxembourg; WEF/IWA Nutrient Removal and Recovery 2013: Trends in Resource Recovery and Use, 28 - 31 July 2013, Vancouver, Canada.

Castro Barros, C..M., **Daelman, M.R.J.**, Mampaey, K.E., van Loosdrecht, M.C.M, Volcke, E.I.P. (2013) Dynamics of N_2O emission from partial nitritation-anammox in a full-scale granular sludge reactor. 11th IWA Conference on Instrumentation Control and Automation, 18-20 September 2013, Narbonne, France; 10th IWA Leading Edge Conference on Water and Waste Water Technologies, 2-6 June 2013, Bordeaux, France; 9th IWA International Conference on Biofilm Reactors, 28 - 31 May 2013, Paris, France.

Guo, L., Lamaire-Chad, C., Bellandi, G., **Daelman, M.R.J.**, Amerlinck, Y., Maere, T., Nous, J., Flameling, T., Weijers, S., van Loosdrecht, M.C.M., Volcke, E.I.P., Nopens, I., Vanrolleghem, P.A. (2013) High-Frequency Field Measurement of Nitrous oxide (N_2O) Gas Emissions and Influencing Factors at WWTPs under Dry and Wet Weather Conditions. WEF/IWA Nutrient Removal and Recovery 2013: Trends in Resource Recovery and Use, 28 - 31 July 2013, Vancouver, Canada.

Daelman, M.R.J., De Baets, B., van Loosdrecht, M.C.M. and Volcke, E.I.P. (2012) Influence of sampling strategies on the estimated N_2O emission from wastewater treatment plants. New Developments in IT & Water Conference, 4 - 7 November 2012, Amsterdam, Netherlands.

Daelman, M.R.J., van Voorthuizen, E.M., van Dongen, L.G.J.M., Volcke, E.I.P. and van Loosdrecht, M.C.M. (2012) Methane and nitrous oxide emissions from municipal wastewater treatment – results from a long-term study. 9th IWA Leading-Edge Conference on Water and Wastewater Technologies, 3 - 7 June 2012, Brisbane, Australia; IWA Nutrient Removal and Recovery Conference, 23 - 25 September 2012, Harbin, China.

Daelman M.R.J., van Dongen L.G.J.M., van Voorthuizen E.M., Kleerebezem R., van Loosdrecht M.C.M. and Volcke E.I.P. (2011). The influence of sampling strategies on the estimated N_2O emission from a wastewater treatment plant. 2nd IWA BeNeLux Young Water Professionals Regional Conference, 20 - 22 September, 2011, Leuven, Belgium.

Daelman M.R.J., van Dongen L.G.J.M., van Voorthuizen E.M., Kleerebezem R., van Loosdrecht M.C.M. and Volcke E.I.P. (2011). Quantification of greenhouse gas emissions from municipal wastewater treatment plants : a case study. 16th PhD Symposium on Applied Biological Sciences, 20 December 2010, Gent.

Poster presentations

Daelman, M.R.J., van Eynde, T., van Loosdrecht, M.C.M., Volcke, E.I.P. (2014). Effect of process design and operating parameters on aerobic methane oxidation in municipal WWTPs. 2nd IWA specialized conference EcoTechnologies for Sewage Treatment Plants (EcoSTP2014), 23-25 June 2014, Verona, Italy; 4th IWA/WEF Wastewater Treatment Modelling Seminar 2014 (WWTmod2014), 30 March – 2 April 2014, Spa, Belgium.

Daelman M.R.J., van Dongen L.G.J.M., van Voorthuizen E.M., Kleerebezem R., van Loosdrecht M.C.M. and Volcke E.I.P. (2011). Controlling greenhouse gas emissions from municipal wastewater treatment plants. First international symposium on Microbial resource management in biotechnology: Concepts & applications. 30 June – 1 July, 2011, Ghent, Belgium.

Acknowledgements

Acknowledgements

Over the past four years, I could not have wished myself a better job than doing a PhD. This is typically the kind of job that is what you yourself make of it, but the impact of others cannot be overestimated.

I had the privilege of working at two institutes, Delft University of Technology and Ghent University, under the guidance of two promoters, Eveline Volcke and Mark van Loosdrecht.

Eveline, I'm the first of your PhD students to graduate and I think we both agree that it went very smoothly. I am grateful for the trust you put in me and the freedom you granted me. I admire the unrelenting thoroughness with which you approach the job at hand and your eye for detail that sometimes had to make up for my own tendency to proceed a tad too briskly. I appreciate that you also value the non-work related things in life. I hope to be the first of a long line of successful PhD students that graduate under your supervision. Ahead of you, there is a career that spans about three decades (taking into account the current age of retirement in Belgium). Even if time flies, that is still a vast amount of opportunities. I can't wait to see what that will result in.

Mark, you too have still many years before retiring (will you ever?), but yet, you have already achieved a status that is far above par in the field of environmental biotechnology, and even in science in general. In the past few years, you received a great many awards and prizes for your achievements as a scientist. From my part in particular, I would like to praise you also as a teacher. Just like Eveline, you realize that life is not only about work. You never put pressure on people's shoulders, but your personality and your radiating energy inspire us to rise above what we thought we could. As the Jesuits say: "Plus est en vous." Well, you know how to bring it out.

This thesis was thoroughly assessed by the committee members Sylvie Gillot, Ingmar Nopens, Nico Boon, Jules van Lier and Geert-Jan Witkamp. I appreciate their effort and their suggestions.

Over the years, I had the opportunity to cooperate with a number of very bright people. Bernard De Baets's contribution to chapter three of this thesis is much appreciated. I was also glad to participate in measurement campaigns on the Eindhoven WWTP, with Lisha and Coralie, and with Jose, students of Peter Vanrolleghem and Ingmar Nopens, respectively.

Because I moved from Delft to Ghent and from Ghent to Delft in the middle of the academic year, I did not have many opportunities to guide students, but the ones I worked with did a very good job. Tamara's MSc thesis resulted in a journal paper and thanks to their tremendous enthusiasm Ella, Jonas, Katrien and Stijn made a well-received BSc thesis.

The first 18 months of my PhD I spent in Delft, working on a project by STOWA. Udo van Dongen was instrumental in helping me to get the practical side of this project going, while Ellen van Voorthuizen was an appreciated sparring partner. I'm also much indebted to the other people involved in this project for their valuable suggestions: Guus IJpelaar, Alex Sengers, Klaas Appeldoorn, Coert Petri, Hardy Temmink, Herman Walthaus and of course, Cora Uijterlinde. Also Marlies Kampschreur was a part of the project committee. It was always a pleasure to tap into her vast knowledge of the nitrogen cycle.

A large part of my research involved full-scale measurements on the wastewater treatment plant of Kralingseveer in Capelle aan den IJssel, near Rotterdam. I spent so much time on this plant that I really started to feel at home there. Of course, that is the merit of the staff. Hans van der Hoek, Marcel van Hees and Manda Milosevic-Bilic were crucial for the success of this research, but they were also very nice people to have a chat with, just like the many other staff members who were always very interested in our work on the plant and always willing to lend us a hand.

During this first term in Delft, I had the pleasure to be part of the nice crowd that the Environmental Biotechnology Section is. Udo, besides being a skilled technician and renown lunch professor, you're foremost an nice pal. Mario, lab wizard and the Bear Grylls of EBT, I'll never forget when you two came to the surprise party for my 30th birthday. You also brought two Italians with you. Marco and Tommaso, thanks for the laughs.

Then there's this bunch of office mates I had during my first term in Delft: Jelmer, Yang, Andrea, Simona, João, Peter. From the silliest jokes to the most elevated discussions, it all had its place. Many other people in the EBT group assured that there never was a dull day: Helena M.G., Shiva, Mari, Helena J., Dmitry, Gerard, Emmanuelle, Robbert, Olga, Florence, Cristian, Gijs, Cees and Ben. Rob and Dirk, your help in all things technical was very valuable, but your contributions to coffee breaks were at least as influential. Life at the Kluyverlab was made a breeze by very capable and very helpful people, such as Ginie, Sjaak and Jos, Herman and Miranda.

After 18 months of assimilation in Delft, I found my way back to Ghent. There I met my new colleagues of the Biosystems Control-group: Celia, Kris, Thomas, Caroline, Salatul. It was nice working with you around. I'm grateful to Jan Pieters for hosting me at his department. While coffee breaks in Delft usually had a very impromptu character, the breaks in Ghent were some kind of institute. I really liked the gatherings around the big table, together with the other colleagues of the department of Biosystems Engineering: Jop, Frederik, Dane, Rob, Wolter, Güray, Diego, Mike, Fons, Gerlinde, Wasan, Eddy and Dieter. To the latter two, I'm also grateful for the technical and administrative support.

During my 18 month stay in Ghent, I met some familiar faces of former classmates that had turned into colleagues, but that had been friends all the time: Katrijn, Linde, Leendert

and Céline. I really enjoyed our lunch breaks at Parnassus. To all the other former classmates that are still sticking together: "De vrienden van de milieu" rock big time!

For the last 6 months of my PhD I returned to Delft, to my new office with some familiar faces: Marco and Emmanuelle, and some new faces as well: Eveline, Bruno, Khaled. Another bunch of new colleagues: Maaike, Gerben, Monica, Geert-Jan, Emma, Leonie, Mitchel, Mabel, Song, Diana and also Julio (who became a regular member of the lunch department). I'm glad I'll be able to enjoy your company in the near future as well.

Katrijn, printed words feel completely inapt to thank you, but anyway I'll type a few: thanks for letting me do what I wanted to do.

In the end, the creation of this thesis can be traced back to the two loving and caring people who raised me, my parents. They made the warmest home imaginable for me and my sister, who in her turn is also creating such a stimulating environment for my nieces and nephews. Having such a great family is invaluable.